SSRC/CCCPR-TR-2015-1

UTOPIA:
The Manual of Version 2015

Claudio Cassardo

EWHA WOMANS UNIVERSITY

UNIVERSITY OF TORINO

INNOVATION
EWHA

UNIVERSITÀ
DEGLI STUDI
DI TORINO

UTOPIA: The Manual of Version 2015

Claudio Cassardo

Department of Physics and NATRISK Center, University of Torino “Alma Universitas Taurinensis”, Torino, Italy

CINFAI, National Inter/University Consortium for Physics of the Atmosphere and Hydrosphere, Turin, Italy

Department of Atmospheric Science and Engeenring, Severe Storm Research Center, and Center for Climate Change Prediction Research, Ewha Womans University, Seoul, Korea

CONTENTS

List of Tables.....vi

List of Figures.....vii

1. Introduction.....1

2. The model and its structure.....6

3. Radiation.....9

3.1. Shortwave radiation.....10

3.2. The incoming (solar) shortwave radiation.....12

3.2.1. The solar angle over titled surfaces.....14

3.3. Longwave radiation.....17

3.3.1. The haze parameterization.....20

3.4. Calculation of surface albedo.....22

3.5. Net radiation.....25

4. Energy balance.....26

4.1. Momentum flux.....27

4.2. Sensible heat fluxes.....28

4.3. Evapotranspiration fluxes.....30

4.4. Latent heat fluxes.....34
4.5. Temperature and humidity in the canopy-air space.....35
4.6. Interface heat fluxes.....35
4.7. Resistances and conductances.....36
4.8. Drag coefficients.....43
4.9. Roughness lengths.....44
5. Heat transfer into soil.....49
5.1. The formulation……...49
5.2. The numerical scheme.....49
6. Vegetation energy and hydrological balances.....54
6.1. Vegetation temperature.....54
6.2. Vegetation water budget.....56
6.3. Roots.....57
7. Soil hydrological budget.....60
7.1. Soil surface hydrological budget.....60
7.2. Soil underground hydrological budget.....61
7.3. Numerical scheme.....64
7.4. Surface and underground runoff.....67
7.5. Water outflow from the bottom layer (drainage).....69
7.6. Modification of all formulations for sloping terrain.....69
8. The snow parametrization.....71

8.1. Definitions.....71
8.2. Melting processes of snow.....72
8.3. Snow energy balance.....74
8.3.1. Net radiation over snowy surfaces.....76
8.3.2. Surface temperature and moisture over snowy surfaces…….76
8.3.3. Conductive fluxes in the snow pack.....77
8.4. Thermal balance in the snow pack.....78
8.5. Hydrological balance in the snow pack.....80
8.6. Snow compactation and density.....82
8.7. Snow coverage.....84
8.7.1. The algorythm proposed for the snow cover in UTOPIA.....89
8.8. Snowfall.....90
9. The soil freezing.....92
9.1. The parameterization of SC01.....92
9.2. The parameterization of V199.....93
9.3. The parameterization of BO10.....94
10. The datasets.....96
10.1. The dataset for the vegetation parameters.....96
10.1.1 Direct initialization.....97
10.1.2 The WH85 global database.....97
10.1.3 The ecoclimap database.....101

10.2. The dataset for the soil parameters.....104
11. Photosynthesis and carbon fixation.....107
11.1. Primary production and carbon assimilation.....107
11.1. Limiting factors for the photosynthesic rate: C3 plants.....108
11.1.1. The rubisco-limited photosynthesis.....109
11.1.1.1. Michaelis-menten coefficients of Rubisco activity..
…..……111
11.1.1.2. The compensation point.....113
11.1.1.3. Maximum rate of Rubisco carboxylation.....113
11.1.2. RunBP-limited photosynthesis.....116
11.1.3. Triose phosphate utilization-limited photosynthesis.....122
11.2. Limiting factors for the photosynthesis rate: C4 plants.....122
11.2.1. RuBP-limited photosynthesis.....122
11.2.2. PEP carboxylase-limited photosynthesis.....123
11.2.3. Rubisco-limited photosynthesis.....124
11.3. Gross and net rate of assimilation.....125
11.3.1. Mitochondrial respiration.....126
11.4. Carbon flux and stomatal conductance.....127
11.4.1. Intercellular gases concentration.....127
11.4.2. Laminar leaf and stomatal resistances.....129
11.4.2.1. The stomatal resistance in the presence of water stress……...132

11.5. The two parameterizations implemented.....133

11.6. Model numerical implementation.....139

11.7. Scaling up photosynthesis from leaf to canopy.....140

12. Useful formulations.....146

12.1. Soil interpolations.....146

12.2. Initialisation of soil temperature and moisture.....149

13. Input/output.....154

13.1. Installation and directory management.....154

13.2 Input: Initial conditions.....155

13.3. Input: Boundart conditions.....165

13.4. Output.....169

13.4.1. Configuration of the required UTOPIA output.....170

13.4.2. Developers' notes: How to make a new variable available for output.....171

14. References.....176

15. Acknowledgements.....184

List of Tables

Table 1: Summary of processes affecting snow pack depending on available energy.....78

Table 2: Vegetation parameters required by UTOPIA.....96

Table 3: List of vegetation codes currently insterd in UTOPIA.....97

Table 4: Distribution of vegetation parameters according with their codes (From Dickinson et al., 1986).....99

Table 5: Soil code types.....105

Table 6: Values of soil parameters according with soil type.....106

Table 7: Coefficients used in the old model parameterization.....134

Table 8: Coefficients related to Rubisco carboxylation used in the new model parameterization.....136

Table 9: Coefficients related to the electron transport used in the new model parameterization.....137

Table 10: An example of PAR_file.....157

Table 11: List of possible input variables for UTOPIA.....167

Table 12: Sample of file memoryout config.....170

List of Figures

Figure 2.1: Structure of UTOPIA…….8

Figure 2.2: Scheme of soil layering in UTOPIA……..8

Figure 3.1: Possibilities of soil coverage: bare soil with and without snow cover, and vegetated soil with and without snow cover…….....9

Figure 3.2: Shortwave radiation components; red arrows indicate downward radiation, while blue arrows indicate upward radiation……...…11

Figure 3.3: Longwave radiation components; red arrows indicate downward radiation, while blue arrows indicate upward radiation……18

Figure 4.1: The resistance network for momentum (up), heat (middle) and water vapor (bottom) transfers in UTOPIA. Left part of figures refers to snowy conditions, while right part refers to snowless conditions……..….37

Figure 5.1: Structure of soil discretization scheme……....50

Figure 7.1: Structure of soil layers for hydrological processes……..63

Figure 8.1: Schematic structure of the snowpack…….……..…72

Figure 8.2: Subdivision of surface according with vegetation and snow coverages……..…….....75

Figure 8.3: Regression lines between (non-fully) snow coverages and snow heights in the Russian stations of RUSWET dataset……...86

Figure 8.4: Behavior of the different parameterizations of the snow coverage. In this plot, FIT0 refers to eq. (8.11), FIT to eq. (8.12), B88 to eq. (8.13), D95 to eq. (8.14), Y94 to eq. (8.15), and OUR to eq. (8.17)..88

Figure 8.5: Geometry of a snowy surface……..….90

Figure 10.1: Behavior of the function f(Ts) (see eq. 10.1)……...100

Figure 10.2: he USDA-NCRS (1997) soil textural database……....105

Figure 11.1: Speed of a non competitive reaction as a function of the substrate concentration [S].Vmax is the maximum reaction rate, while KM is the Michaelis-Menten coefficient of the reaction activity. Image source:www.knowledgerush.com/kr/encyclopedia/Enzyme……...….110

Figure 11.2: The rate of photosynthesis is plotted as a function of the PAR flux density. Note that a negative net CO2 uptake indicates a loss of carbon due to the respiration. The light saturation point will be descripted subsequently. Image source: Pearson Education, Inc……...…112

Figure 11.3: Arrhenius and Arrhenius modified function plotted using the coefficients values of a Sessile Oak tree Quercus petraea Source: Cerenzia (2012)……...115

Figure 11.4: Parameters required for modeling RuBPlimited photosynthesis according to Collatz model (1991), solid line, and to Bonan (2002), dashed line, based on the response of electron transport to incident photon flux. β is a constant (Bernacchi et al. (2009)).119

Figure 11.5: Sample responses of Jmax to leaf temperature. Value are normalized to 1 at 25 °C. From Medlyn et al. (2002)……...121

Figure 11.6: Heat, CO2 and water vapor fluxes at the leaf surface interface. The subscripts a, s and i, refer to ambient air, leaf surface and leaf, respectively. From Sellers et al. (1992)……....128

Figure 11.7: Measured photosynthetic capacity shows a direct proportionality with the canopy nitrogen amount for different trees species. Jack pine and black spruce are needleleaf evergreen trees, while aspen is a broadleaf tree. From Bonan (2002)……....142

Figure 13.1: Example of input data file……166

1. Introduction

The “land surface” (LS) is the surface that comprises vegetation, soil and snow, coupled with the way these influence the exchange of water, energy and carbon within the Earth system (Pitman (2003)). For more than three decades, it has been widely accepted that the land surface processes (LSP) are a key and critical component for the study of the weather and climate. They control the partitioning of available energy at the surface between sensible and latent heat, and the partitioning of available water between evaporation, runoff, soil storage, or groundwater recharge, as well as its regulation of biogeochemical cycles with processes such as photosynthesis and respiration. These exchanges between the atmosphere and the LS are known to significantly impact weather and climate, which has motivated significant advancement in the understanding of the physical processes that govern these exchanges.

Several recent review papers have addressed the issue of whether the state of the LS can influence weather and climate, concluding that such influence exists and is strong (Avissar and Verstraete (1990); Betts et al. (1996); Pielke et al. (1998); Sellers (1992)). Despite some preliminary studies founded that LSP at small time and space scales affect the atmosphere (Pielke (2001)) but not the climate as modeled by climate models (Avissar and Pielke (1991)), there is now a long series of evidences (see Pitman (2003) for a detailed review) that the LS matters also in climate models, at regional to global scales. Among the series of parameters involved in the LS processes in the climate, the leaf area index (LAI), the water-holding capacity of the soil, the role of roots, and in general the land cover characteristics (LCC) can be highlighted. Perhaps this is also because, with the aim to attempt to represent more accurately the land-atmosphere

interactions, many LS parametrization schemes have been developed, implemented, and tested for various climate conditions around the world. Thus, LSP in climate models have evolved from a very simple, implicit approach representing the surface energy balance and hydrology (Manabe (1969)), to complex models that represent many of the key processes through which the land surface influences the climate simulated by climate models (Pitman (2003)).

These land surface schemes vary in complexity from the very simple bucket method (Manabe (1969); Deardorff (1978)) to more physically based schemes (Sellers et al. (1986); Sellers et al. (1996); Noilhan and Planton (1989); Verseghy (1991); Verseghy et al. (1993); Yang and Dickinson (1996)); preliminary but non exhaustive reviews can be found on Avissar and Verstraete (1990) and Garratt (1993). Generally speaking, land surface models (LSM) can be categorized into three generations of models.

The **first-generation models** use simple bulk aerodynamic transfer formulations, and uniform and prescribed surface parameters. Vegetation is treated implicitly and do not changes in time. These models include only one to two layers for soil temperature, inadequate to capture the temperature variations at different scales, and only a single layer for soil moisture. The evapotranspiration do not explicitly includes the canopy resistance, and all fluxes have the same aerodynamic resistances for heat, water and momentum. Runoff is parametrized very simply. All these simplified parametrizations have as result an inappropriate representation of hydrology, is inadequate to capture the observed behavior of hydrological processes.

There are several **second-generation models** innovative in the way some components have been developed or tested, but all are fundamentally built from the leadership of

Deardorff (1978), Dickinson et al. (1986), and Sellers et al. (1986). These models usually represent the vegetation–soil system such that the surface interacts with the atmosphere, rather than being passive as in the first-generation models (Sellers et al. (1997)). They differentiate between soil and vegetation at the surface, and explicitly represent the impact of vegetation on momentum transfer. The canopy resistance is usually based on the relationship developed by Jarvis (1976), able to capture the key responses of stomata to PAR, humidity and temperature. Finally, most of these models have a reasonably sophisticated snow sub-model. According to Pitman (2003), there is evidence strongly suggesting that the second-generation models do improve the modelling of surface–atmospheric exchanges, at least on the time scale of days.

The **third-generation models** try to go beyond the major limitation of second-generation ones, i.e. the empirical modeling of canopy conductance. With the addition of an explicit canopy conductance, it has been possible to improve the simulation of the evapotranspiration pathway, as well as to address the issue of carbon uptake by plants. Thus, third-generation schemes are identifiable by the method used to model carbon, while they tend to use representations of other processes quite similar to those included in second-generation LSM.

In the Project for Intercomparison of Land-surface Parameterization Schemes, several studies have reported on and discussed the performances of some well-known LSM (Henderson-Sellers et al. (1993); Yang et al. (1997); Shao and Henderson-Sellers (1996); Chen et al. (1997)). Although most LSM have been validated and calibrated with the help of field data, the differences between individual models are still large. Nevertheless, the physically based LSM have a well-recognized promising potential for meteorological,

hydrological, and agricultural applications, also in the context of short-range and high spatial resolution precipitation forecasts (Wen et al. (2000)).

Mintz (1984), and later Oglesby (1991) and Beljaars et al. (1996), who used GCMs, studied the sensitivity of numerically simulated climates to land surface boundary conditions, analyzing the precipitation response to evaporation, and concluding that a positive feedback from the recirculation of precipitation should be expected through the soil moisture reservoir. However, how this response works in detail at high spatial resolution is still unknown and, as previously mentioned, differences between individual land surface schemes can be large.

Given such a wide spectrum of land surface models, it is a big challenge for atmospheric modelers, both for meteorological or climatic purposes, to select a land surface scheme appropriately adapt to their needs. The ideal land surface model for meteorological purposes should be sufficiently complex in order to well represent several physical processes of interaction, but also sufficiently simple in order to require few parameters and a small cpu-time to run (Chen et al. (1996)). Due to the similarity between second- and third-generation LSMs, actually many of these models continue to be developed via improvements in scheme components, data input, computational efficiency, etc. This because an advanced understanding of soil temperature physics, soil moisture processes, large-scale hydrology, snow physics, radiative transfer, photosynthesis-level biochemistry and large-scale ecology, boundary-layer processes, bio-geochemical cycling and advanced computer science are all required, especially when a good understanding of climate and climate feedbacks are concerned. The ultimate boundary of the LS research nowadays pushes scientists to design flexible LSM, in which

LS physical processes are realistically parameterized, in order that such LSMs could be linked into different climate models Polcher et al. (1998).

Following these directives, this paper aims to present the UTOPIA (University of TOrino land Process Interaction model in Atmosphere), which is the modern version of the old Land Surface Process Model (LSPM), developed by a team of Italian researchers and continuously updated and improved in the last quarter of century.

2. The model and its structure

The **U**niversity of **TO**rino land surface **P**rocess **I**nteraction model in **A**tmosphere (UTOPIA) is the upgraded version of the LSPM (Land Surface Process Model: Cassardo et al. (1995); Cassardo et al. (2006)), a diagnostic one-dimensional model studying the interactions at the interface between the atmospheric surface layer, the vegetation and the soil (Figure 3.2).

Both UTOPIA and its ancestor LSPM have been tested several times using routinely measured data, or field campaigns data, or coupled with an atmospheric circulation model. Among the most relevant studies, the LSPM was compared (Ruti et al. (1997)) with the BATS (the land surface scheme used by RegCM3) in the Po Valley; the dependence of the results by the initial conditions was analyzed (Cassardo et al. (1998)); the LSPM was used (Cassardo et al. (2005)) to analyse the surface energy and hydrological budgets at synoptic scale. The LSPM was also used (Cassardo et al. (2002) and Cassardo et al. (2006)) to analyze two extreme flood events occurred in Piedmont (Italy), and to study the 2003 heat wave in Piedmont (Cassardo et al. (2007)). The UTOPIA was also used for determining the hydrological and energy budgets in the Piedmontese vineyards (Francone et al. (2011)). The LSPM was also applied to extra-European climates, with simulations performed in very dry sites (Feng et al. (1997); Loglisci et al. (2001)) or to evaluate the hydrological and energy budgets during the Asian summer monsoon (Cassardo et al. (2009)). The most recent application is the coupling of the UTOPIA with the Weather Research and Forecast (WRF) model; this

coupled model WRF-UTOPIA was applied to study a flash flood caused by a landfalled typhoon (Zhang et al. (2011)).

The UTOPIA is able to represent the physical processes at the interface between atmospheric surface, vegetation and soil layers. The UTOPIA can be categorized as a big leaf model, meaning that a single vegetation element contributing to the various processes is considered, without considering its real extension. As SVAT models, it can, known the system initial conditions , to describe the energy, momentum, and humidity exchanges between the atmosphere and the soil, in the different ways they may occur.

The UTOPIA is a soil multilayer model, and discretizes the soil into a certain number of layers defined by the user. UTOPIA is a one-dimensional model, meaning that it works on a single point (station) in which the only direction allowed is the vertical one (from the surface layer to the deep soil). Fluxes are evaluated by building a resistances scheme. In UTOPIA, the vegetation and the soil are represented according to their physical parameters: a big leaf approximation is used. Momentum, heat and water vapor exchanges are the main physical processes considered in UTOPIA. In addition to the above mentioned physical processes, the model solves the hydrological processes, e.g. those involving water, water vapor and ice.

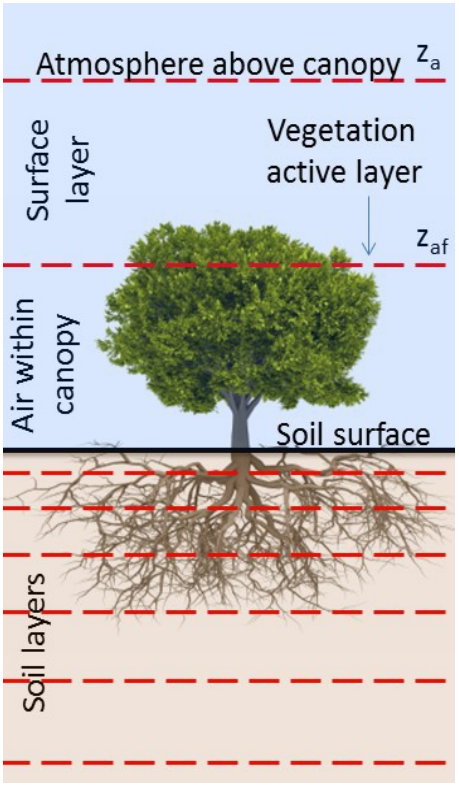

Figure 2.1: Structure of UTOPIA.

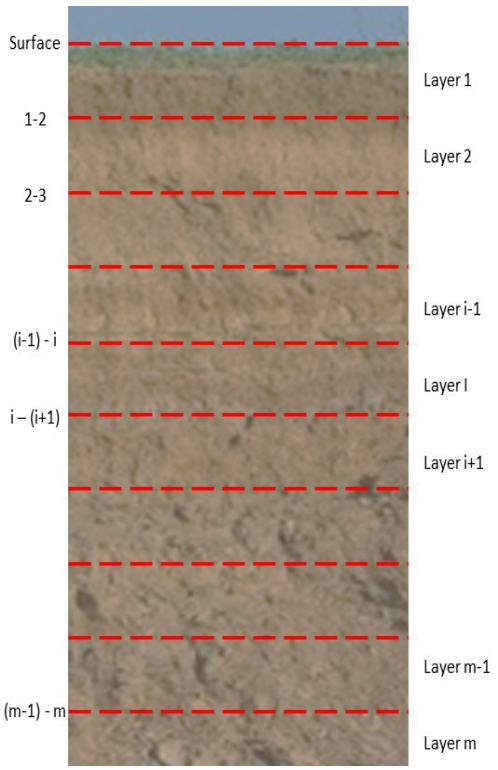

Figure 2.2: Scheme of soil layering in UTOPIA.

3. Radiation

A model point is characterized by a specific soil type and land use type. Furthermore, there can also be snow cover. The main subdivision consists in bare soil with and without snow cover, and vegetated soil with and without snow cover (Fig. 3.1).

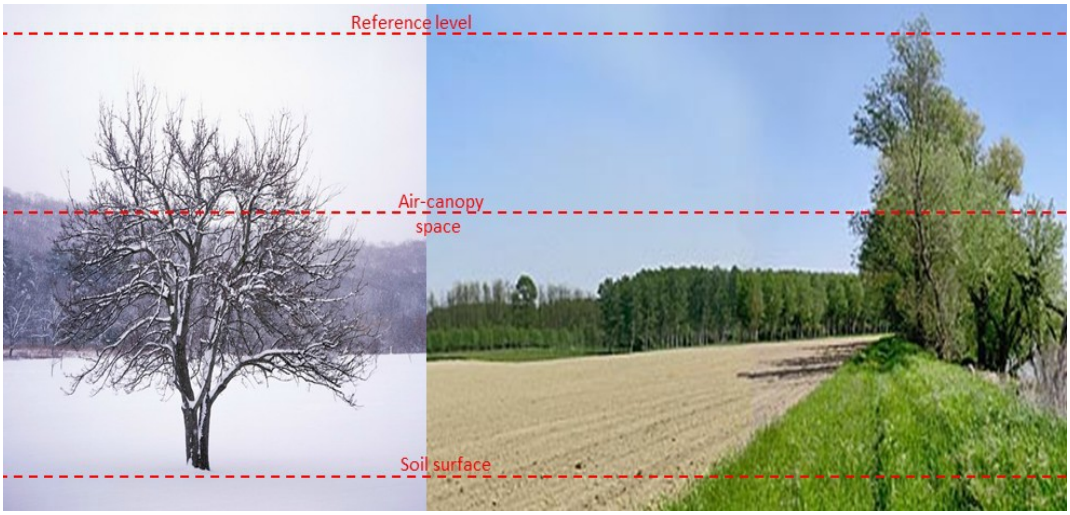

Figure 3.1: Possibilities of soil coverage: bare soil with and without snow cover, and vegetated soil with and without snow cover.

3.1. SHORTWAVE RADIATION

The shortwave radiative balance is given by:

$$R_s = R_{sd} - R_{su}$$

Where the subscript *s*, *d* and *u* mean shortwave, downward and upward, respectively (Fig. 10.1). Both variables R_{sd} and R_{su} are partitioned in contributions coming from canopy and bare soil fractions, indicated with the subscripts *v* and *g*, respectively. Each of them can be covered by snow or not (snow is indicated with the subscript *sn*). We have the following relationships:

$$G = R_{sfd} + R_{sgd} + R_{sfsnd} + R_{sgsnd}$$

$$R_{su} = R_{sfu} + R_{sgu} + R_{sfsnu} + R_{sgsnu}$$

$$R_{sfd} = G f_v (1 - Sn_f)$$

$$R_{sgd} = G (1 - f_v)(1 - Sn_g)$$

$$R_{sfu} = G f_v \alpha_v (1 - Sn_f)$$

$$R_{sgu} = G (1 - f_v) \alpha_g (1 - Sn_g)$$

$$R_{sfsnd} = G f_v Sn_f$$

$$R_{sfsnu} = G f_v \alpha_v Sn_f$$

$$R_{sgsnd} = G (1 - f_v) Sn_f$$

$$R_{sgsnu} = G (1 - f_v) \alpha_g Sn_g$$

Where G is the incoming solar shortwave radiation, f_v is the vegetated fraction (also called vegetation cover), Sn_f is the fraction of vegetation covered by snow, Sn_g is the fraction of bare soil covered by snow, and α is the specific surface albedo

(see section 3.4.). Fig. 10.1 shows a useful scheme that represents the shortwave radiative fluxes occurring between soil and atmosphere.

The amount of incident solar global radiation G can be given to UTOPIA as input, but UTOPIA could also calculate it by modulating the clear sky radiation evaluated using specific schemes, discussed in section 3.2., by means of the values of total and low cloud cover. The evaluation of clear sky radiation depends on the Earth's orbit, the optical mass and the thickness of the crossed air (see section 3.2), and is evaluated also considering the tilt of the surface (see section 3.2.1.).

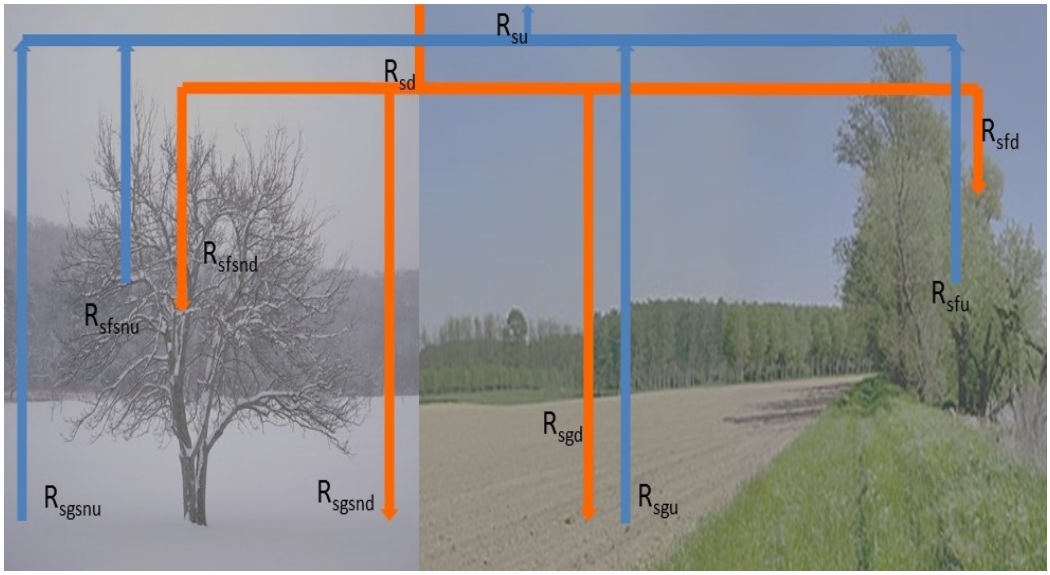

Figure 3.2: Shortwave radiation components; red arrows indicate downward radiation, while blue arrows indicate upward radiation.

3.2. THE INCOMING (SOLAR) SHORTWAVE RADIATION

This formulation is used only if the observed values of solar radiation are unavailable. The global solar radiation on the specified site is calculated taking into account the period of the year and the observed cloudiness (Page (1986)). The following variables are used: the Julian day J, the latitude ϕ, the longitude λ (used in the section 3.2.1), the summer time code C_{leg}, the pressure p, the coefficient R (used in the formulation of the turbidity factors), and the low (C_{nl}) and total (C_n) cloud cover.

At a first stage, the routine SOLAR_ANGLE calculates the solar angle γ (section 3.2.1). Subsequently, the direct and diffuse components of solar radiation are calculated. The direct radiation (R_{im}) has three distinct components: the clear sky one (R_{im0}) and those relative to the fractions of low (R_{iml}) and middle-high (R_{iml}) clouds:

$$R_{im} = R_{imh} + R_{iml} + R_{imo}$$

They are defined as:

$$R_{imh} = C_{nh} \exp(-\alpha_h C_{nh}) R_{ic}$$

$$R_{iml} = C_{nl} \exp(-\alpha_l C_{nl}) R_{ic}$$

$$R_{im0} = (1 - C_{nh} - C_{nl}) R_{ic}$$

The direct clear sky radiation is given by:

$$R_{ic} = K_d R_{i0} \exp[-\Delta r m T_l(\gamma)]$$

Where $R_{i0} = 1367\, W\, m^{-2}$ is the solar constant, i.e. the solar radiation at the top of the atmosphere, and

$$K_d = 1 + 0.03344 \cos(J' - 2.8)$$

is the correction due to the eccentricity of the earth orbit (elliptic). Here J' is the day angle, given by:

$$J' = J_{day}\frac{360}{365}$$

With J_{day} the Julian day. Finally, m is the relative optical air mass crossed by the solar radiation:

$$m = \frac{p}{1013.25}\frac{1}{\sin(\gamma) + 0.15(\gamma + 3.885)^{-1.253}}$$

And Δr is the Rayleygh optical thickness per unit of m :

$$\Delta r = \frac{1}{0.9\,m + 9.4}$$

The second air mass Linke turbidity factor T_{2L} is evaluated as:

$$T_{2L} = 22.76 + 0.0536\,\phi - 27.78\left(0.69051 + 0.00193\,\phi + R\right)$$

Ranging between 0 and 1, is used to define the Linke turbidity factor $T_L(\gamma)$ as:

$$T_L(\gamma) = \begin{cases} T_{2L} - [0.85 - 2.25\sin(\gamma).1.11\sin(\gamma)^2] & if\ T_{2L} \geq 2.5 \\ T_{2L} - [0.85 - 2.25\sin(\gamma).1.11\sin(\gamma)^2]\dfrac{T_{2L} - 1}{1.5} & if\ T_{2L} < 2.5 \end{cases}$$

The diffuse radiation at the top of the atmosphere is evaluated as:

$$R_{iabs} = R_{i0}K_d(1 - Q_{AM})$$

And is corrected for the earth elliptic orbit (K_d) and the atmosphere trasmissivity (Q_{AM}), the latter given by:

$$Q_{AM} = A_X\left[0.506 - 0.010788\ T_L(\gamma)\right]$$

Where:

$$A_A = \sum_{i=1}^{6} A_i\gamma^{(i-1)}$$

And A_i coefficients are defined in Page (1986) on the basis of experimental fits.

The total diffuse radiation includes two components: one ($R_{d,clear}$) relative to clear sky and the other ($R_{d,cloud}$) relative to the cloudy sky. Moreover:

$$R_{d,clear} = 0.5\left[R_{i0}K_d - R_{ic} - R_{iabs}\right]\sin\gamma$$

$$R_{d,cloud} = K_d\left(2.61 + 182.6\sin\gamma\right)$$

And they may be combined as:

$$R_{dm} = \left[\left(1 - C_n\right)R_{d,clear} + C_n R_{d,cloud}\right]$$

In conclusion, the global solar radiation can be expressed as:

$$G = R_{\mathrm{im}}\sin\gamma + R_{dm}$$

3.2.1. The solar angle over tilted surfaces

The complete formula for the solar angle for a tilted surface, reported in Allen et al. (2006) is:

$$\begin{aligned}\cos(\theta) = {} & \sin\delta\sin\phi\cos s - \sin\delta\cos\phi\sin s\cos\gamma + \\ & + \cos\delta\cos\phi\cos s\cos\omega + \cos\delta\sin\phi\sin s\cos\gamma\cos\omega + \\ & + \cos\delta\sin\gamma\sin s\sin\omega\end{aligned} \tag{3.1}$$

That, by putting $s = \gamma = 0$ (horizontal surface), simplifies in:

$$\cos(\theta_{hor}) = \sin\delta\sin\phi + \cos\delta\cos\phi\cos\omega \tag{3.2}$$

Where θ is the solar angle, δ is the declination of the Earth (positive during northern hemisphere summer), ϕ the latitude of the site (positive for the northern hemisphere and negative for the southern hemisphere), s the surface slope (where $s = 0$ for horizontal and $s = \pi/2$ radians for vertical slope; s is always positive and

represents the slope in any direction), and γ is the surface aspect angle (where $\gamma=0$ for slopes oriented due South, $\gamma=-\pi/2$ radians for slopes oriented due East, $\gamma=\pi/2$ radians for slopes oriented due West, and $\gamma=\pm\pi$ radians for slopes oriented due North). The parameter ω is the hour angle, where $\omega=0$ at solar noon, $\omega<0$ in the morning, and $\omega>0$ in the afternoon.

The hourly solar angle ω is defined in function of the apparent local time $T[hours]$ as:

$$\omega=15(T-12)$$

To evaluate the apparent local time T from the actual one $t[hours]$, the method used determines the mean longitude λ_{st} of the Earth segment of amplitude 15° (in longitude) in which the specific site is located:

$$T=t-C_{leg}-E_t+\left(\frac{\lambda-\lambda_{st}}{15°}\right)$$

Where λ is the longitude of the site and C_{leg} the summer time code or, more generally, the difference of time between local time and Greenwich meridian time.

This value is needed for evaluating the equation of time (in hours), which includes a correction due to the difference between terrestrial and sidereal day:

$$E_t=-0.128\sin(d_a-2.8)-0.165\sin(2d_a+19.7)$$

In which d_a is the day angle, evaluated from the Julian day J_{day} as:

$$d_a=\frac{360\,J_{day}}{365.25}$$

The Earth declination is instead given by:

$$\delta=\arcsin\left\{0.3978\sin[d_A-80.2+1.92\sin(d_a-2.8)]\right\}$$

It is possible to reconstruct the radiation incident on a tilted surface by combining the parameterization of Page (1986) with the method proposed by Allen et al. (2006). This method, in fact, allows to modify the radiation observed or modeled over a horizontal surface.

The ratio of expected direct beam radiation on the slope to direct beam radiation on the horizontal surface F_b is evaluated as:

$$F_b = \frac{\cos\theta}{\cos\theta_{hor}}$$

Where the cosines have been previously evaluated using the formulation for tilted (eq. 3.1) and horizontal (s=γ=0: eq. 3.2) surface.

The theoretical solar global radiation $R_{A,hor}$ on a horizontal surface is given by:

$$R_{A,hor} = \frac{G_{SC}\cos\theta_{hor}}{d^2}$$

To compute the radiation over a tilted surface, some further variables are needed. The actual atmospheric transmissivity (direct plus diffuse) for the horizontal surface is:

$$\tau_{swh} = \frac{R_{sw,hor}}{R_{A,hor}}$$

The clearness index for direct beam radiation for horizontal surface is:

$$K_{B,hor} = \begin{cases} 1.56\,\tau_{swh} - 0.55 & if\ \tau_{swh} \geq 0.42 \\ 0.016\,\tau_{swh} & if\ \tau_{swh} \leq 0.175 \\ 0.022 - 0.280\,\tau_{swh} + 0.828\,\tau_{swh}^2 + 0.765\,\tau_{swh}^3 & if\ 0.175 < \tau_{swh} < 0.42 \end{cases}$$

While the clearness index for diffuse beam radiation on horizontal surface is:

$$K_{D,hor} = \tau_{sw,hor} - K_{B,hor}$$

The ratio between diffuse radiation on a tilted surface vs diffuse radiation on a flat surface (using the isotropic hypothesis) is given by:

$$F_i = 0.75 + 0.25 \cos s - \frac{s}{360}$$

And finally the ratio between diffuse radiation on a tilted surface vs diffuse radiation on a flat surface (still using the isotropic hypothesis) is given by:

$$F_{ia} = (1 - K_{B,hor}) \left[1 + \sqrt{\frac{K_{B,hor}}{K_{B,hor} + K_{D,hor}}} \sin\left(\frac{s}{2}\right)^3 \right] F_i + F_B K_{B,hor}$$

Finally, the solar global radiation on tilted surface R_s can be evaluated starting from the one referred to horizontal surface $R_{sm,hor}$:

$$R_s = R_{sm,hor} \left[\frac{F_B K_{B,hor}}{\tau_{swh}} + \frac{F_{ia} K_{D,hor}}{\tau_{swh}} + \alpha (1 - F_i) \right]$$

Considering that it is important to evaluate the projection of such radiation in the vertical direction, we obtain:

$$R_{sp} = \frac{R_s}{\cos s}$$

3.3. LONGWAVE RADIATION

The downward longwave radiation could be an observation and thus be part of the input dataset. In this case, the UTOPIA do not evaluate it, but simply takes the input datum.

In the case in which the longwave radiation is not available, UTOPIA estimates it using an empirical formulation (Mutinelli (1998)):

$$R_{ld} = \epsilon_a \sigma T_a^4$$

In which the atmospheric emissivity ϵ_a is parametrized in function of the atmospheric cloudiness C_n , the possible presence of fog and the air humidity, according with the espression (Brutsaert (1982)):

$$\epsilon_a = [1 + 0.22\, C_n^2 + 0.22(1 - C_n^2)\, F_{haze}]\, 0.67\, [1670\, q_a]^{0.08}$$

Where F_{haze} is a function accounting for the presence of haze (section 3.3.1).

Since the vegetation, being composed in large part by water, is also able to emit radiation in the longwave band, the scheme is a bit more complicated than in the case of the shortwave radiation, as there are additional terms of exchange between vegetation and soil. Looking at Fig. 오류: 참조 소스를 찾을 수 없습니다., at which we refer for the meaning of symbols used, different contributions are visible; these should be considered separately in the budget. Note that, in agreement with the literature, the emissivity ϵ is used instead of albedo α , being $\epsilon = 1 - \alpha$ (in the radiation bands typical of atmospheric processes, transmissivity can be neglected).

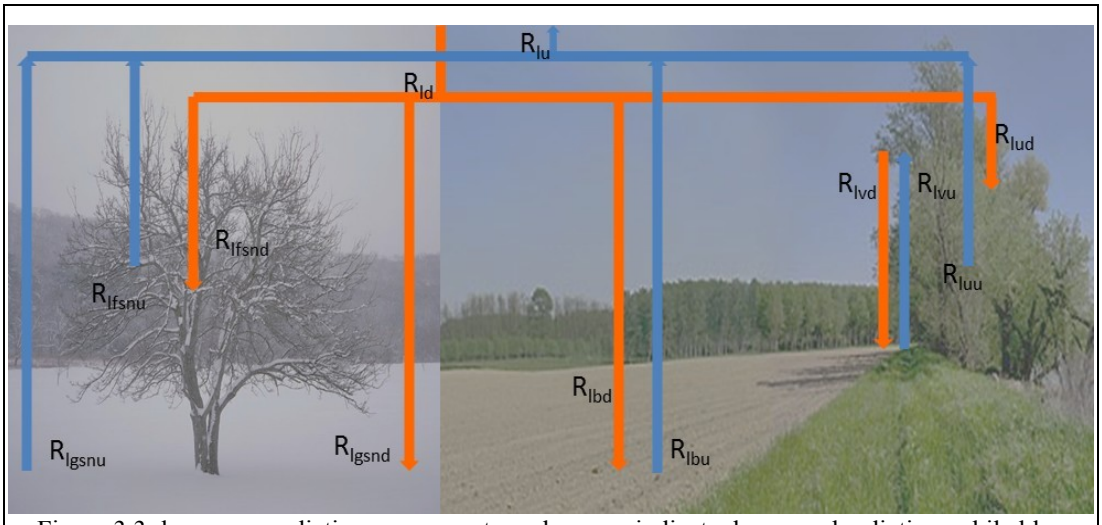

Figure 3.3: longwave radiation components; red arrows indicate downward radiation, while blue arrows indicate upward radiation.

The downward and upward longwave radiation above snowless vegetation are:

$$R_{lud} = R_{ld}\, f_v (1 - Sn_f)$$

$$R_{luu} = f_v (1 - Sn_f)\, \epsilon_f \sigma T_f^4 + (1 - \epsilon_f)\, R_{lud}$$

The downward and upward longwave radiation above snowless bare soil are:

$$R_{lbd} = (1 - f_v)(1 - Sn_g)\, R_{ld}$$

$$R_{lbu} = (1 - f_v)(1 - Sn_g)\, \epsilon_g \sigma T_1^4 + (1 - \epsilon_g)\, R_{lbd}$$

The downward and upward longwave radiation in the vegetation-bare soil space, without snow, are respectively given by ("d" means from vegetation to bare soil, and "u" vice versa):

$$R_{lvd} = f_v \frac{\epsilon_f \sigma T_f^4 + (1 - \epsilon_f)\epsilon_g \sigma T_1^4}{\epsilon_f + \epsilon_g - \epsilon_f \epsilon_g}$$

$$R_{lvd} = f_v \frac{\epsilon_g \sigma T_1^4 + (1 - \epsilon_g)\epsilon_f \sigma T_f^4}{\epsilon_f + \epsilon_g - \epsilon_f \epsilon_g}$$

The downward and upward longwave radiation from/to snowless bare soil are:

$$R_{lgd} = R_{lbd} + R_{lvd}$$

$$R_{lgu} = R_{lbu} + R_{lvu}$$

The net downward radiation on vegetation without snow (downward incident radiation from top minus downward emitted radiation from bottom) is:

$$R_{lfd} = R_{lud} - R_{lvd}$$

While the upward counterpart is given by:

$$R_{lfu} = R_{luu} - R_{lvu}$$

Regarding snow, the total upward longwave radiation emitted from snow is:

$$R_{ls} = \epsilon_{sn} \sigma T_{sn}^4 + (1 - \epsilon_{sn})\, R_{ld}$$

The downward and upward longwave radiation on snowy vegetation are given respectively by:

$$R_{lfsnd} = f_v Sn_f R_{ld}$$

$$R_{lfsnu} = f_v Sn_f R_{ls}$$

The downward and upward longwave radiation on snowy bare soil is:

$$R_{lgsnd} = (1 - f_v) Sn_g R_{ld}$$

$$R_{lgsnd} = (1 - f_v) Sn_g R_{ls}$$

The total downward longwave radiation incident on snow is given by:

$$R_{lsnd} = R_{lfsnd} + R_{lgsnd}$$

while the total upward longwave radiation emitted by snow is given by:

$$R_{lsnu} = R_{lfsnu} + R_{lgsnu}$$

The total longwave radiation emitted from the surface (includes snow, vegetation and bare soil) is:

$$R_{lu} = R_{luu} + R_{lbu} + R_{lsnu}$$

3.3.1 The haze parameterization

The explicit parametrization of the haze was originally introduced in Cassardo et al. (1995) to obviate the too low values of net radiation predicted by the model in the Po valley during nighttime. The successive modifications introduced in Mutinelli (1998) altered only the shape of the formulas used. The haze event is parametrized on the basis of the values assumed by the following variables: relative humidity $RH[\%]$, horizontal wind speed $v[m\,s^{-1}]$, and solar global radiation $G[W\,m^{-2}]$. The

calculation assigns a value to the probability of haze formation on the basis of three factors:

a) relative humidity: the haze can form if relative humidity exceed a certain threshold RH_{min} (that should be lower than 96%):

$$F_1 = \begin{Bmatrix} 0 & if\ RH < RH_{min} \\ \sqrt{\dfrac{RH - RH_{min}}{RH_{max} - RH_{min}}} & if\ RH \geq RH_{min} \end{Bmatrix}$$

b) horizontal wind speed: the haze will form with a sinusoidally increasing probability if wind is blowing below a certain threshold v_{max} and its formation will not have restrictions if wind speed is lower than v_{min} :

$$F_2 = \begin{Bmatrix} 0 & if\ v \geq v_{max} \\ 0.5[1 + \cos(180° \dfrac{v - v_{min}}{v_{max} - v_{min}})] & if\ v_{min} < v < v_{max} \\ 1 & if\ v \leq v_{min} \end{Bmatrix}$$

c) solar global radiation: above a certain value of solar radiation, haze is assumed as impossible, while there will not be restrictions when solar radiation is null (i.e. during nighttime):

$$F_3 = \begin{Bmatrix} 0 & if\ G \geq G_{max} \\ 0.5[1 + \cos(180° \dfrac{G - G_{max}}{G_{max}})] & if\ 0 < G < G_{max} \\ 1 & if\ G \leq 0 \end{Bmatrix}$$

The various parameters are experimental thresholds that depend on the observation site. For instance, for the central Po valley, it has been suggested $v_{min} = 2\, m\, s^{-1}$ and $v_{max} = 5\, m\, s^{-1}$, $G_{max} = 100\, W\, m^{-2}$, $RH_{min} = 84$ and $RH_{max} = 96$.

The haze function can thus be evaluated as:

$$F_{haze}=0\le(F_1 F_2 F_3)\le 1$$

And F_{haze} represents the probability that haze can form.

3.4. CALCULATION OF SURFACE ALBEDO

A specific routine has been dedicated in UTOPIA to the evaluation of the surface albedo. The input variables needed are the following: the mean vegetation albedo α_{ffh}, the dry soil albedo α_{sdmax}, the water albedo $\alpha_w(=0.14)$, the saturation ratio of the first soil layer q_1, the actual time t, the latitude ϕ and the longitude λ of the location. The variables calculated are: the soil albedo α_s, the vegetation albedo α_v, the snow albedo α_{sn} and the total albedo α_{tot}. The soil, vegetation and snow albedo are calculated in function of the day of the year and of the hour of the day. The bare soil albedo α_g is calculated as sum of two components:

$$\alpha_g=\alpha_h+\alpha_z-0.03 \tag{3.3}$$

Where the numerical value *0.03* represents a rough estimate of the α_z daily mean value. The former (α_h), specific of the soil type, depends on the relative humidity in the first soil layer q_1 and on its temperature T_1 according with the formula:

$$\alpha_h=\begin{cases}\alpha_w & if\ q_1\ge 0.5 \text{ and } T_1>0\,^\circ C\\ \alpha_{sdmax}-(\alpha_{sdmax}-\alpha_w)q_1 & if\ q_1<0.5 \text{ and } T_1>0\,^\circ C\\ \alpha_{sdmax} & if\ T_1\le 0\,^\circ C\end{cases}$$

Where α_w is the albedo of water. On the contrary, the second one (α_z), used for all albedoes during daytime, is a function of the solar angle γ according with the formulation:

$$\alpha_z = \begin{cases} 0 & if\ \gamma \le 3° \\ \dfrac{\exp[0.003286(90° - \gamma)^{1.5} - 1]}{100} & if\ \gamma > 3° \end{cases}$$

The vegetation albedo α_v is given by:

$$\alpha_v = \alpha_{vh} + \alpha_z - 0.03 \tag{3.4}$$

Where the numerical value *0.03* represents a rough estimate of the α_z daily mean value, as in eq. 3.3, and where α_{vh} is the characteristic vegetation albedo.

The snow albedo α_{sn} is calculated only in presence of snow. Its value varies between a maximum value α_{snmax} (fresh snow) and a minimum value $\alpha_{sn,min} = 0.50$ (old or dirty snow). The former is not assumed as fixed, but varies according with the snow temperature:

$$\alpha_{snmax} = \alpha_{sn0} + 0.05 \frac{T_m - T_{sn}}{10}$$

With $\alpha_{sn0} = 0.85$ and where the fraction must be limited in the range 0-1: in this way, the maximum value varies in the range 0.80÷0.85. These extreme values are in agreement with the literature (see for instance Dingman (1994)). There are several parameterizations of snow albedo in literature: see for instance Robinson and Kukla (1984), Verseghy (1991), Douville et al. (1995), and Sun et al. (1999). In UTOPIA, snow albedo is initialized to the maximum value in occasion of the first snowfall, and then it is parametrized as decreasing to take into account the smoke deposition and other

processes. The parameterization actually set in UTOPIA is a mix of the schemes proposed by Douville et al. (1995) for the French LSM ISBA (some numerical values refer to Verseghy (1991)) and that of Sun et al. (1999). In particular, the distinction is between deep and shallow snowfall, and the discriminating factor is $h_s = 0.2\,m$. Albedo of deeper snow decreases exponentially with time, while shallower snow amount has a linear, smoother, decay of albedo, with a rate depending on the snow temperature. More specifically:

$$\alpha_{sn0} = \begin{cases} \alpha_{sn,min} + (\alpha_{sn} - \alpha_{sn,min}) \exp\left(\frac{\tau_f \Delta t}{\tau_1}\right) & if\ h_{sn} > 0.2 \\ \alpha_{sn} - \frac{\tau_a \Delta t}{\tau_1} & if\ h_{sn} \le 0.2 \end{cases}$$

Where the experimental parameters are: $\tau_f = 0.24$ and $\tau_1 = 86400\,s$ and where:

$$\tau_a = \begin{cases} 0.071 & if\ T_{sn} = T_m \\ 0.006 & if\ T_{sn} < T_m \end{cases}$$

In the exponential decay of albedo, the time needed for albedo to change from its maximum value $\alpha_{sn} = \alpha_{snmax}$ to its minimum value $\alpha_{sn} = \alpha_{snmin}$, in absence of snowfalls and other phenomena, is about 10 days. This formulation has proven to behave in a very satisfactory way in Siberian environment (experiment RUSWET: Robock et al. (1995)).

In case of fresh snowfall above pre-existing snow cover, we assume that, if the fresh snowfall $(P_{sn} \Delta t)$ exceeds the empirical threshold $(h_{snwhite} = 10^{-5} m)$ (snow at the ground surface, expressed in units of water equivalent), the snow albedo is completely refreshed and set to its maximum value (α_{snmax}) (Dingman (1994)); otherwise the snow albedo is calculated as the weighted average of fresh and old snow albedoes:

$$\alpha_{sn0}=\begin{cases}\alpha_{sn,max} & if\ \Delta t\ P_{sn}\geq P_{sn,white}\\ \alpha_{sn,max}P_{sn}\Delta t+\alpha_{sn0}\dfrac{P_{sn,white}-P_{sn}\Delta t}{P_{sn,white}} & if\ \Delta t\ P_{sn}<P_{sn,white}\end{cases}$$

The values calculated using the above equation represent the daily mean albedo; during daytime, the contribution due to solar elevation (Mc Cumber (1980)) is also considered, using a formulation similar to that for the bare soil (eq. 3.3) or vegetation (eq. 3.4):

$$\alpha_{sn}=\alpha_{sn0}+\alpha_z-0.03$$

The total albedo is evaluated as the weighted average of the bare soil, vegetation and snow albedoes, according with the expression:

$$\alpha_{tot}=Sn\,\alpha_{sn}+(1-Sn)[f_v\alpha_v+(1-f_v)\alpha_g]$$

Where Sn is the snow fraction.

3.5. NET RADIATION

Net radiation at the surface is the sum of the net solar (shortwave, suffix '*s*') and terrestrial-atmospheric (longwave, suffix '*l*') radiation (according to Deardorff (1978) and Mc Cumber (1980)), given in each case by the difference between incident (downward, suffix '*d*') and upward (suffix '*u*') radiation. It is also possible to evaluate separately the budgets for vegetation and bare soil components:

$$\begin{aligned}R_n&=(R_{sd}-R_{su})+(R_{ld}-R_{lu})\\ R_{nf}&=(R_{sfd}-R_{sfu})+(R_{lfd}-R_{lfu})\\ R_{ng}&=(R_{sgd}-R_{sgu})+(R_{lgd}-R_{lgu})\\ R_{nsn}&=(R_{ssnd}-R_{ssnu})+(R_{lsnd}-R_{lsnu})\end{aligned}\qquad(3.5)$$

4. Energy balance

The zonal and meridional momentum fluxes τ_x and $\tau_y [kg\, m^{-1} s^{-2}]$, the sensible heat flux SH and $LH [W\, m^{-2}]$ and the water vapor flux $E [kg\, m^{-2} s^{-1}]$ between the atmosphere at the reference height(*) and the surface are described using the analog electric scheme, by means of appropriate resistances or conductances. Over bare soil, their expression is simple:

$$\tau_x = -\rho_a s_{am} (u_a - u_s)$$

$$\tau_y = -\rho_a s_{am} (v_a - v_s)$$

$$SH_g = \rho_a c_p s_d (\theta_a - \theta_1)$$

$$E_g = \rho_a s_s [q_a - f_h q_s (T_1)]$$

Where u and v are zonal and meridional horizontal wind speed components, respectively, θ is the potential temperature, q the specific humidity, $q_s(T)$ the saturate specific humidity at temperature T , ρ_a the air density, $c_p = 1003\, J\, kg^{-1} K^{-1}$ the specific heat of dry air at constant pressure, f_h is the relative humidity of soil surface, and $s [m\, s^{-1}]$ indicate the appropriate conductance for every flux, defined as the inverse of the appropriate resistance $r [s\, m^{-1}]$ (their expression will be specified in section 4.7.). Here the suffix '*a*' refers to the height z_a above the soil surface, while the suffix '*1*' refers always to the soil surface. Note that, for the temperature, the surface temperature is approximated by the soil temperature of the

* The reference height is the height at which the atmosphere interacts with the land surface, including vegetation canopy.

first layer T_1 , while, for the humidity, there is the function f_h (humidity factor) accounting for the difference with respect to the true humidity.

These fluxes, used also for water and ice surfaces, are derived from the Monin-Obukhov similarity theory applied to the surface layer (constant flux layer), as described by Brutsaert (1982) and Arya (1988). In this derivation, surface wind velocity components are null ($u_s = v_s = 0$) because they refer to the height $z_{0\mathrm{gm}}$. r_{am} is the aerodynamic resistance for momentum between the atmosphere in the layer between z_a and the surface at the height $z_{0\mathrm{gm}}$. Likewise, the surface temperature θ_g and specific humidity q_g are defined at the heights $z_{0\mathrm{gh}}$ and $z_{0\mathrm{gw}}$, respectively. Consequently, r_{ah} and r_{aw} are the aerodynamic resistances to sensible heat and water vapor transfer between the atmosphere in the layers between the height z_a and the surface, at the heights $z_{0\mathrm{gh}}$ and $z_{0\mathrm{gw}}$, respectively.

A portion of the routine FLUXES (in which most calculations reported in this section are performed) is dedicated to carry out some quality control checks in such a way to force UTOPIA to continue its run even when numerical errors are present, by artificially limiting the value of such fluxes. 4.1. The current limit is set to 1000 W m^{-2}.

4.1. MOMENTUM FLUX

If vegetation is present, the situation is more complicated. Both vegetation and bare soil emit fluxes from their active surface to a level within the canopy, indicated by the suffix '*af*'. The momentum flux is evaluated between the reference level z_a and this level z_{af} :

$$\tau_x = \rho_a \overline{(u'w')} = -\rho_a s_{am} (u_a - u_{af}) \simeq -\rho_a s_{am} u_a$$

$$\tau_y = \rho_a \overline{(v'w')} = -\rho_a s_{am} (v_a - v_{af}) \simeq -\rho_a s_{am} v_a$$

Aerodynamic resistances and conductances are defined as above, however the layer is bounded below by the level $z_{0m} + d$, d being the zero displacement height.

The friction velocity u_* is then evaluated as:

$$u_* = \sqrt{\overline{(u'w')} + \overline{(v'w')}}$$

For convenience, in UTOPIA actually u_{af} and v_{af} are considered null in the above formulations for momentum tensor.

4.2. SENSIBLE HEAT FLUXES

For the bare soil fraction, the sensible heat flux SH is indicated by the suffix '*g*'. For the vegetated part, f_v being the vegetation cover, the flux is indicated by the suffix '*f*'. The surface temperatures θ_1 and θ_f are defined at the heights z_{0gh} and $z_{0h} + d$, respectively. Consequently, $r_b(s_b)$ and $r_d(s_d)$ are the appropriate resistances (conductances) to sensible heat transfer to the atmosphere in the layers between the height z_a and the respective surface, at the heights $z_{0h} + d$ and z_{0gh} , respectively. The heat capacity of air $c_p [J\, kg^{-1} K^{-1}]$ is assumed constant $(1003\, J\, kg^{-1} K^{-1})$.

In the case in which there is snow, two additional sensible heat fluxes, from the snowy bare soil fraction Sn_g and the snowy vegetated fraction Sn_f , are present.

For vegetated surfaces, the surface temperatures θ_1 and θ_f are defined at the heights z_{0gh} and $z_{0h} + d$, respectively. Consequently, $r_b(s_b)$ and $r_d(s_d)$ are the appropriate resistances (conductances) to sensible heat transfer to the atmosphere in the layers

between the height z_a and the respective surface, at the heights $z_{0h}+d$ and z_{0gh}, respectively. The heat capacity of air $c_p[J\,kg^{-1}K^{-1}]$ is assumed constant $(1003\,J\,kg^{-1}K^{-1})$.

The vegetated fraction emits the sensible heat flux:

$$SH_f=\rho_a c_p s_b(\theta_f-\theta_{af}) f_v(1-Sn_f)$$

While the bare soil emists the following heat flux:

$$SH_g=\rho_a c_p s_d(\theta_1-\theta_{af})(1-f_v)(1-Sn_g)$$

In presence of snow, the snowy vegetated and bare soil fractions emit the flux:

$$SH_{snf}=\rho_a c_p s_{dsn}(\theta_{sn}-\theta_{af}) f_v Sn_f$$

$$SH_{sng}=\rho_a c_p s_{dsn}(\theta_{sn}-\theta_{af})(1-f_v) Sn_g$$

Which can be sumarized in the total sensible heat flux from snow:

$$SH_{sn}=SH_{snf}+SH_{sng}$$

The total flux from the surface layer is:

$$SH_a=SH_f+SH_g+SH_{sn}$$

The discussion is a bit different for the following types of land use: ice (soil code: 12), water (14 or 15), dense settlement (20), asphalt and concrete (27 and 28). In these cases, since there is not vegetation on the ground ($f_v=0$), thus the terms related to the vegetation (SH_f, Sn_f) are set to zero. In this case, the scheme simplifies as there are only two components: the layer above the soil and the soil surface. In the first case (condensation), it will occur independently on the presence of a dry and wet component of the soil, thus:

$$SH_g=\rho_a c_p s_d[\theta_1-\theta_a](1-Sn_g)$$

Regarding the snow, since vegetation is absent there, then $SH_{snf}=0$. Over water surfaces (soil codes 14 and 15) it is assumed that snow will not be present, thus also $SH_{sng}=0$ and thus $SH_{sn}=0$. Over ice and other surfaces, snow can be present over the terrain. In this case:

$$SH_{sn}=SH_{sng}=\rho_a c_p s_{ah}[\theta_{sn}-\theta_a]Sn_g$$

4.3. EVAPOTRANSPIRATION FLUXES

The word *evapotranspiration* is composed by the contraction of *evaporation* and *transpiration*, which are two distinct processes. The former occur when liquid water over the soil (or within its upper few millimeters) or vegetation surfaces change phase becoming water vapor, and this phenomenon is regulated almost exclusively by the atmospheric conditions (for the water evaporating by the soil, also from the soil moisture conditions). The latter, instead, is the process with which the vegetation extracts liquid water by the soil root zone and, through a series of complicated internal mechanisms, emits in the atmosphere through the stomata. The calculation of the evapotranspiration thus depends on the type of soil and the concentration of water vapor with respect to the considered surface.

A single leaf can simultaneously evaporate and transpire. The evaporation can occur from its eventual wet fraction (in the case in which a fraction of the leaf is covered by water), while the transpiration can occur from the remaining dry part. Thus, it is necessary to introduce a variable accounting for the fraction of vegetation wet; this is R_f , the wet fraction of the vegetation, defined as the ratio between the wet area of the leaves and their total area.

In the following equations, r_b and r_d , as in the case of the sensible heat flux, are the appropriate resistances to evaporation flux to the atmosphere in the layers between the height z_a and the respective surface, at the heights $z_{0v}+d$ and z_{0gv} , respectively. However, since the evaporation and transpiration processes will be constrained by the conditions of the respective surface (bare soil or vegetation), each flux is subject to an additional resistance: the soil resistance r_{soil} and the canopy resistance r_f . Likewise, the humidity of the soil-atmosphere interface q_g , approximated by the expression $f_h q_s(T_1)$, is defined at the height z_{0gv} , while the humidity at the canopy-atmosphere q_f , approximated by the simple expression $q_s(T_f)$, is defined at the height $z_{0v}+d$. In presence of snow, the humidity of the snow surface q_{sn} is approximated by the simple expression $q_s(T_{sn})$ and defined at the height $z_{0sn}+d$.

Also for evaporation fluxes, in the case in which there is snow, the expressions for the fluxes from vegetation and bare soil will include the appropriate snow cover fractions, and two additional sensible heat fluxes, from the snowy bare soil fraction Sn_g and the snowy vegetated fraction Sn_f , are present.

At this point, it is necessary to consider another additional constraint. Evaporation or transpiration can only occur if the water vapor concentration of the evaporating or transpiring component is lower than the saturated water vapor in the atmosphere; otherwise, the water vapor in the atmosphere cannot increase.

For **vegetated surfaces**, regarding the dry portion of the leaves, there is transpiration only when the canopy humidity is larger than the humidity in the air within the vegetation, i.e. if $q_s(T_f) \geq q_{af}$ and if the mean root zone temperature is above 0°C

($T_s \geq 0\,°C$). In this case, the transpiration (which means the water extracted from roots) occur only from the dry part of the canopy at the rate given by:

$$E_{trtot} = \rho_a s_{fdry} [q_s(T_f) - q_{af}] f_v (1 - Sn_f) \quad if\ q_s(T_f) \geq q_{af} \text{ and } T_s \geq 0\,°C$$

The evaporation from the wet part of the vegetation is given by:

$$E_{fw} = \rho_a s_{fwet} [q_s(T_f) - q_{af}] f_v (1 - Sn_f) \qquad if\ q_s(T_f) \geq q_{af}$$

And is independent on the mean root zone temperature.

In the case in which $q_s(T_f) < q_{af}$, there will be condensation over the leaves, preferentially on their upper side, and this process does not involve the canopy resistance:

$$E_{fw} = \rho_a \frac{s_b}{2} [q_s(T_f) - q_{af}] f_v (1 - Sn_f) \qquad if\ q_s(T_f) < q_{af}$$

Where the factor "2" in the conductance accounts for the fact that the condensation will occur only on the upper part of the leaves, and where the only difference with respect to the previous equations is in the conductance involved.

The total evapotranspiration from the vegetation will be thus given by:

$$E_f = E_{trtot} + E_{fw}$$

The total transpiration is shared among the soil layers in the root zone using the variable $RP_{total,i}$, which accounts on the percentage of roots in each soil layer:

$$E_{tr,i} = \begin{cases} RP_{total,i} E_{trtot} & if\ T_s > 0\,°C \\ 0 & if\ T_s \leq 0\,°C \end{cases}$$

Where T_s is the mean temperature in the root zone.

Also for the **bare soil**, it is possible to use a similar method of partition between the wet and dry part of the soil surface. The difference in the conductances will be similar: in case of evaporation, both aerodynamic and soil surface resistances will act, while in case

of condensation, only the aerodynamic resistance will be involved. The formulations will thus be:

$$E_{gdry}=\rho_a s_{gdry}[f_h q_s(T_1)-q_{af}](1-f_v)(1-Sn_g)$$

$$E_{gwet}=\rho_a s_{gwet}[f_h q_s(T_1)-q_{af}](1-f_v)(1-Sn_g)$$

In case of evaporation, with the total evaporation from the bare soil surface:

$$E_g=E_{gdry}+E_{gwet}$$

And:

$$E_g=\rho_a s_d[f_h q_s(T_1)-q_{af}](1-f_v)(1-Sn_g)$$

In case of condensation.

Regarding the snowy portions of vegetation and bare soil, evaporation rates are:

$$E_{snf}=\rho_a s_{ssn}[q_s(T_{sn})-q_{af}]f_v Sn_f$$

$$E_{sng}=\rho_a s_{ssn}[q_s(T_{sn})-q_{af}](1-f_v)Sn_g$$

$$E_{sn}=E_{snf}+E_{sng}$$

The discussion is a bit different for the following types of land use: ice (soil code: 12), water (14 or 15), dense settlement (20), asphalt and concrete (27 and 28). In these cases, there is not vegetation on the ground, thus terms related to the vegetation (E_{trtot}, E_{fw}, E_f) are set to zero, as also $f_v=0$. In this case, the scheme simplifies as there are only two components: the layer above the soil and the soil surface. Even in this case, according with the proportion of moistures at the soil surface and in atmosphere, there could be condensation or evaporation. In the first case (condensation), it will occur independently on the presence of a dry and wet component of the soil, thus:

$$E_g=\rho_a s_d[f_h q_s(T_1)-q_a](1-Sn_g) \quad if\ f_h q_s(T_1)<q_a$$

In the second case (evaporation), it is possible to divide the soil in dry and wet portions; in the former, evaporation involves also the resistance of the soil, while in the latter, only aerodynamic resistance is involved:

$$E_{gdry}=\rho_a s_{gdry}[f_h q_s(T_1)-q_a](1-Sn_g) \quad if\ f_h q_s(T_1)\geq q_a$$

And the former by:

$$E_{gwet}=\rho_a s_{gwet}[f_h q_s(T_1)-q_{af}](1-Sn_g) \quad if\ f_h q_s(T_1)\geq q_a$$

And the total evaporation from the bare soil surface will be thus given by:

$$E_g=E_{gdry}+E_{gwet}$$

Regarding the snow, since vegetation is absent there, then $E_{snf}=0$. Over water surfaces (soil codes 14 and 15) it is assumed that snow will not be present, thus also $E_{sng}=0$ and thus $E_{sn}=0$. Over ice and other surfaces, snow can be present over the terrain. In this case:

$$E_{sn}=E_{sng}=\rho_a s_d[q_s(T_{sn})-q_a]Sn_g$$

4.4. LATENT HEAT FLUXES

The latent heat flux can be derived from the evaporation flux by multiplying it by the latent evaporation and/or fusion heat $\lambda(T)$ (see section 11.1.), which vary with the temperature T according to the approximate expression $\lambda(T)=A-B(T-T_0)$, where $T_0=273.15\,K$ and A and B are numerical values accounting for evaporation and eventual fusion. Thus, latent heat fluxes LH above bare and vegetated soil, both covered or not by snow, can be expresses as:

$$LH_f=\lambda(T_f)E_f$$

$$LH_g=\lambda(T_1)E_g$$

$$LH_{fsn} = \lambda(T_{sn}) E_{fsn}$$

$$LH_{gsn} = \lambda(T_{sn}) E_{gsn}$$

4.5. TEMPERATURE AND HUMIDITY IN THE CANOPY-AIR SPACE

The sensible heat and evaporation fluxes coming from the soil surface and vegetation combine to give the fluxes to the atmosphere:

$$H_a = H_f + H_g + H_{fsn} + H_{gsn}$$

$$E_a = E_f + E_g + E_{fsn} + E_{gsn}$$

At the same time, these fluxes can also be expressed using the analogue of the Ohm law referred to the levels '*a*' and '*af*':

$$H_a = \rho_a c_p s_{ah} (\theta_a - \theta_{af})$$

$$E_a = \rho_a s_{av} (q_a - q_{af})$$

By equaling the above two expressions, it is possible to calculate the two unknown values at the level '*af*':

$$T_{af} = \frac{T_a s_{ah} + f_v [s_b (1 - Sn_f) T_f + s_d Sn_f T_{sn}] + (1 - f_v) s_d [(1 - Sn_g) T_1 + Sn_g T_{sn}]}{s_{ah} + f_v [s_b (1 - Sn_f) + s_d Sn_f] + (1 - f_v) s_d}$$

$$q_{af} = \frac{q_a s_{ah} + f_v [s_f (1 - Sn_f) q_s(T_f) + s_d Sn_f q_s(T_{sn})]}{s_{ah} + f_v [s_f (1 - Sn_f) + s_d Sn_f] + (1 - f_v)[s_s (1 - Sn_g) + s_d Sn_g]} + \frac{(1 - f_v)[s_s (1 - Sn_g) f_h q_s(T_1) + s_d Sn_g q_s(T_{sn})]}{s_{ah} + f_v [s_f (1 - Sn_f) + s_d Sn_f] + (1 - f_v)[s_s (1 - Sn_g) + s_d Sn_g]}$$

4.6. INTERFACE HEAT FLUXES

Soil and vegetation heat fluxes are given by (respectively):

$$Q_f = R_{nf} - SH_f - LH_f - Q_{rainf} + Q_{snf}$$

$$Q_g = R_{ng} - SH_g - LH_g - Q_{raing} + Q_{sng}$$

Where the direct conductive heat flux produced by the rainfall can be evaluated as:

$$Q_{rainf} = C_w P_f \rho_w (T_a - T_f)$$

$$Q_{raing} = C_w P_g \rho_w (T_a - T_1)$$

In these formulations, $C_{sw} = 4186\, J\, m^{-3}\, K^{-1}$ is the water heat capacity, P_f and P_g are the rainfall rates over vegetation and bare soil, respectively, and $\rho_w = 1000\, kg\, m^{-3}$ is the water density. Regarding interface heat fluxes involving snow, (Q_{snf} and Q_{sng}), they are reported in detail in section 8.3.3.

4.7. RESISTANCES AND CONDUCTANCES

It is possible to represent the differences in the contribution to the resistances that occur taking into account the kind of surface described by the model, and depending if latent or sensible heat flux is considered.

All formulations, whenever not explicitly referenced, are taken by Dai and Zeng (1998). The resistance networks are represented in Figure 10.1.

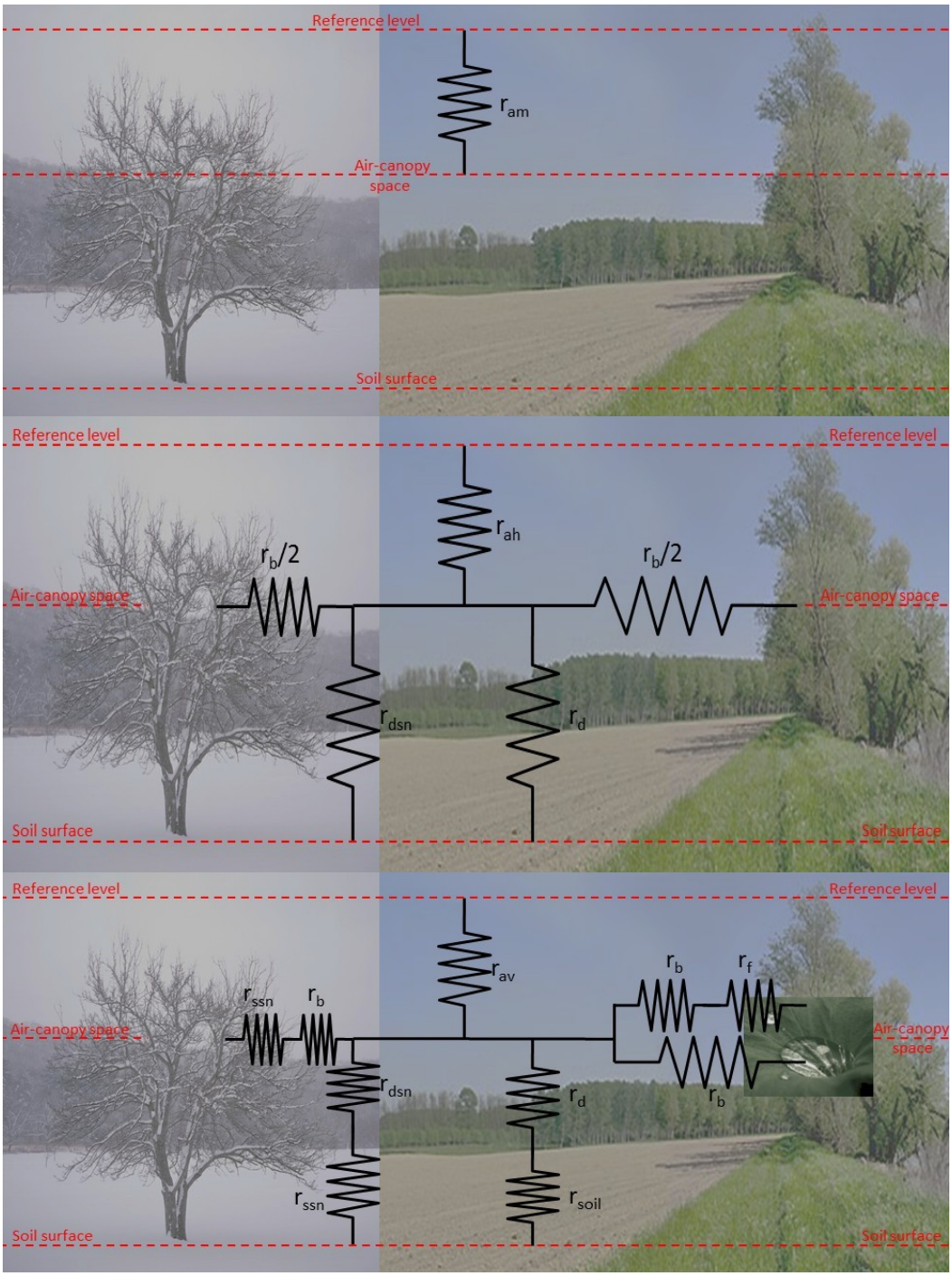

Figure 4.1: The resistance network for momentum (up), heat (middle) and water vapor (bottom) transfers in UTOPIA. Left part of figures refers to snowy conditions, while right part refers to snowless conditions.

Drag coefficients are derived in section 4.8.

Aerodynamic resistances for momentum (suffix '*m*'), heat ('*h*') and water vapor ('*v*') above canopy are respectively calculated as:

$$r_{am} = \frac{1}{C_{Dm} u_a}$$
$$r_{ah} = \frac{1}{C_{Dh} u_a}$$
$$r_{av} = \frac{1}{C_{Dv} u_a}$$

Where the C_{Di} are the appropriate drag coefficients, discussed in section 4.8..

Laminar leaf resistance beneath canopy r_b is calculated as:

$$r_b = \frac{193.0825}{LAI} \sqrt{\frac{d_0}{u_{af}}} \tag{4.1}$$

Following a formulation adapted by Bonan (1996), where d_0 is the second leaf dimension and u_{af} is the wind speed within the canopy, given by the expression:

$$u_{af} = U_a [1 - f_v (1 - \sqrt{C_{Dm}})] \geq 0.5\, m\, s^{-1}$$

Where U_a is the wind speed modulus at the reference level z_a . A minimum threshold of $0.5\, m\, s^{-1}$ for u_{af} is kept.

Aerodynamic resistance beneath canopy r_d over snowless bare soil is calculated according to the Bonan (1996) formulation:

$$r_d = \frac{h_f}{3\, k\, u_* (h_f - d)} [e^{3(1 - \frac{z_{0fh}}{h_f})} - e^{3(1 - \frac{z_{0gh} + d}{h_f})}]$$

Where h_f is the canopy height, u_* the friction velocity, d the zero displacement height, z_{0fh} and z_{0gh} the roughness lengths for heat relative to vegetation and bare soil, respectively, z_a the reference level above the vegetation, and the coefficient '*3*' is experimental.

Aerodynamic resistance beneath canopy r_{dsn} over snowy bare soil is calculated in strict analogy with previous formulation as:

$$r_{dsn}=\frac{h_f}{3\,k\,u_*(h_f-d)}\left[e^{3\left(1-\frac{z_{0sn}}{h_f}\right)}-e^{3\left(1-\frac{z_{0sn}+d}{h_f}\right)}\right]$$

Where z_{0sn} is the roughness lengths for heat relative to the snow.

Resistance to water evaporation from bare soil is calculated for almost every kind of land cover according to Sellers et al. (1992) as:

$$r_{soil}=\mathrm{e}^{8.206-4.255q_1}$$

Where q_1 is the soil moisture (in terms of saturation rate) of first soil layer, and the numbers in the parameterization have been kept equal to the original ones. The only exceptions in terms of land cover are water surfaces and ice, for which $r_{soil}=0$ and $r_{soil}=100\,sm^{-1}$ have been set, respectively.

Canopy resistance is calculated, adapting the proposal of Dickinson (1984), as the combination of five functions, depending on solar radiation, soil moisture, atmospheric humidity (air moisture deficit), atmospheric temperature, and carbon dioxide in the following way:

$$r_f=\frac{1}{LAI}\left(\frac{r_{min}}{F_1F_2F_3F_4}\right) \qquad (4.2)$$

Where $r_{min}[sm^{-1}]$ is the minimum stomatal resistance and *LAI* the Leaf Area Index, and the term in the bracket must be limited to $5000\,sm^{-1}$. The five functions $F_1, F_2, F_3, F_4,$ and F_5 account for the dependence on solar radiation, soil moisture in the root zone, atmospheric water vapor deficit, air temperature, and carbon dioxide concentration, respectively, and are given by:

$$F_1 = \frac{\frac{r_{min}}{5000} + f}{1 + f} \qquad with\ f = \frac{1.1\, R_{sd}}{R_{GL}\, LAI}, \qquad 0 \le F_1 \le 1 \tag{4.3}$$

Which is taken from Dickinson (1984), and where R_{sd} is the shortwave incident radiation, $R_{GL}[W\,m^{-2}]$ the Noilhan parameter (Noilhan and Planton (1989)), which varies according with the vegetation type;

$$F_2 = \frac{q_s - q_{wi}}{q_{fc} - q_{wi}}, \qquad 0.15 \le F_2 \le 1 \tag{4.4}$$

Which is taken from ISBA version (Verseghy (1991)), and where q_{wi} is the wilting point, q_{fc} the field capacity and q_s the root zone soil moisture (all expressed in units of saturation ratio);

$$F_3 = 1 - 60[q_s(T_a) - q_a], \qquad 0 \le F_3 \le 1 \tag{4.5}$$

Which follows Dickinson (1984), and where the coefficient "*60*" is expressed in $kg_{air}\, kg^{-1}_{water\ vapor}$;

$$F_4 = 1 - 0.0016(T_{opt} - T_a), \qquad 0 \le F_4 \le 1 \tag{4.6}$$

Which also follows Dickinson (1984), but in which the optimum temperature T_{opt}, i.e. the temperature at which the vegetation behaves best, has been set according to the vegetation type (but, for most vegetation types, this threshold is assumed equal to $298\,K$);

$$F_5 = \begin{cases} e^{0.0027(C_{CO2} - 400)} & if\ C_{CO2} \le 400 \\ 1 - 0.0013(C_{CO2} - 400) & if\ C_{CO2} > 400 \end{cases} \qquad 0 \le F_5 \le 1 \tag{4.7}$$

Which follows Prino et al. (2009), and which is obviously used only if carbon dioxide concentration data C_{CO2} are available (otherwise, the value $F_5 = 1$ is set.

All functions above defined are bounded between a minimum value of 0 (meaning infinite resistance) and a maximum value of 1 (meaning minimum resistance), but the minimum value of F_2 and F_3 has been set equal to 0.15 and 0.25, respectively.

The expression for r_f force this resistance to become ∞ (in practice, its upper limit is bounded to 5000 s m^{-1}, to avoid numerical under/overflows) in the limit $f_v \to 0$, while, for the same limit, $r_d \to 0$. On the other way, in absence of vegetation, r_b is not defined.

The conductances are defined generically as the inverse of the resistances. Their formulation is quite simple and immediate for momentum:

$$s_{am} = \frac{1}{r_{am}}$$

And heat transfers:

$$s_{ah} = \frac{1}{r_{ah}}$$

$$s_b = \frac{2}{r_b}$$

$$s_d = \frac{1}{r_d}$$

$$s_{dsn} = \frac{1}{r_{dsn}}$$

(the factor "2" in s_b definition accounts for the fact that both sides of the leaf exchange heat), while it is a bit more complicated for water vapor transfers, as there are

additional resistances accounting for "internal" processes: the resistance of soil r_{soil} for the evaporation from bare soil (which represents the additional resistance for the evaporation from a soil with respect to a free lake), and that of the vegetation r_f, which accounts of all regulatory mechanisms of the plant. Thus:

$$s_{av} = \frac{1}{r_{av}}$$

$$s_{fdry} = \frac{1 - R_f}{r_b + r_f}$$

$$s_{fwet} = \frac{R_f}{r_b}$$

$$s_f = s_{fdry} + s_{fwet}$$

$$s_{gdry} = \frac{1 - R_g}{r_d + r_{soil}}$$

$$s_{gwet} = \frac{R_g}{r_d}$$

$$s_s = s_{gdry} + s_{gwet}$$

$$s_{ssn} = \frac{1}{r_{dsn} + r_{soilsn}}$$

Where R_f and R_g are the relative leaf and soil surface wetness, corresponding to the percentage of leaves or bare soil covered by water. In the limit $f_v \to 0$, $s_b, s_{fdry}, s_{fwet}, s_f \to 0$ too, while, since $r_d \to 0$, thus $s_{gwet} \to \infty$.

Note also that the conductance for the evaporation from vegetation (bare soil) has two components: one referred to the dry part, when stomatal (soil surface) resistance sums to the laminar boundary-layer (aerodynamic below-canopy) resistance, and another for the

eventual wet portion of the leaf (bare soil), which does not involve stomatal (bare soil) resistance.

Finally, the expression of boundary layer conductance s_b for sensible heat flux contains a factor two because both parts of the leaf are exchanging heat, while just one surface is involved in the processes related to the transpiration (the lower one) or the evaporation from the wet portion and the condensation (the upper one).

4.8. DRAG COEFFICIENTS

Neutral drag coefficients $(C_{DFM})_N$, $(C_{DFH})_N$ and $(C_{DFV})_N$ for momentum, heat and water vapor, respectively, are calculated following Garratt (1994) (eqq. 3.43 & 3.48):

$$(C_{Dfm})_N = \frac{k^2}{\ln^2[\frac{z_a - d_f}{z_{0\text{fm}}}]}$$

$$(C_{Dfh})_N = \frac{k^2}{\ln[\frac{z_a - d_f}{z_{0\text{fm}}}]\ln[\frac{z_a - d_f}{z_{0\text{fh}}}]}$$

$$(C_{Dfv})_N = \frac{k^2}{\ln[\frac{z_a - d_f}{z_{0\text{fm}}}]\ln[\frac{z_a - d_f}{z_{0\text{fv}}}]}$$

Where all roughness lengths are defined in section 4.9. The dependence on atmospheric stability is included by introducing the Richardson number, adapted from Garratt (1994):

$$Ri = \frac{g(z_a - z_s)(T_a - T_s)}{T_s u_a}$$

Where $z_s = f_v h_f$ is the height of the active surface.

The effect of the stability is accounted by multiplying the neutral drag coefficients by stability functions, for which the Louis (1979) formulation, adapted by Garratt (1994), has been used. First, some variables are calculated depending of the property:

$$b_{sm}=13.7-\frac{0.34}{\sqrt{(C_{Dfm})_N}} \qquad b_m=9.4\,b_{sm}(C_{Dfm})_N\sqrt{\frac{z_a-d_f}{z_{0\mathrm{fm}}}}$$

$$b_{sh}=6.3-\frac{0.18}{\sqrt{(C_{Dfh})_N}} \qquad b_h=9.4\,b_{sh}(C_{Dfh})_N\sqrt{\frac{z_a-d_f}{z_{0\mathrm{fh}}}}$$

$$b_{sv}=6.3-\frac{0.18}{\sqrt{(C_{Dfv})_N}} \qquad b_v=9.4\,b_{sv}(C_{Dfv})_N\sqrt{\frac{z_a-d_f}{z_{0\mathrm{fv}}}}$$

Then, the stability functions are calculated as:

$$f_m(Ri)=\begin{cases}1-\dfrac{9.4\ Ri}{1+b_m\sqrt{-Ri}} & Ri<0\\ \dfrac{1}{(1+4.7\,Ri)^2} & Ri\geq 0\end{cases}$$

$$f_h(Ri)=\begin{cases}1-\dfrac{9.4\ Ri}{1+b_h\sqrt{-Ri}} & Ri<0\\ \dfrac{1}{(1+4.7\,Ri)^2} & Ri\geq 0\end{cases}$$

$$f_v(Ri)=\begin{cases}1-\dfrac{9.4\ Ri}{1+b_v\sqrt{-Ri}} & Ri<0\\ \dfrac{1}{(1+4.7\,Ri)^2} & Ri\geq 0\end{cases}$$

Finally, the non-neutral drag coefficients are respectively evaluated as:

$$C_{Dfm}=(C_{Dfm})_N\ f_m(Ri)$$
$$C_{Dfh}=(C_{Dfh})_N\ f_h(Ri)$$
$$C_{Dfv}=(C_{Dfv})_N\ f_v(Ri)$$

4.9. ROUGHNESS LENGTHS

The roughness lengths are defined differently according with the surface type. At a first stage, the zero displacement level d is evaluated as (Garratt (1994), p. 86):

$$d = f_v 0.67 h_f$$

Where h_f is the vegetation height and f_v the vegetation cover. Since d is used as an argument of a logarithm for the calculation of the drag coefficient, it is required that $z_a - d > 0$, z_a being the quote of the observations (also called reference level), i.e. $z_a > d$. This control is included in the model initialization phase.

Over land, the momentum roughness length for bare soil $z_{0\mathrm{gm}}$ is calculated following Garratt (1994) (page 290 table A6) as:

$$z_{0\mathrm{gm}} = 0.005\,[m]$$

For all kinds of bare soil, excepting concrete and asphalt (for which $z_{0\mathrm{gm}} = 0.001\,m$) and water, ice and snow, discussed later.

The corresponding values for heat and water vapor for every ground surface are (Garratt (1994), p. 244):

$$z_{0\mathrm{gh}} = z_{0\mathrm{gv}} = \left(z_{0\mathrm{gm}} / 7.4\right)$$

The momentum roughness length for vegetated soil is (Garratt (1994), eq. 4.4, adapted from Monteith (1973)):

$$z_{0\mathrm{fm}} = 0.13\,h_f \qquad (4.8)$$

In presence of snow, the snow momentum roughness length depends on air kinematic viscosity ν_a and friction velocity u_* (Dingman (1994), p. 190):

$$z_{0\mathrm{sn}} = 0.135\frac{\nu_a}{u_*} + 0.035\frac{u_*^2}{g}\{1 + 5\exp[-(\frac{u_* - 0.18}{0.10})^2]\}$$

Where, in turn, ν_a is function of the air temperature T_a :

$$\nu_a = 1.3432\,10^{-5} + 9.3571\,10^{-8}\left(T_a - T_m\right)$$

The average roughness length for momentum is evaluated as:

$$z_{0\mathrm{m}}=(1-Sn_f)\,f_v\,z_{0\mathrm{fm}}+(1-f_v)(1-Sn_g)\,z_{0\mathrm{gm}}+Sn\,z_{0\mathrm{sn}}$$

Where Sn_f and Sn_g are the fractions of vegetation and bare soil covered by snow, respectively, and Sn the fraction of soil surface covered by snow. Averaged roughness lengths for heat and water vapor are evaluated as:

$$z_{0\mathrm{h}}=z_{0\mathrm{v}}=\left(z_{0\mathrm{m}}/7.4\right)$$

If the database Ecoclimap (Masson et al. (2003)) is used, this database contains directly the mean values of roughness lengths for the non-snowy soil surface $z_{0\mathrm{m}}^{ECO}$ and $z_{0\mathrm{h}}^{ECO}$; thus, the averaged values, which keep their names $z_{0\mathrm{m}}$ and $z_{0\mathrm{h}}$, are evaluated as:

$$z_{0\mathrm{m}}=z_{0\mathrm{m}}^{ECO}(1-Sn)+Sn\,z_{0\mathrm{sn}}$$

$$z_{0\mathrm{v}}=z_{0\mathrm{h}}=z_{0\mathrm{h}}^{ECO}(1-Sn)+Sn\,z_{0\mathrm{sn}}$$

When the soil surface is completely covered by ice, in the hypothesis that there cannot be any vegetation there, it is assumed $Sn=1$, and the “bare” soil surface roughness length is set equal to that for bare soil:

$$z_{0\mathrm{gm}}=0.005\,[m] \qquad\qquad z_{0\mathrm{gh}}=z_{0\mathrm{gv}}=\left(z_{0\mathrm{gm}}/7.4\right)$$

In this case, the averaged values $z_{0\mathrm{m}}, z_{0\mathrm{h}}$ and $z_{0\mathrm{v}}$ assume the same values relative to the bare soil (as said, it is assumed that there is not vegetation over ice):

$$z_{0\mathrm{m}}=z_{0\mathrm{gm}} \qquad\qquad z_{0\mathrm{h}}=z_{0\mathrm{v}}=\left(z_{0\mathrm{m}}/7.4\right)$$

Or, in the case Ecoclimap is used, they will be assumed equal to the Ecoclimap values.

Over ocean, the formulation follows Garratt (1994) (pp. 98-102). u_* allows to distinguish among smooth and rough flow. In case of smooth flow ($u_* \le 0.23\, m\, s^{-1}$), the roughness lengths are defined as:

$$z_{0\mathrm{gm}} = 0.11\, \nu_a / (u_*) \qquad z_{0\mathrm{m}} = z_{0\mathrm{gm}}$$

$$z_{0\mathrm{gh}} = 0.20\, \nu_a / (u_*) \qquad z_{0\mathrm{m}} = z_{0\mathrm{gh}}$$

$$z_{0\mathrm{gv}} = 0.11\, \nu_a / (u_*) \qquad z_{0\mathrm{m}} = z_{0\mathrm{gv}}$$

In case of rough flow ($u_* > 0.23\, m\, s^{-1}$):

$$z_{0\mathrm{gm}} = 0.016 \left(u_*^2 / g\right) \qquad z_{0\mathrm{m}} = z_{0\mathrm{gm}}$$

$$z_{0\mathrm{gh}} = z_{0\mathrm{gm}} \exp\left[2 - 2.48 \left(\mathrm{Re}^{0.025}\right)\right] \qquad z_{0\mathrm{m}} = z_{0\mathrm{gh}}$$

$$z_{0\mathrm{gv}} = z_{0\mathrm{gm}} \exp\left[2 - 2.28 \left(\mathrm{Re}^{0.025}\right)\right] \qquad z_{0\mathrm{m}} = z_{0\mathrm{gv}}$$

Where 0.016 is the Charnook constant, and the other numbers are empirical coefficients.

If the Ecoclimap database is used, in both cases its values are assumed for $z_{0\mathrm{gm}}$, $z_{0\mathrm{gh}}$ and $z_{0\mathrm{gv}} = z_{0\mathrm{gh}}$.

An important note is the automatic correction of the level at which observations refer (z_a or z_v), in order to get a reasonable value for the drag coefficient. The main reason for such corrections is that, in most drag formulations, the logarithm has an argument in which the numerator is something like $(z_a - d)$, thus a negative value in the bracket is not acceptable. The second reason is that, in this case, despite there is not any theoretical reason for this position, all formulations have been verified against observations normally referring to meteorological measurements, often carried out at standard heights: 2m above soil surface for temperature, humidity and pressure observations, and 10 m above

soil surface for the wind. Thus, in the case in which $z_a < d$ or $z_v < d$, the following corrections for z_a or z_v are performed:

$$z_a = d + 2[m]$$

$$z_v = d + 10[m]$$

5. Heat transfer into soil

5.1. THE FORMULATION

With the heat flux $F_z[W\,m^{-2}]$ at depth *z* given by the law of Fourier:

$$F_z = -k_T \frac{\partial T}{\partial z} \tag{5.1}$$

The one dimensional energy conservation requires that:

$$\rho c \frac{\partial T}{\partial t} = -\frac{\partial F}{\partial z} = \frac{\partial}{\partial z}\left(k_T \frac{\partial}{\partial z}\right) \tag{5.2}$$

Where $\rho c[J\,m^{-3}\,K^{-1}]$ is the volumetric soil heat capacity, $T[K]$ the soil temperature and $k_T[W\,m^{-1}\,K^{-1}]$ the thermal conductivity. The above equation is solved by discretizing the soil column into *m* layers with thickness $\Delta Z_i[m]$ (i = 1, 2, …, m).

5.2. THE NUMERICAL SCHEME

The temperature T_i and the volumetric heat capacity $(\rho c)_i$ are defined at the center of each layer, while the thermal conductivity k_{Ti} and heat flux F_{zi} are defined at the interface of each layer (Fig. 5.1).

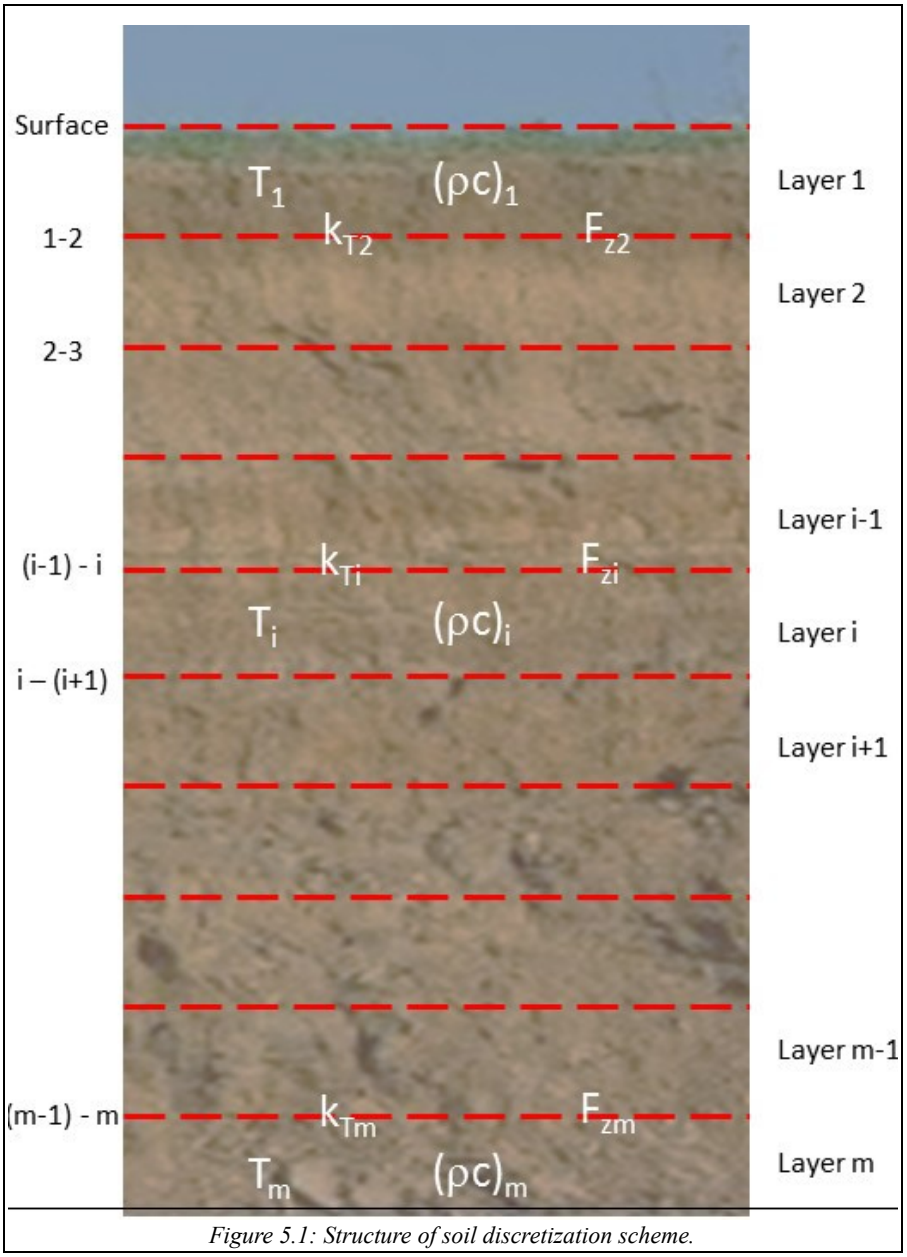

Figure 5.1: Structure of soil discretization scheme.

The heat flux F_{zi} at the interface between the *i-th* and the *(i+1)-th* soil layers is evaluated as:

$$F_{zi} = -k_{Ti} \frac{T_i - T_{i+1}}{0.5(\Delta z_i + \Delta z_{i+1})}$$

The energy balance for the *i-th* layer is:

$$(\rho c)_i \frac{\Delta z_i}{\Delta t}(T_i^{n+1} - T_i^n) = F_{z\,i-1} + F_{zi}$$

Where the superscripts *n* and *n+1* indicate the values at the beginning and end of the time step Δt (seconds), respectively. This equation is solved by using the Crank-Nicholson method (Crank and Nicolson (1947)), which combines the explicit method, with fluxes evaluated at time *n*, and the implicit method, with fluxes evaluated at time *n+1*:

$$(\rho c)_i \frac{\Delta z_i}{\Delta t}(T_i^{n+1} - T_i^n) = 0.5(-F_{z,i-1}^{n+1} + F_{z,i}^{n+1} - F_{z,i-1}^{n} + F_{z,i}^{n})$$

Resulting in a tridiagonal system of equations:

$$d_i = a_i T_{i-1}^{n+1} + b_i T_i^{n+1} + c_i T_{i+1}^{n+1}$$

For the first (uppermost) soil layer (i=1), the top boundary condition for the heat flux is $F_{z\,i-1} = F_{z0} = -Q_g$, where Q_g is the heat flux into the soil (positive into the soil) evaluated from the energy balance. The resulting equations for this layer (*i=1*) are:

$$\frac{(\rho c)_i \Delta z_i}{\Delta t}(T_i^{n+1} - T_i^n) = Q_g - k_{T,i}\left(\frac{T_i^{n+1} - T_{i+1}^{n+1}}{\Delta z_i + \Delta z_{i+1}} + \frac{T_i^n - T_{i+1}^n}{\Delta z_i + \Delta z_{i+1}}\right)$$

$$a_i = 0$$

$$b_i = -\frac{(\rho c)_i \Delta z_i}{\Delta t} + \frac{k_{T,i}}{\Delta z_i + \Delta z_{i+1}}$$

$$c_i = -\frac{k_{T,i}}{\Delta z_i + \Delta z_{i+1}}$$

$$d_i = -\frac{(\rho c)_i \Delta z_i}{\Delta t} T_i^n + Q_g - k_{T,i}\frac{T_i^n - T_{i+1}^n}{\Delta z_i + \Delta z_{i+1}}$$

The boundary condition for the flux at the bottom of the soil column ($i=m$) can be assumed as null flux in case of deep soil layers (some meters); however, in general, it will be $F_{zm}=-Q_{g,bot}$. The resulting equations are:

$$\frac{(\rho c)_i \Delta z_i}{\Delta t}(T_i^{n+1}-T_i^n)=Q_{g,bot}+k_{T,i-1}(\frac{T_{i-1}^{n+1}-T_i^{n+1}}{\Delta z_{i-1}+\Delta z_i}+\frac{T_{i-1}^n-T_i^n}{\Delta z_{i-1}+\Delta z_i})$$

$$a_i=-\frac{k_{T,i-1}}{\Delta z_{i-1}+\Delta z_i}$$

$$b_i=\frac{(\rho c)_i \Delta z_i}{\Delta t}+\frac{k_{T,i-1}}{\Delta z_{i-1}+\Delta z_i}$$

$$c_i=0$$

$$d_i=\frac{(\rho c)_i \Delta z_i}{\Delta t}T_i^n+k_{T,i-1}\frac{T_{i-1}^n-T_i^n}{\Delta z_{i-1}+\Delta z_i}-Q_{g,bot}$$

$Q_{g,bot}$ is evaluated adapting the analytical formulation for the heat transfer into soil for a homogeneous soil, in the hypothesis of a sinusoidal forcing thermal wave at the surface. The coefficients used are the average of the considered soil profile, while, as upper forcing flux, the Q_g value was used. The formulation is:

$$Q_{g,bot}=Q_g \exp(-\frac{z_{bot}}{D})\sin(\omega t-\frac{180° z_{bot}}{\pi D}+45°)$$

Where $\omega t=(180° t)/12-90°$ represents the hourly angle (see section 3.2.1.), with $\omega=7.292\ 10^{-5} rad\ s^{-1}$, z_{bot} is the depth of the lowest boundary, and D is defined as:

$$D=\sqrt{\frac{2k_T}{\omega \rho c\, z_{bot}}}$$

And all properties refer to the averaged soil layer.

For the intermediate soil layers, m-1 ≥ i ≥ 2:

$$\frac{(\rho c)_i \Delta z_i}{\Delta t}(T_i^{n+1} - T_i^n) = k_{T,i-1}\left(\frac{T_{i-1}^{n+1} - T_i^{n+1}}{\Delta z_{i-1} + \Delta z_i} + \frac{T_{i-1}^n - T_i^n}{\Delta z_{i-1} + \Delta z_i}\right) - k_{T,i}\left(\frac{T_i^{n+1} - T_{i+1}^{n+1}}{\Delta z_i + \Delta z_{i+1}} + \frac{T_i^n - T_{i+1}^n}{\Delta z_i + \Delta z_{i+1}}\right)$$

$$a_i = -\frac{k_{T,i-1}}{\Delta z_{i-1} + \Delta z_i}$$

$$b_i = -\frac{(\rho c)_i \Delta z_i}{\Delta t} + \frac{k_{T,i}}{\Delta z_i + \Delta z_{i+1}} + \frac{k_{T,i-1}}{\Delta z_{i-1} + \Delta z_i}$$

$$c_i = -\frac{k_{T,i}}{\Delta z_i + \Delta z_{i+1}}$$

$$d_i = \frac{(\rho c)_i \Delta z_i}{\Delta t} T_i^n + k_{T,i-1}\frac{T_{i-1}^n - T_i^n}{\Delta z_{i-1} + \Delta z_i} - k_{T,i}\frac{T_i^n - T_{i+1}^n}{\Delta z_i + \Delta z_{i+1}}$$

This solution conserves energy. For numerical stability, the time step Δt is suggested to be not higher than 60÷120 s, especially with thin uppermost soil layers.

6. Vegetation energy and hydrological balances

6.1. VEGETATION TEMPERATURE

The equation regulating the energy budget in the vegetation is:

$$\frac{\partial T_f}{\partial t} = \frac{Q_f}{C_f}$$

Where T_f is the vegetation (or canopy) temperature, $Q_f [W\, m^{-2}]$ is the net input of energy and $C_f [J\, m^{-2} K^{-1}]$ the integrated heat capacity of vegetation, parametrized as:

$$C_f = C_{fw} LAI + 4.186\, 10^6 P_{mf}$$

Here the value C_{fw} derives from the assumption that vegetation possesses the same heat capacity of 0.55 mm of water (Garratt (1994)), while the second term in the r.h.s. considers the eventual presence of water on the leaves. The numerical solution of this equation is different from the one used for soil temperature, due to the large value of C_f with respect to the other terms, which could cause numerical instability. Thus a simple solution like:

$$T_f^{n+1} = T_f^n + \Delta t \frac{Q_f}{C_f}$$

Where the suffices *n* and *n+1* indicate the time interval, may be not applicable in certain conditions.

The following numeric scheme is more suitable:

$$T_f^n + 1 = T_f^n + \frac{Q_f}{\frac{C_f}{\Delta t}\frac{1}{2}\left(\frac{\partial Q_f}{\partial T_f}\right)} \tag{6.1}$$

Thus we need to explicit the dependence of Q_f from T_f .

Looking at sections 3.1., 3.3., 4.2., 4.3. and 4.6., the explicit formulation for Q_f in function of the vegetation temperature T_f can be written as:

$$Q_f = -\epsilon_f f_v \sigma T_f^4 + \frac{(\epsilon_g - \epsilon_f + \epsilon_f \epsilon_g)}{\epsilon_f + \epsilon_g - \epsilon_f \epsilon_g} \sigma T_f^4 - \rho_a c_p s_b \theta_f f_v (1 - Sn_f) +$$
$$-\lambda(T_f)\rho_a f_v (1 - Sn_f)(s_{dry} + s_{wet}) q_s(T_f) - C_{sw} P_f \rho_w T_f + K$$

Where the last term K accounts for all other terms not explicitly depending on T_f . Note also that, in the above expression, s_{dry} should be replaced by s_b if $q_s(T_f) < q_{af}$.

The derivative of the previous equation with respect to T_f can be written as:

$$\frac{\partial Q_f}{\partial T_f} = -4\epsilon_f f_v \sigma T_f^3 + \frac{(\epsilon_g - \epsilon_f + \epsilon_f \epsilon_g)}{\epsilon_f + \epsilon_g - \epsilon_f \epsilon_g} 4\sigma T_f^3 - \rho_a c_p s_b \frac{\theta_f}{T_f} f_v (1 - Sn_f) +$$
$$-\lambda(T_f)\rho_a f_v (1 - Sn_f)(s_{dry} + s_{wet}) \frac{\partial q_s(T_f)}{\partial T_f} - C_{sw} P_f \rho_w$$

Being $\partial \theta_f / \partial T_f = \theta_f / T_f$.

In the above calculations, it has been implicitly neglected, for T_{af} and q_{af} , as well as the latent heat of evaporation $\lambda(T_f)$, their implicit dependence on T_f . This is actually not true, but it could be considered as a first order approximation. In fact, as T_{af} and q_{af} contain also all snow coefficients, the complete formulation of eq. 6.1 may become quite long. In the opinion of the authors, the increase of precision does not justify the increase in computational time.

6.2. VEGETATION WATER BUDGET

Precipitation is either intercepted by the canopy or falls to the ground as throughfall and stemflow. The maximum water amount which can be held by the canopy is given by (Garratt (1994), page 237):

$$M_{fmax} = 2\ 10^{-4} f_v LAI$$

Canopy water is evaluated using a mass balance equation in which the components are: interception, dew and evaporation, respectively. All terms are expressed in rates (m s^{-1}):

$$\frac{\Delta M_f}{\Delta t} = q_{inter} + q_{cdew} - q_{ceva}$$

The wet fraction of canopy, also called leaf wetness, R_f, is defined as:

$$R_f = \left(\frac{M_f}{M_{fmax}} \right) \leqslant 1$$

The rate of water (rain, snow, dew or frost) intercepted by the vegetation p_f is calculated as:

$$p_f = f_v p_a (1 - Sn_f)$$

When p_a is the atmospheric precipitation, and both variables are expressed as rates [m s^{-1}]. The variation of water above vegetation $M_f[m]$ is evaluated as:

$$\Delta M_f = \Delta t \left(p_f - \frac{E_{fw}}{\rho_{fw}} \right) \qquad \Delta M_f \geq -M_f$$

Where E_{fw} is the evaporation from the wet portion of canopy (if positive) or the condensation of water vapor above leaves (if negative). The water exceeding the maximum water content above vegetation M_{fmax} (m) is used to evaluate the drainage from vegetation according with the formula:

$$d_f = \begin{cases} M_f - M_{fmax} & if\ M_f > M_{fmax} \\ 0 & if\ M_f < M_{fmax} \end{cases}$$

UTOPIA evaluates also, for each timestep, the time (in units of the internal timestep, converted in minutes) in which the leaves are "wet". This calculation is done by counting for how many minutes R_f (the fraction of leaves wet) is larger than the threshold $R_{thre} = 3.44\,10^{-9}\,m$, evaluated experimentally in Cassardo et al. (2003).

The water not intercepted by the vegetation and the leaf drainage reaches the ground and contribute to the precipitation rate reaching the soil p_g, defined as:

$$p_g = (p_a - p_f + d_f)(1 - Sn_f)$$

In the case in which the temperature of the vegetation T_f is smaller than 0 °C, the water above leaves is considered as snow, thus the eventual water present on the vegetation is added to the snow content, and M_f is set equal to zero. In this way, frost and galaverna are considered as snow.

Finally, in the case in which it snows, the entire precipitation p_a in each timestep is assumed as being fresh snow ($p_{sn} \equiv p_a [m\,s^{-1}]$). In the case in which there is snow at the ground during a rainfall, the water balance of snow must include also the rainfall over snow $p_{gonsnow}[m\,s^{-1}]$:

$$p_{gonsnow} = (p_a - p_f + d_f)\,Sn_g$$

6.3. Roots

As far as the roots, two coefficients have been introduced in order to account of their geometrical distribution, as in LSPM (Cassardo (2006)). For the calculation of soil mean

temperature and moisture in the roots layer, the volume of soil in which there are roots is compared to the total soil volume, assuming an uniform distribution of the roots.

Expressing such volumes for unit of surface area, the fractional root percentage $FRP_{occ}(i)$ (i.e. the percentage of occupation of soil by roots in the *i-th* layer) depends on the layer depth $\Delta z(i)$ and the root depth d_R according to the formula:

$$FRP_{occ}(i)=\begin{cases} \dfrac{d_i}{d_R} & if \sum_{j=1}^{i} d_j \le \Delta z \\ d_i - \dfrac{\sum_{j=1}^{i} d_j - \Delta z}{d_R} & if \sum_{j=1}^{i} d_j > \Delta z \end{cases}$$

Where $\Delta z = Min\left(d_r, \sum_{j=1}^{m} d_j\right)$

For the calculation of the contribution of every layer to the transpiration and the heat capacity, we assume that the roots are uniformly distributed in a cone of height d_R and base radius d_R (it can be demonstrated that the dimension of the base area does not influence the calculations under the assumption of uniform distribution of roots). The total volume occupied by the roots $V_{rootTOT}$ can be thus evaluated as:

$$V_{rootTOT} = \pi \frac{\Delta z^3}{3}$$

Then, for each *i-th* layer of soil, the volume occupied by roots V_{root} is given by the difference between the volume of the fraction of cone included between the top and the bottom of the layer:

$$V_{root}(i)=\frac{\pi}{3}MIN[\sum_{j=1}^{i-1}d_j,d_R]-\frac{\pi}{3}MIN[\sum_{j=1}^{i}d_j,d_R]$$

While the total volume of the *i-th* layer $V_{TOT}(i)$ is:

$$V_{TOT}(i)=\pi d_R^2\Delta z(i)$$

The fraction in volume of the *i-th* layer occupied by roots is thus:

$$RP_{layer}(i)=\frac{V_{root}(i)}{[V_{TOT}(i)]}$$

While the percentage of roots in the *i-th* layer with respect to the total volume of roots (useful to establish the contribution of *i-th* layer to the total evapotranspiration) is:

$$RP_{total}(i)=K_R f_v \frac{V_{root}(i)}{[V_{rootTOT}(i)]}$$

Where K_R is an empirical coefficient accounting for the root density. In the model, it has been assumed $K_R=0.05$.

7. Soil hydrological budget

7.1. Soil surface hydrological budget

In analogy with vegetation, the maximum water amount that can be stored (without infiltrating into soil) above the soil surface is given by:

$$M_{gm} = 2\,10^{-4}[m]$$

For all types of land use, except for the categories corresponding to urban areas (*settlement* and *large settlement*), for which $M_{gm} = 4.8\,10^{-4}[m]$ (Grimmond et al. (1991)).

Given p_g as the precipitation occurring over bare soil, and E_g the evaporation from the wet portion of the bare soil, or the condensation above it, the actual soil water content M_g will be varied by the quantity ΔM_g so evaluated:

$$\Delta M_g = \Delta t\left(p_g - E_{gwet}/\rho_w\right)$$

Where $\rho_w = 1000\,kg\,m^{-3}$ is the water density.

To discriminate solid from liquid accumulation, the presence of ice in the first layer of soil is analyzed. More specifically, if $\eta_i > 0 \quad [m_{ice}^3\, m_{soil}^{-3}]$, then it is supposed that water will freeze, thus all liquid water is considered as ice:

$$M_i = M_g, M_g = 0, \Delta M_g = 0$$

If then M_g(or M_i) are exceeding th maximum quantity, then the excess:

$$d_g = \begin{cases} M_g - M_{gmax} & if\ M_g > M_{gmax} \\ 0 & if\ M_g \le M_{gmax} \end{cases}$$

Will become water available for the infiltration (and same for M_i in case of ice).

7.2. SOIL UNDERGROUND HYDROLOGICAL BUDGET

Soil water is calculated from the conservation equation:

$$\frac{\partial \eta}{\partial t} = \frac{\partial Q}{\partial z} \tag{7.1}$$

Where $\eta [m^3_{void} m^{-3}_{soil}]$ is the volumetric soil water content and $Q[m\,s^{-1}]$ is the total water flux. In the desert land surface, besides the liquid water flux Q_l , also the water vapor flux Q_v must be considered, and it has been introduced into UTOPIA. Q_v is usually neglected by most of the land surface models, due to its very small contribution in non-arid zones. Hovever, several studies have demostrated that it may become important in the desert, arid and semi-arid regions. Based on Philip and de Vries (1957), Sun (1982), and Niu et al. (1997) papers, the water flux Q is partitioned into liquid water flux Q_l and water vapor flux Q_v :

$$Q = Q_l + Q_v$$

$$Q_l = -D_{l\eta}\frac{\partial \eta}{\partial z} + D_{lT}\frac{\partial T}{\partial z} - K_\eta$$

$$Q_v = -D_{v\eta}\frac{\partial \eta}{\partial z} + D_{vT}\frac{\partial T}{\partial z} - K_\eta$$

Where $D_{l\eta}$ is the liquid water diffusivity due to the soil water content gradient, D_{lT} is the liquid water diffusivity due to the temperature gradient (this term is small as compared with other terms), $D_{v\eta}$ is the water vapor diffusivity due to the soil water content gradient, D_{vT} is the water vapor diffusivity due to the temperature gradient, and finally K_η is the hydraulic conductivity.

$D_{v\eta}$ and D_{vT} can be derived from the vapor diffusion process under a the local equilibrium assumption, and are equal to (Niu et al. (1997)):

$$D_{v\eta} = -\frac{D_v \tau(\eta_s - \eta)\rho_v g \Psi_s b \eta_s^b}{\rho_w R_v T \eta^{b+1}}$$

$$D_{vT} = -D_v \tau(\eta_s - \eta)\frac{\rho_v}{\rho_w}\left[\frac{1}{T} + \frac{g\Psi_s b \eta_s^b}{R_v T \eta^b} - \frac{a_v b_v}{(T - c_v)^2}\right]$$

Where $a_v = 17.269, B_v = 273.3, \text{and} c_v = 35.86$ are empirical parameters, τ is the soil tortuosity coefficient (connected to the size of sand grains; typical values are about 30 to 40), ρ_w the water density, and $R_v = 287\, J\, kg^{-1} K^{-1}$ the water vapor constant. The water vapor density ρ_v is parameterised as:

$$\rho_v = \frac{e_s(T)\exp\left(\frac{g\Psi}{R_v T}\right)}{R_v T}$$

Where $e_s(T)$ is the saturated vapor pressure over the free water surface at the local averaged soil temperature *T*, and *g* is the acceleration of gravity. Finally D_v is the water vapor diffusivity, parametrized by: $D_v = 2.3\ \ 10^{-5}\left(\frac{T}{273.16}\right)^{1.75}$

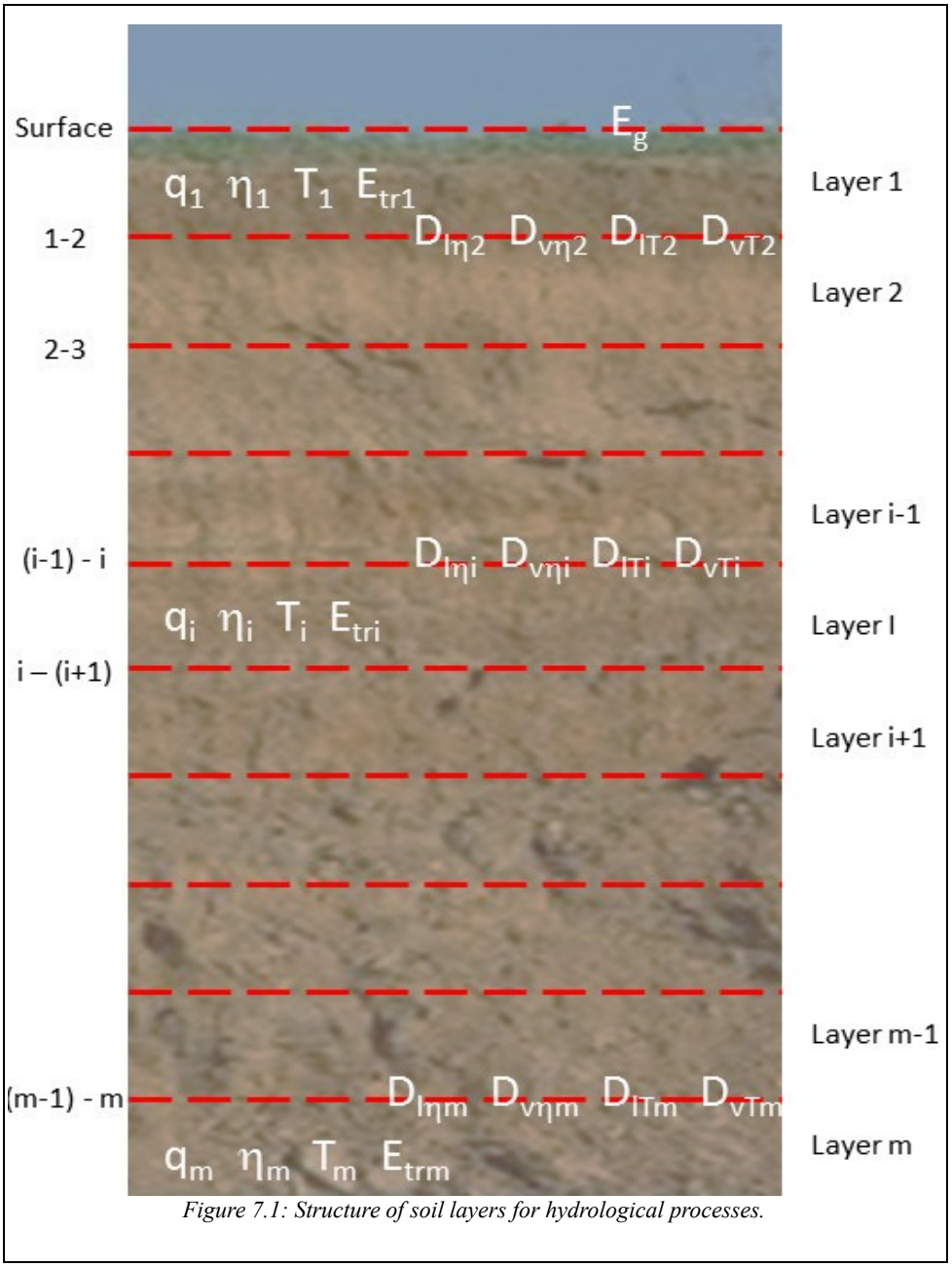

Figure 7.1: Structure of soil layers for hydrological processes.

7.3. NUMERICAL SCHEME

With reference to Fig. 7.1, the vertical water flow at the depth z is:

$$Q_z = -(D_{l\eta} + D_{v\eta})\frac{\partial \eta}{\partial z} - K_\eta - (D_{vt} + D_{v\eta})\frac{\partial T}{\partial z}$$

One dimensional water conservation requires that:

$$\frac{\partial \eta}{\partial t} = -\frac{\partial Q_z}{\partial z} = \frac{\partial}{\partial z}[(D_{l\eta} + D_{v\eta})\frac{\partial \eta}{\partial z}] + \frac{\partial K_\eta}{\partial z} + \frac{\partial}{\partial z}[(D_{vT} + D_{v\eta})\frac{\partial T}{\partial z}]$$

Similarly to the soil temperature case, the soil moisture η is defined at the centre of each layer. The hydraulic conductivity and the diffusivities are defined at the interfaces.

Thus, the water flux from layer *i-th* to layer *(i+1)-th* is:

$$Q_i = -2(D_{l\eta i} + D_{v\eta i})\frac{\eta_i - \eta_{i+1}}{\Delta z_i + \Delta z_{i+1}} - K_{\eta i} - 2(D_{lTi} + D_{vTi})\frac{T_i - T_{i+1}}{\Delta z_i + \Delta z_{i+1}}$$

The water balance for the *i-th* layer can be expressed as:

$$\frac{\Delta z_i}{\Delta t}(\eta_i^{n+1} - \eta_i^n) = (Q_i - Q_{i-1})\cos^2 s - e_i \qquad (7.2)$$

Where $e_i = E_{tri} + E_g \delta_{1i}$ includes transpiration and surface evaporation, and where the function of the slope angle will be discussed in detail in section 7.6..

Likewise the soil temperature equation, also the above equation is solved using the Crank-Nicholson method (Crank and Nicolson (1947)).

For the first soil layer (*i=1*):

$$e_i = E_{tri} + E_g \delta_{1i}$$

$$Q_{i-1} = P_{infiltr}$$

Where $P_{infiltr}$ is the infiltration, and e_i accounts for the transpiration E_{tri} and surface evaporation E_g, the latter only for the first soil layer. The complete equation thus can be written as:

$$\frac{\Delta z_i}{\Delta t}(\eta_i^{n+1} - \eta_i^n) = P_{infiltr} - E_{tri} - \delta_{1i} E_g - K_{\eta i}\cos^2 s +$$
$$-2(D_{l\eta i} + D_{v\eta i})\frac{\eta_i^{n+1} - \eta_{i+1}^{n+1}}{\Delta z_i + \Delta z_{i+1}}\cos^2 s - 2(D_{l\eta i} + D_{v\eta i})\frac{\eta_i^n - \eta_{i+1}^n}{\Delta z_i + \Delta z_{i+1}}\cos^2 s +$$
$$-2(D_{lTi} + D_{vTi})\frac{T_i^n - T_{i+1}^n}{\Delta z_i + \Delta z_{i+1}}\cos^2 s$$

And its solution results from the tridiagonal system of equations:

$$d_i = a_i \eta_{i-1}^{n+1} + b_i \eta_i^{n+1} + c_i \eta_{i+1}^{n+1}$$

With the coefficients given by:

$$a_i = 0$$

$$b_i = \frac{\Delta z_i}{\Delta t} + \frac{D_{l\eta i} + D_{v\eta i}}{\Delta z_i + \Delta z_{i+1}}\cos^2 s$$

$$c_i = -\frac{D_{l\eta i} + D_{v\eta i}}{\Delta z_i + \Delta z_{i+1}}\cos^2 s$$

$$d_i = \frac{\Delta z_i}{\Delta t}\eta_i^n + P_{infiltr} - E_{tri} - \delta_{1i} E_g - K_{\eta i}\cos^2 s +$$
$$-2(D_{l\eta i} + D_{v\eta i})\frac{\eta_i^n - \eta_{i+1}^n}{\Delta z_i + \Delta z_{i+1}}\cos^2 s - 2(D_{lTi} + D_{vTi})\frac{T_i^n - T_{i+1}^n}{\Delta z_i + \Delta z_{i+1}}\cos^2 s$$

For the bottom layer ($i=m$), the boundary conditions are:

$$Q_i = -K_i$$

$$e_i = E_{tri}$$

So the complete equation is:

$$\frac{\Delta z_i}{\Delta t}(\eta_i^{n+1} - \eta_i^n) = -E_{tri} + 2(D_{l\eta} + D_{v\eta})_{i-1} \frac{\eta_{i-1}^{n+1} - \eta_i^{n+1}}{\Delta z_{i-1} + \Delta z_i} \cos^2 s +$$
$$+ 2(D_{l\eta} + D_{v\eta})_{i-1} \frac{\eta_{i-1}^{n} - \eta_i^{n}}{\Delta z_{i-1} + \Delta z_i} \cos^2 s - K_{\eta i} \cos^2 s +$$
$$+ 2(D_{lT} + D_{vT})_{i-1} \frac{T_{i-1}^{n} - T_i^{n}}{\Delta z_{i-1} + \Delta z_i} \cos^2 s$$

And the solution is:

$$a_i = -\frac{(D_{l\eta} + D_{v\eta})_{i-1}}{\Delta z_{i-1} + \Delta z_i} \cos^2 s$$

$$b_i = \frac{\Delta z_i}{\Delta t} + \frac{(D_{l\eta} + D_{v\eta})_{i-1}}{\Delta z_{i-1} + \Delta z_i} \cos^2 s$$

$$c_i = 0$$

$$d_i = \frac{\Delta z_i}{\Delta t} \eta_i^n + 2(D_{l\eta} + D_{v\eta})_{i-1} \frac{\eta_{i-1}^{n} - \eta_i^{n}}{\Delta z_{i-1} + \Delta z_i} \cos^2 s + K_{\eta(i-1)} \cos^2 s +$$
$$- K_{\eta(i)} \cos^2 s + 2(D_{lT} + D_{vT})_{i-1} \frac{T_{i-1}^{n} - T_i^{n}}{\Delta z_{i-1} + \Delta z_i} \cos^2 s - (E_{tr})_i$$

For the other layers, m-1 ≥ i ≥ 2, the only boundary condition is:

$$e_i = E_{tri}$$

So the complete equation is:

$$\frac{\Delta z_i}{\Delta t}(\eta_i^{n+1}-\eta_i^n)=-(E_{tr})_i+(K_\eta)_{i+1}-(K_\eta)_i\cos^2 s+$$
$$+2(D_{l\eta}+D_{v\eta})_{i-1}\frac{\eta_{i-1}^{n+1}-\eta_i^{n+1}}{\Delta z_{i-1}+\Delta z_i}\cos^2 s-2(D_{l\eta i}+D_{v\eta i})\frac{\eta_i^{n+1}-\eta_{i+1}^{n+1}}{\Delta z_i+\Delta z_{i+1}}\cos^2 s$$
$$+2(D_{lT}+D_{vT})_{i-1}\frac{T_{i-1}^n-T_i^n}{\Delta z_{i-1}+\Delta z_i}\cos^2 s-2(D_{lTi}+D_{vTi})\frac{T_i^n-T_{i+1}^n}{\Delta z_i+\Delta z_{i+1}}\cos^2 s$$

And the solution is:

$$a_i=-\frac{(D_{l\eta}+D_{v\eta})_{i-1}}{\Delta z_{i-1}+\Delta z_i}\cos^2 s$$

$$b_i=\frac{\Delta z_i}{\Delta t}+\frac{(D_{l\eta}+D_{v\eta})_{i-1}}{\Delta z_{i-1}+\Delta z_i}\cos^2 s+\frac{(D_{l\eta}+D_{v\eta})_i}{\Delta z_i+\Delta z_{i+1}}\cos^2 s$$

$$c_i=-\frac{(D_{l\eta}+D_{v\eta})_i}{\Delta z_i+\Delta z_{i+1}}\cos^2 s$$

$$d_i=\frac{\Delta z_i}{\Delta t}\eta_i^n+2(D_{l\eta}+D_{v\eta})_{i-1}\frac{\eta_{i-1}^n-\eta_i^n}{\Delta z_{i-1}+\Delta z_i}\cos^2 s+$$
$$-2(D_{l\eta i}+D_{v\eta i})\frac{\eta_i^n-\eta_{i+1}^n}{\Delta z_i+\Delta z_{i+1}}\cos^2 s-2(D_{lT}+D_{vT})_i\frac{T_i^n-T_{i+1}^n}{\Delta z_i+\Delta z_{i+1}}\cos^2 s+$$
$$+2(D_{lT}+D_{vT})_{i-1}\frac{T_{i-1}^n-T_i^n}{\Delta z_{i-1}+\Delta z_i}\cos^2 s-(E_{tr})_i+(K_\eta)_{i-1}\cos^2 s-(K_\eta)_i\cos^2 s$$

To ensure the numerical stability of the scheme, the authors suggest that the time step Δt should vary in the range 60÷120 s.

7.4. SURFACE AND UNDERGROUND RUNOFF

The treatment of the water which does not increase the soil moisture content is developed in many ways. At beginning, the effective precipitation $P_{geff}[m\,s^{-1}]$, taking into account also the eventual inclination of the soil, is calculated by eq. (7.2) (see Section 7.6.). Subsequently, the maximum soil infiltration capacity over flat surface

$P_{infiltr,max,0}$ is calculated according with the formulation of NCAR model (Bonan (1996)):

$$P_{infiltr,max,0} = K_{\eta s1}\left[1 - \frac{\psi_{s1}}{0.5\,d_1} b_1 \left(1 - \frac{\eta_{w1}}{\eta_{s1} - \eta_{i1}}\right)\right] \tag{7.3}$$

Where η_{w1} and η_{i1} are the liquid and ice water content in the first soil layer, respectively, and η_{s1} is the porosity. Note that, in case of soil freezing, the denominator decreases, as the size of the pores also decreases, due to the presence of some ice within the pores.

This parametrization has been preferred to that of Boone and Wetzel (1996), originally used in the ancestor model LSPM, as the infiltration values seem more reasonable, especially in case of dry soil.

The effective infiltration is then evaluated as:

$$P_{in} = P_{eff} \le P_{infiltr,max}$$

And the eventual excess water is considered as surface runoff $R_{s1}[m]$:

$$R_{s1} = \Delta t\,(P_{infiltr,max} - P_{geff}) \ge 0$$

The saturation runoff can occur at each soil layer in the case in which soil moisture content exceed the porosity of that layer, and is calculated as $R_{s2}[m]$ for each *i-th* layer:

$$(R_{s2})_i = \eta_{si}\, d_i\,(q_i - 1) \ge 0$$

The total surface runoff R_s is now calculated as:

$$R_s = R_{s1} + (R_{s2})_1$$

While underground runoff R_u , which includes both drainage and all intermediate layer runoff, is given by:

$$R_u = \sum_{i=2}^{M} (R_{s2})_i + (Q_{out})_M + \sum_{i=2}^{M} (R_{s3})_i$$

Where $(Q_{out})_M$ is the water outflow from the *M-th* and last layer, i.e. the drainage, evaluated in section 7.5., and the additional term $(R_{s3})_i$ will be described in section 7.6..

7.5. WATER OUTFLOW FROM THE BOTTOM LAYER (DRAINAGE)

Gravitational drainage from the bottom soil layer is defined in function of the bottom layer hydraulic conductivity as:

$$(Q_{out})_M = C_{dren} K_\eta \Delta t \ \cos^2 s$$

Where C_{dren} is the drainage parameter, ranging between *0* (no drainage) and *1* (full drainage), and *s* is the slope angle. The use of the square in the cosine is due to the consideration that the sum of the water movement along the terrain slope, and perpendicularly to it, must equal the value for horizontal surface.

7.6. MODIFICATION OF ALL FORMULATIONS FOR SLOPING TERRAIN

If the terrain is not horizontal but possesses a slope angle *s*, there are three main differences in the physical processes: (i) the incidence of the solar radiation; (ii) the path of the water entering into soil; (iii) the effectiveness of the precipitation.

The first one has already been included in the formulation of solar radiation (section 3.2.1.). The other two points can be treated together in the following way.

The effective precipitation rate $P_{geff}[m\,s^{-1}]$ is affected by the surface inclination, because the apparent surface seen by the falling drop is different (in UTOPIA, the fact that the precipitation may fall following a tilted line, not vertical, is not considered at present), but also because a portion of the precipitation will become surface runoff, as the infiltration capacity for flat soil $P_{infiltr,max,0}$ (eq. 7.3) will decrease by the quantity $\cos s$:

$$P_{infiltr,max} = P_{infiltr,max,0}\cos s \geq 0$$

Also in a generic *i-th* layer of soil, the flux of water, which over a flat terrain will flow perpendicularly to the layer itself, in presence of a slope will flow vertically, and thus can be decomposed in a flux parallel to the terrain and a flux perpendicular to it (figure XXX):

$$Q_i = (Q_i)_{//} + (Q_i)_{\perp} = Q_i \sin^2 s + Q_i \cos^2 s$$

It is thus possible to define for each soil layer, the lateral slope runoff $(R_{s3})_i[m]$ given by:

$$(R_{s3})_i = \Delta t (Q_i - Q_{i-1}) \sin^2 s$$

While the correction accounting for the term $(Q_i)_{\perp}$ appears into eq. 7.2.

8. The snow parametrization

8.1. DEFINITIONS

A generic snow pack is characterized by a depth h_s , a volume V_s , and a base area A (Fig. 8.1). The water equivalent of the snow pack is defined as the ratio between of the volume of liquid water V_w and ice V_i present in the snow pack and the base area A:

$$h_m = \frac{V_m}{A} = h_i + h_w$$

Where $V_m = V_w + V_i$ is the volume of water and ice expressed in terms of volume of equivalent water (where "*m*" stands for *melt*), $h_w = V_w / A$ is the liquid water content and $h_i = V_i / A$ the ice content. Defining the snow density as:

$$\rho_s = \frac{\rho_i V_i + \rho_w V_w}{V_s} \tag{8.1}$$

(where the contribution of air density ρ_a has been neglected, as $\rho_a \ll \rho_i < \rho_w$), the relation between the snow height h_s and the corresponding snow water equivalent h_m becomes:

$$h_m = \frac{\rho_s}{\rho_w} h_s \tag{8.2}$$

Provided these basic definitions, for which we have followed Dingman (1994), it is possible to analyze all parameterizations in the following subsections.

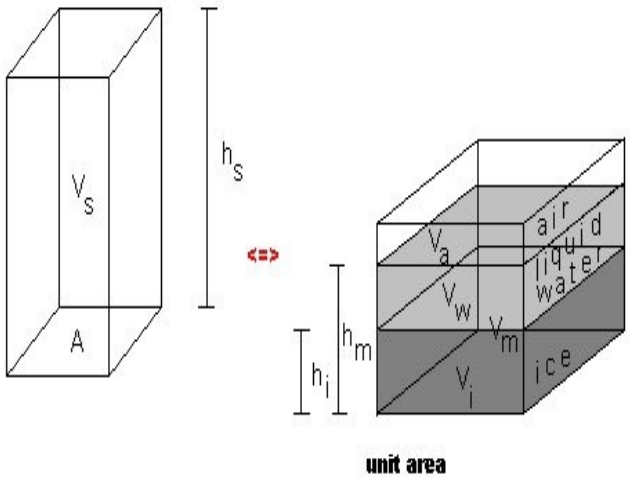

Figure 8.1: Schematic structure of the snowpack

8.2. MELTING PROCESSES OF SNOW

The melting of snow pack begins when the budget of incoming net energy on the snow ΔQ_{av} is positive. By considering a snow pack at an initial temperature $T_s < 0\,°C$, the melting process can be considered subdivided into three separate phases (Dingman (1994)):

- the warming phase;
- the ripening phase;
- the real melting phase.

In the **warming phase**, the snow pack temperature increases from the initial value $T_s < 0\,^\circ C$ to the melting point $T_m = 0\,^\circ C$. The specific (i.e. per unit area) energy needed to increase the snow temperature up to the melting point is:

$$Q_{warm} = c_i \rho_s h_s (T_m - T_s) = c_p \rho_w h_m (T_m - T_s) \tag{8.3}$$

In the **ripening phase**, the snow pack is heated at a constant temperature of $T_s = T_m = 0\,^\circ C$. In this case, part of the snow melts but the resulting water remains in the snow pack pores, retained by the surface tension forces. The snow is completely ripe (saturated) when the liquid water content h_w equals the maximum water retention of the snow h_{wret}. According to Dingman (1994), the following dependence of h_{wret} from snow density and depth has been assumed:

$$h_{wret} = \left(C_1 \frac{\rho_s^2}{\rho_w} - C_2 \frac{\rho_s}{\rho_w}\right) h_s \geq C_3 h_s \tag{8.4}$$

Where $C_1 = 0.267\ m^3 kg^{-1}$ and $C_2 = 0.0735$ are experimental values, and $C_3 = 0.00698\, m^{-1}$ has been evaluated using eq. 8.2 with $\rho_s = 350\, kg\, m^{-3}$, value assumed as empirical maximum for the snow density.

The specific energy required to ripe a snow pack at temperature $T_s = T_m = 0\,^\circ C$ is:

$$Q_{ripe} = (h_{wet} - h_w) \rho_w \lambda_f \tag{8.5}$$

In the **melting phase**, a ripe snowpack at temperature $T_s = T_m = 0\,^\circ C$ will receive heat used for melting until all snow melts and the water produced drains out as runoff. The energy necessary to melt all the snow pack is then given by:

$$Q_{melt,tot} = \rho_w \lambda_f h_m \tag{8.6}$$

Until here, we have only analyzed warming processes. Let's study cooling ones.

When a snow pack with a liquid water content h_w is cooled, the energy amount Q_{solid}, given by:

$$Q_{solid} = \rho_w \lambda_f h_w \tag{8.7}$$

Is required to freeze all liquid water.

A further amount of negative specific energy Q_{cool} will cool the dry snowpack by the quantity (in analogy with eq. 8.3):

$$Q_{cool} = c_p \rho_w h_m (T_s - T_m) \tag{8.8}$$

The scheme proposed in this paper considers the snow pack as a homogeneous layer of snow. In real cases, snow starts to melt at the top surface of the snow pack, and melted water can percolate inside the snow pack, in some cases re-freezing (if the snow temperature is low enough), and in any case altering the thermal vertical profile of the snow pack. These processes have not been considered yet in this version of UTOPIA.

8.3. SNOW ENERGY BALANCE

UTOPIA is considering separately the snow cover above vegetation and that above bare soil, each one having a proper budget. In the following, we will use the suffix '*snf*' and '*sng*' to indicate snowy vegetation and snowy bare soil, respectively, while we will use the generic suffix '*sn*' for the general equations that are equal in the two budgets.

To express each term of snow processes as a function of the surface parameters, it is necessary to split the surface area into four sub-areas, of which each extent represents the percentage of different coverages (a sort of tiling approach: see Fig. 8.2).

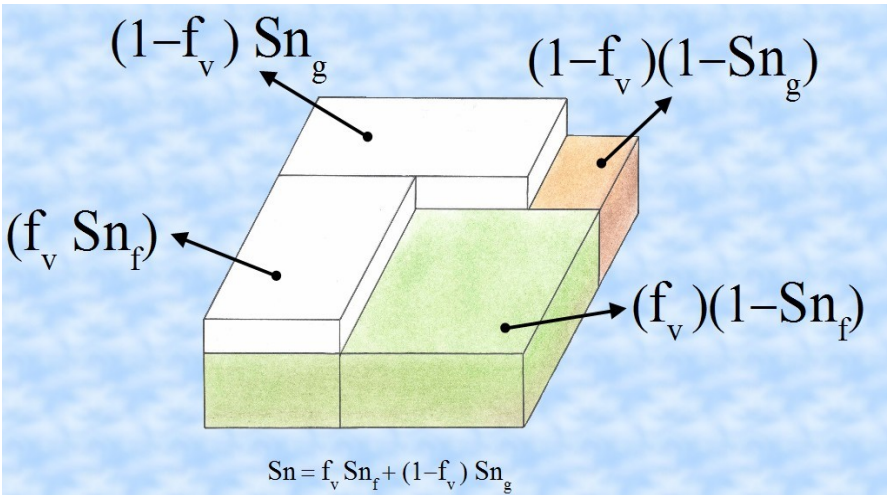

Figure 8.2: Subdivision of surface according with vegetation and snow coverages

As in the case of vegetation cover, these four sub-areas are expressed by the ratio of their area to the total area. Both vegetated (f_v) and bare soil $(1-f_v)$ fractions can be covered with or without snow. The snow coverage on vegetation (Sn_f) can be different from the snow coverage on bare soil (Sn_g), considering the different roughness of canopy and bare soil. The total area covered by snow is given by:

$$Sn = f_v Sn_f + (1-f_v) Sn_g$$

The energy balance of the entire snow pack can be explicited (see for instance Koren et al. (1999), or Cox et al. (1999)) by summing the net radiation, the conductive heat flux coming from soil, canopy and eventual rainfall (all considered positive when entering in the snow), and of sensible and latent heat fluxes (considered positive when leaving the snow). The resulting equation is:

$$\Delta Q_{av} = \left(R_{Nsn} - H_{sn} - F_{sn} + Q_{gsn} + Q_{fsn} + Q_{rain} \right) \Delta t \qquad (8.9)$$

The variable ΔQ_{av} will be hereafter called as ***available energy***. Note that, in eq. 8.9, ΔQ_{av} is expressed in units of energy per unit of surface $[J\,m^{-2}]$ while all other terms are energy fluxes $[J\,m^{-2}s^{-1} = W\,m^{-2}]$. Each term of eq. 8.9 will be analyzed separately in the following subsections.

8.3.1. Net Radiation over Snowy Surfaces

Net radiation over snow is given by eq. 3.5 While individual terms are evaluated in sections 3.2. and 3.3..

8.3.2. Surface temperature and moisture over snowy surfaces

The temperature and specific humidity for canopy and soil surfaces are defined as weighted averages between the snow and snow-free fractions in the following way:

$$T_{canopy} = Sn_f T_{snf} + \left(1 - Sn_f\right) T_f$$

$$T_{surf} = Sn_g T_{sng} + \left(1 - Sn_g\right) T_1$$

$$q_{canopy} = Sn_f q_s\left(T_{snf}\right) + \left(1 - Sn_f\right) q_s\left(T_f\right)$$

$$q_{surf} = Sn_g q_s\left(T_{sng}\right) + \left(1 - Sn_g\right) f_h q_s\left(T_1\right)$$

Where f_h is the relative humidity at the soil surface, q_s denotes the saturated specific humidity, and $T_{snf}, T_{sng}, T_f, T_1$ are snowy-vegetation, snowy-bare-soil, snowless-vegetation and snowless-bare-soil surface temperatures, respectively.

8.3.3. Conductive fluxes in the snow pack

Heat fluxes can be transmitted to the snow from both canopy and bare soil by conduction. According to Fourier's law, these contributions have been parameterized as:

$$Q_{snf} = 2\mathrm{K}_{snf} Sn_f \frac{T_{snf} - T_f}{h_{snf} + h_f}$$

$$Q_{sng} = 2\mathrm{K}_{sng} Sn_g \frac{T_{sng} - T_1}{h_{sng} + d_1}$$

For vegetation and bare soil, respectively. The thermal conductivities K_{snf} and K_{sng} are evaluated as weighted averages between the surface and the snow thermal conductivities by using the following equations:

$$K_{snf} = \frac{h_f K_f + h_{snf} K_{sn}}{h_f + h_{snf}}$$

$$K_{sng} = \frac{d_1 K_1 + h_{sng} K_{sn}}{d_1 + h_{sng}}$$

Where $K_f = 6\ 10^{-4} LAI\,[W\,m^{-1}K^{-1}]$ and K_1 (eq. 12.3) are the thermal conductivities of vegetation and bare soil, respectively; the snow conductivity, following Dingman (1994), has been expressed in function of the snow density ρ_{sn} as:

$$K_{sn} = C_1 (\rho_{sn}/\rho_w)^{1.88}$$

With $C_1 = 2.22\,W\,m^{-1}K^{-1}$ (note that the dependence of K_{sn} by ρ_{sn} is similar to the formulation of Gel'fan (1989)) for both vegetated and bare soil components (using the respective snow density). These formulations, despite their greater simplicity with respect to those used in other models (see for instance Cox et al. (1999)), have been

selected in UTOPIA because the energy involved in the conductive heat flux exchange between the snow and the underlying surface is generally low, thus the error can be considered small.

The heat flux transmitted to the snow pack by rainfall when it rains over snow at a rate of $P_{g\_on\_snow}$, and Q_{rain} is given by:

$$Q_{rain} = \rho_w c_w P_{g\_on\_snow}(T_a - T_{sn}) + \rho_w C_{Lf} P_{g\_on\_snow}$$

Where last term of this equation occurs only when $T_{sn} < 273.15\,°C$ and the rain temperature is assumed to equal the air temperature at raingauge (or snow-gauge) level T_a, and the rainfall rate over snow is given by $P_{g\_on\_snow} = Sn_f\left(P_a - P_f + D_f\right)$.

$\Delta Q_{av} > 0$	$\Delta Q_{av} < Q_{warm}$	$\Delta T_s > 0$, $T_s < 0$ °C increases	Phase 1
		$h_w = 0$	
		h_m remains constant	
	$\Delta Q'_{av} < Q_{ripe}$	$T_s \rightarrow 0$ °C	Phase 2
	$\Delta Q_{av} \geq Q_{warm}$	$\Delta h_w > 0$, $h_w < h_{wret}$ increases	
		h_m remains constant	
	$Q_{ripe} \leq \Delta Q'_{av} < Q_{melt,tot}$	$T_s \rightarrow 0$ °C	Phase 3
		$h_w \rightarrow h_{wret}$ increases	
		$\Delta h_m < 0$, h_m decreases	
	$\Delta Q'_{av} \geq Q_{melt,tot}$	melt of all snow	Phase 4
$\Delta Q_{av} < 0$	$\lvert\Delta Q_{av}\rvert < Q_{solid}$	$T_s < 0$ °C remains constant	Phase 5
		$\Delta h_w < 0$, h_m decreases	
		h_m remains constant	
	$\lvert\Delta Q_{av}\rvert > Q_{solid}$	$\Delta T_s < 0$, $T_s < 0$ °C decreases	Phase 6
		$h_w \rightarrow 0$	
		h_m remains constant	

Tab 1: Summary of processes affecting snow pack depending on available energy

8.4. THERMAL BALANCE IN THE SNOW PACK

The snow pack temperature T_{sn} is supposed to be uniform at its interior: this option is certainly reasonable for the snow cover above vegetation, which will not exceed a certain amount, while it may be rough for the snow cover above bare soil, which may be quite deep. However, this is a basic assumption in UTOPIA. The behavior of T_{sn}

depends on the energy balance. According to the value of the available energy ΔQ_{av} (eq. 8.9), it is possible to evaluate the snow temperature T_{sn} using the scheme reported in Table 1. In particular, in the phase 1, if there is not any liquid water inside snow pack and $T_{sn} < T_m$, the latter being the ice melting point $(T_m = 273.15\,°C)$, and when the available energy ΔQ_{av} is lower than the energy Q_{warm} required to warm up the whole snow pack up to the temperature T_m, the snow pack temperature would increase by:

$$\Delta T_{sn} = \frac{\Delta Q_{av}}{\rho_w h_m c_i}$$

Where c_i is the specific heat of ice.

If the available energy is negative $(\Delta Q_{av}) < 0$ and its absolute value is larger than the energy Q_{solid} required to refreeze all liquid water inside snow pack, then the energy deficit is used to cool the snow pack by the quantity:

$$\Delta T_{sn} = -\frac{|\Delta Q_{av}| - Q_{solid}}{\rho_w h_m c_i}$$

When new snow is precipitating at the rate $P_{sn}[m\,s^{-1}]$, the resulting temperature is assumed as the average between the temperature of falling snow (assumed to be equal to the air temperature T_a and T_{sn}, weighted by the water equivalent increment caused by snowfall P_{sn} and the actual snow water equivalent:

$$T_{sn}^{n+1} = \frac{(P_{sn}\Delta t)\,T_a + h_m T_{sn}^{n}}{P_{sn}\Delta t + h_m}$$

Where it has been indicated explicitly the time relative to the variable T_{sn} ('*n*' refers to the present value and '*n+1*' to the future value).

8.5. HYDROLOGICAL BALANCE IN THE SNOW PACK

By close analogy with the thermal balance, the scheme of Table 1 can also be used to predict the water equivalent, the liquid water content of the snow pack, and the runoff, if one (Dingman (1994)). The proposed scheme has a similar structure to that proposed by Sun et al. (1999). The snow depth is calculated at each time step by inverting the equation 8.1. If the available energy ΔQ_{av} is positive, the (excess) energy $\Delta Q'_{av} = \Delta Q_{av} - Q_{warm}$ will be considered. The following three possibilities arise:

a. $\Delta Q'_{av} < Q_{ripe}$ (phase 2): in this case, the available energy is lower than the energy Q_{ripe} required for saturating completely the snow pack. In this circumstance the water equivalent h_m is kept constant, while the liquid water content h_w increases by:

$$\Delta h_w = \frac{\Delta Q'_{av}}{\rho_w \lambda_f}$$

But remains lower or equal than its maximum value h_{wret} (eq. 8.4);

b. $Q_{ripe} \le \Delta Q'_{av} < Q_{melttot}$ (phase 3): in this case, the available energy is larger than Q_{ripe} but lower than the one required for the complete melting of the snow pack ($Q_{melt,tot}$, eq. 8.6). The water equivalent decreases by the quantity:

$$\Delta h_m = -\frac{\Delta Q'_{av} - Q_{ripe}}{\rho_w \lambda_f}$$

While the liquid water content in the snow pack is forced to approach the riped value ($h_w = h_{wret}$). The exceeding water equivalent is considered as runoff.

c. $\Delta Q'_{av} \geq Q_{melttot}$ (phase 4): in this case the whole snow pack will melt.

If the available energy is negative, the water equivalent h_m doesn't change, thus there is not runoff. Two possibilities arise, according to the value of ΔQ_{av} compared with Q_{solid} (eq. 8.7):

a. $|\Delta Q_{av}| < Q_{solid}$ (phase 5): the available energy is insufficient to refreeze all liquid water, if any. The liquid water content decreases by the quantity:

$$\Delta h_w = -\frac{|\Delta Q_{av}|}{\rho_w \lambda_f}$$

b. $|\Delta Q_{av}| \geq Q_{solid}$ (phase 6): all liquid water solidifies, thus $h_w = 0$.

When new snow is precipitating at the rate P_{sn} , the water equivalent is incremented by the quantity $h_m^{n+1} = h_m^n + P_{sn} \Delta t$.

When it rains over the snow pack at the rate $P_{g\_on\_snow}$, the liquid water content h_w of snow pack is incremented up to the value h_{wret} , the remainder of water being expelled as runoff:

$$\Delta h_w = P_{g\_on\_snow} \Delta t \leq (h_{wret} - h_w)$$

In this case, also the water equivalent content is incremented by the same value: $\Delta h_m = \Delta h_w$.

Finally, in the case in which the water equivalent content decreases, the runoff can be calculated as:

$$R_{sn}^{n+1} = R_{sn}^{n} + \left(h_m^n - h_m^{n+1}\right) \quad if\ h_m^n > h_m^{n+1}$$

Furthermore, the contribution coming by eventual rainfall exceeding ripe snow should be also added:

$$R_{sn}^{n+1} = R_{sn}^{n} + \begin{Bmatrix} P_{g\_on\_snow}\Delta t - \left(h_{wret} - h_w\right) & if \quad h_w > h_{wret} \\ P_{g\_on\_snow}\Delta t & if\ h_w \le h_{wret} \end{Bmatrix}$$

8.6. SNOW COMPACTATION AND DENSITY

Since the snow height h_{sn} is used in UTOPIA to evaluate some parameters (such as the roughness length), it is important to obtain an accurate physical description of this variable. This parameter is defined by equation 8.2, and it is evident that h_{sn} is strongly related to the value of the snow density ρ_{sn}. The snow compaction is a complex process because it depends not only from the actual values of some snow parameters (height, temperature, liquid water content, etc.), but also from the "history" of the snow pack. Several parameterizations used in literature have been compared in this study. The formulation of Verseghy (1991), in which the snow density is assumed to increase exponentially (about 10 days are needed to have a complete compaction), has been initially used. Nevertheless, the obtained results seemed not sufficiently realistic, since this formulation is independent from the snow temperature.

Then, the formulation of Anderson (1976) was tested, which has been adapted in the models of Sun et al. (1999) and Koren et al. (1999). In the former, the destructive metamorphism, the densification process and the snow melting are considered separately, while in the latter case there is a general equation for the snow compaction and a specific equation accounting for the new

snow. After some numerical tests, it has been decided to use an adapted version of the parameterization reported in the Koren et al. (1999) model, which will be resumed here shortly.

According to Anderson (1976), the change of snow density due to compaction can be expressed as:

$$\frac{1}{\rho_{sn}(z)}\frac{d\,\rho_{sn}(z)}{dt}=C_1 h_m(z)\exp[C_2 T_{sn}(z)-C_3\rho_{sn}(z)] \tag{8.10}$$

Where C_1 is the fractional increase in snow density per unit water equivalent of load per unit time at the temperature $T_{sn}(z)=0\,°C$ and density $\rho_{sn}(z)=0$ while C_2 and C_3 are observational constants. Since UTOPIA usually uses $\Delta t<60\,s$, if a short integration time like this one is considered, the r.h.s. of eq. 8.10 can be supposed constant in this time interval, thus snow density can be integrated over time. The average snow density of the snow pack, composed by a single snow layer, can be expressed by the integration of the previously obtained solution over the snow depth h_{sn}, giving:

$$\rho_{sn}^{n+1}=\rho_{sn}^{n}+\frac{\exp\{\Delta t\,C_1\exp[C_2 T_{sn}-C_3\rho_{sn}^{n}]\,h_m\}-1}{\Delta t\,C_1\exp[C_2 T_{sn}-C_3\rho_{sn}^{n}]\,h_m}$$

The value of the coefficient C_1 selected for UTOPIA was higher than that suggested by Anderson (1976), i.e. $C_1=2.78\,10^{-5}\,m^{-1}s^{-1}$, and by Kojima (1967), i.e. $C_1=7.22\,10^{-4}\,m^{-1}s^{-1}$. After several numerical tests, the value $C_1=2.78\,10^{-3}\,m^{-1}s^{-1}$ has been adopted. For the other two constants, the values suggested in the paper of Anderson (1976), i.e. $C_2=0.08\,°C^{-1}$ and $C_3=0.021\,m^3kg^{-1}$ have been selected.

Since new snowfalls also affect snow density and depth, snow density is assumed to vary during snowfall/snowmelt according to the following expression (adapted by Koren et al. (1999)):

$$\rho_{sn}^{n+1} = \frac{\rho_{sn}^{n} h_m + \rho_{sn\_new} P_{sn} \Delta t}{h_m + P_{sn} \Delta t}, \qquad \rho_{snmin} \le \rho_{sn}^{n+1} \le \rho_{snmax}$$

Where the density of the new snowfall ρ_{sn_new} is estimated on the basis of the air temperature T_a as (Gottib (1980)):

$$\rho_{sn\_new} = \rho_{snmin} + 17(T_a + C_4)^{1.5,} \qquad \rho_{snmin} \le \rho_{sn\_new} \le \rho_{snmax}$$

With $C_4 = 15\,K$. Minimum and maximum thresholds for snow density have been assumed respectively as $\rho_{snmin} = 50\,kg\,m^{-3}; \rho_{snmax} = 400\,kg\,m^{-3}$ (Dingman (1994); Koren et al. (1999); Douville et al. (1995)).

8.7. SNOW COVERAGE

The snow coverage is one of the most important physical parameters in the snow scheme. In fact, snow coverage is an important parameter needed to determine the correct share of incoming and outgoing radiative energy and of the turbulent and conductive heat fluxes. A small error in the evaluation of the snow coverage can produce significant errors in the evaluation of the snow pack despite other sophisticated snow processes parameterisations.

Due to the importance of this parameter, a great attention to its formulation has been made. As starting point, a crude linear regression to the observed snow depth h_{sn} and

the observed coverage Sn gathered in 6 Siberian stations (Ruswet experiment[1], Robock et al. (1995), where surface vegetation is short grass) has been applied. By considering only the Sn values lower than 100% (see Fig. 8.3), the following regression lines has been obtained:

$$Sn = C_1 h_{sn} \tag{8.11}$$

$$Sn = C_2 h_{sn} + C_3 \tag{8.12}$$

With $C_1 = 8.34\, m^{-1}$, $C_2 = 3.78\, m^{-1}$ and $C_3 = 0.44$. By analyzing the behavior of the above equations (and also their plot shown in Fig. 8.3), it is possible to notice that, in case of short grass, (as in the Siberian stations), the observed threshold value of snow height above which the 99% snow coverage is reached lies in the range 12-15 cm. Comparing between each other the two eqq. (8.11) And (8.12), it is possible to see that the former gives a more realistic value for low snow heights, tending to zero, while the latter assumes $\lim_{h_{sn} \to 0} Sn = C_3$, which is unrealistic. Thus, the relation (8.11) will be used as reference for sake of comparison with the other following formulations.

1 Web site for Ruswet data: http://www.meto.umid.edu/~alan/soil_moisture/ruswet.forcing.6sta.readme.html.

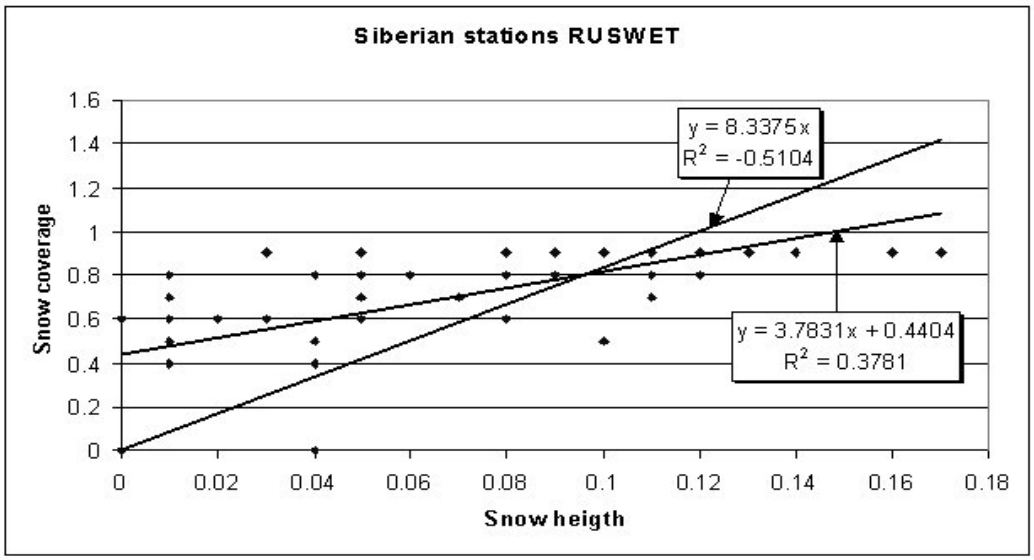

Figure 8.3: Regression lines between (non-fully) snow coverages and snow heights in the Russian stations of RUSWET dataset.

Many models evaluate snow coverage in a simple way, not taking into account the type of surface that is covered by snow. For instance, the formulation of Blondin (1988), used also in the ECMWF GCM, calculates the snow coverage as:

$$Sn = \frac{h_m}{h_{m,max}} \leq 1 \tag{8.13}$$

Where $h_{m,max}$ is the threshold above which full coverage is get. This equation can be considered realistic in the case in which the surface vegetation is composed by shrubs, because the snow equivalent corresponding to 99% coverage is about 0.07 m, i.e. roughly $h_m \simeq 0.7\,m$ if an average snow density of 100 kg m^{-3} is considered. But this formulation seems clearly inadequate if other kind of surface cover, like forests or short grass, is considered.

For this reason, it has been decided to analyse other relationships in which the dependence of the surface type is included. A good way to include the surface

characteristics is obtained by including the surface roughness length z_0 in its formulation. For instance, the equation taken from Douville et al. (1995) and used in their land surface scheme ISBA1, reads as follows:

$$Sn = \frac{h_s}{h_s + 5z_0} \leq 1 \tag{8.14}$$

and is similar to the one proposed by Yang et al. (1997):

$$Sn = \frac{h_s}{h_s + 10z_0} \leq 1 \tag{8.15}$$

The only difference being in the z_0 multiplying coefficient. The inclusion of z_0 in the equations (8.14) and (8.15) makes they suitable to be used in the determination of snow coverage of vegetation and bare soil separately, according to their different values of z_0. However, these expressions have been designed to work mainly in the GCMs, in which generally each grid box of the domain covers a large area and is strongly inhomogeneous. By trying to verify the correctness of these formulations comparing their predictions over short grass, it is possible to see (fig. 8.4) that equation (8.14) predicts $h_{sn} \simeq 5.1\,m$ for 99% coverage over a short grass field (if $h_f = 8\,cm$, then $z_{0f} = 0.13 h_f = 10.4\,mm$), and equation (8.15) predicts, in the same conditions, $h_{sn} \simeq 10.3\,m$, values which looks unrealistic with regards to equation (8.11) or fig. 8.3, for which the snow height corresponding to $Sn = 0.99$ is $h_{sn} = 0.99 / C_1 = 12\,cm$.

For this reason, it has been decided to work out an alternative formulation, which is derived in detail in the next subsection, and whose final equation (eq. (8.17)) has been rewritten here for sake of convenience:

$$Sn = \frac{0.26\,h_{sn}}{z_0} - \frac{0.0169\mathrm{h}_{sn}^2}{z_0^2} \le 1 \qquad for \quad h_{sn} \le \frac{z_0}{0.13}$$

Where the numerical coefficients are dimensionless, and the roughness length is related to the type of surface (bare soil, vegetation). Using this formulation, the 99% snow coverage over a short grass field occurs with $h_{sn} \simeq 7\,cm$, a value slightly lower but comparable with the about 12 cm given by eq. (8.11). The behaviour of all equations discussed in this section is shown in Fig. 8.4, and also comparing the various trends it is evident that eq. (8.17) performs better than others. On the basis of this discussion, eq. (8.17) has been selected in UTOPIA to parameterize the snow coverage.

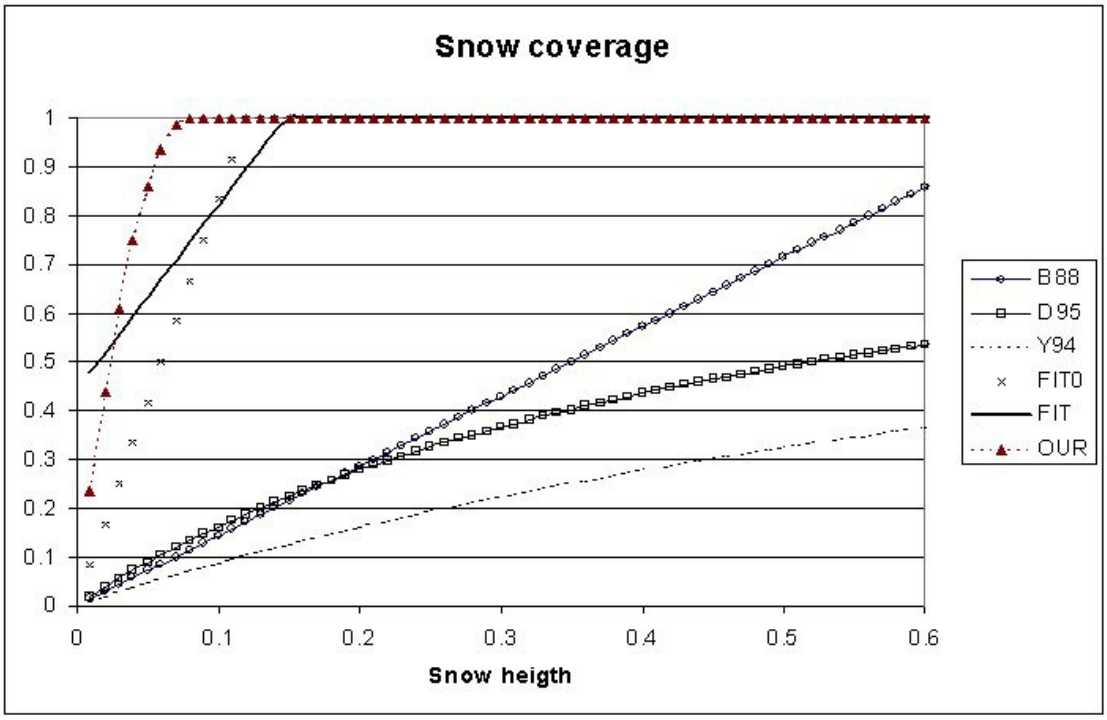

Figure 8.4: Behavior of the different parameterizations of the snow coverage. In this plot, FIT0 refers to eq. (8.11), FIT to eq. (8.12), B88 to eq. (8.13), D95 to eq. (8.14), Y94 to eq. (8.15), and OUR to eq. (8.17).

8.7.1. The algorythm proposed for the snow cover in UTOPIA

Looking at Fig. 8.5, the basic hypotheses for this derivation are that the roughness elements can be considered as regular pyramids of square area whose side is l and whose depth is h, and that snow doesn't adhere to oblique surface but simply fill the space between pyramids according to its depth h_{sn}. In these conditions, according to the geometry of Fig. 8.5, it can be written:

$$tg\,\theta = \frac{h_{sn}}{y} = \frac{2h}{l}$$

And, for a pyramid, the area covered by snow can be evaluated as:

$$A_{sn} = l^2 - (l - 2y)^2 = \frac{2l^2 h_{sn}}{h} - \frac{l^2 h_{sn}^2}{h^2}$$

Now, the ratio between the area covered by snow (A_s) and total pyramid area (l^2) gives the snow coverage relative to the pyramids:

$$Sn = \frac{2h_{sn}}{h} - \frac{h_{sn}^2}{h^2} \tag{8.16}$$

That is obviously valid only for $h_{sn} < h$ (otherwise $Sn \to 1$). Since it is more easily to use the roughness length z_0 instead of element's depth h, using eq. 4.8, it is possible to rewrite the eq. (8.16) for the snow cover in function of the roughness length as:

$$Sn = \frac{0.26\,h_{sn}}{z_0} - \frac{0.0169\,h_{sn}^2}{z_0^2} \qquad if \quad h_{sn} \le \frac{z_0}{0.13} \tag{8.17}$$

Where h_{sn} and z_0 are given in m.

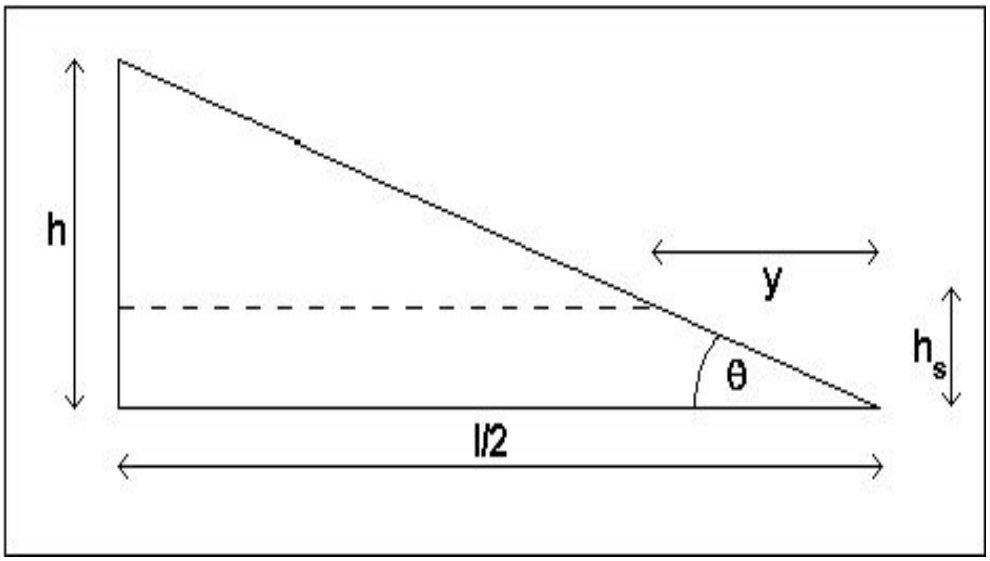

Figure 8.5: Geometry of a snowy surface

8.8. SNOWFALL

When the snow scheme becomes a part of a land surface process simulation model, as in this case, it is necessary to establish a method to provide, in default of direct observations of snowfall, the amount of precipitation that has to be considered as snow.

The method used in UTOPIA is the following. In presence of precipitation $(P_a > 0)$, it is supposed to have snowfall $(P_{sn} = P_a)$ if the following two conditions are verified:

$$T_{aw} < T_{snow\_threshold} \quad \text{and} \quad P_a > 0 \tag{8.18}$$

Where $T_{snow\_threshold}$ is the wet bulb temperature threshold between rainfall and snowfall, assumed equal to 1 °C.

Despite the approximation given by eq. (8.18) is rather crude, it has proven to be satisfactory not only in the extreme Siberian climatic conditions, but also in the Alpine weather, where the model has been tested. It is also necessary to remember that this assumption will work only during off-line simulations because, when the UTOPIA (and its snow subscheme) will become a component of an atmospheric circulation model, this assumption is not necessary as the snowfall rate will be provided by the parent model.

The presence of snow will be accounted, in the model, by the logical variable *LSNOW*, that will assume a positive value if:

- there is old snow, or
- it is snowing now, or
- there is frost on soil/canopy

9. The soil freezing

The soil temperature and moisture are calculated by solving the eqq. 5.2 and7.1, in which the variable η will be here rewritten as η_w for indicating that it refers to the liquid water. More specifically, the variable $\eta_w [m^3_{water} m^{-3}_{soil}]$ indicates the volumetric soil (liquid) content, while $\eta_i [m^3_{ice} m^{-3}_{soil}]$ the volumetric soil ice content, and $\eta = \eta_w + \eta_i$ their sum, or the total water content of the soil. The soil saturation ratio $q = \eta_w / (\eta_s - \eta_i)$ indicates, instead, the degree of saturation only of the liquid water component, considering that a part of the soil porosity $\eta_s [m^3_{voil} m^3_{soil}]$ is occupied by ice.

The actual version of UTOPIA includes three formulations in order to consider the soil freezing. These parametrizations, who can be selected by specifying a code, are here briefly described.

If no soil freezing scheme is selected, η_i is kept equal to zero for all simulation (thus $q \rightarrow \eta_w / \eta_s$). Otherwise, volumetric soil water and ice contents are calculated separately.

9.1. THE PARAMETERIZATION OF SC01

This formulations, due to Schrödin and Heise (2001), considers the freezing from the energetic point of view. Practically, when in each soil layer the increasing (decreasing) temperature crosses the 0°C isotherm, the energy ΔE due to the melting (freezing) of ice (liquid water) into soil allows to calculate both the variation of soil ice content

$\Delta\eta_{i,max}$ (liquid water $\Delta\eta_{w,max}$), and the consequent variation of effective temperature of the soil layer. The formulations are the following:

$$\Delta\eta_{w,max} = -\Delta\eta_{w,max} = \frac{\Delta E}{L_f \rho_w}$$

$$T = T_0 + (\Delta\eta_i - \Delta\eta_{i,max}) \frac{L_f \rho_w}{(\rho c)_s \Delta z}$$

Where Δz is the depth of soil layer considered and T_0 is the threshold temperature for snow fusion (assumed equal to 0°C).

The advantage of this method is that it conserves the energy, while the disadvantage is the imposition of a fixed threshold (T_0) for the water-ice transition.

9.2. THE PARAMETERIZATION OF VI99

This formulations, due to Viterbo et al. (1999), considers the contribution of the latent heat of fusion L_f directly in the prognostic equation for the soil temperature:

$$(\rho c)_s \frac{\partial T}{\partial t} = \frac{\partial}{\partial z}\left(\lambda \frac{\partial T}{\partial z}\right) + L_f \rho_w \frac{\partial \eta_i}{\partial t} \tag{9.1}$$

Where ρ_w is the water density. The soil ice content depends on the temperature *T* and on the volumetric soil water content at the field capacity η_{wf} according with the relation:

$$\eta_i = f(T) f_v \eta_{wf} \tag{9.2}$$

Where the function *f(T)* is defined as:

$$f(T)=\begin{cases} 0 & if \quad T>T_1 \\ 0.5\left[1-\sin\left(\pi\dfrac{T-0.5\,T_1-0.5\,T_2}{T_1-T_2}\right)\right] & if \quad T_2\le T\le T_1 \\ 1 & if \quad T<T_2 \end{cases} \tag{9.3}$$

In this relation, f_v is the vegetation cover and normally the two tunable parameters assume the values $T_1=0\,°C\,; T_2=-3\,°C$.

Including eqq. (9.2) and (9.3) into eq. (9.1), the final formulation is thus:

$$\left[(\rho c)_s-L_f\rho_w\eta_f\frac{\partial f}{\partial T}\right]\frac{\partial T}{\partial t}=\frac{\partial}{\partial z}\left(\lambda\frac{\partial T}{\partial z}\right)$$ lambda o KT?

In which it is evident that the contribution of the freezing of the liquid water in the soil consists in modifying the thermal capacity of the soil.

The advantage of this method is the introduction of a temperature interval $(T_1 \div T_2)$ for the water-ice transition, while the disadvantages are mainly two: the soil temperature is not strictly related to the energy released or assumed, and the presence of the factor f_v limits the maximum quantity of soil ice in the non-vegetated soils.

9.3. THE PARAMETERIZATION OF BO10

In the formulation of Bonanno et al. (2010), the equation (9.2) for the evaluation of soil ice content is modified in the following way:

$$\eta_i=f(T)\eta-\eta_{w,min}$$

Where $\eta_{w,min}$ is the minimum quantity of water into soil and η is the total (liquid plus ice) volumetric soil water content.

The advantages of this parameterization are that, in the derivative of η_w , there is a term related to the derivative of the soil water content (not present in the original formulation), while the unrealistic dependence from the vegetation cover f_v has been eliminated. The disadvantage, common with the original parameterization, is that the soil temperature is still not strictly related to the energy released or assumed.

10. The datasets

10.1. THE DATASET FOR THE VEGETATION PARAMETERS

Variable	Unit	Symbol
Vegetation cover	$m^2 m^{-2}$	f_v
2nd dimension of the leaf	m	d_f
Vegetation albedo	--	$\alpha_{f,sw}$
Minimum stomatal resistance	$s m^{-1}$	r_{min}
LAI, Leaf Area Index	$m^2 m^{-2}$	LAI
Vegetation height	m	h_f
Vegetation emissivity	--	ϵ_f
Vegetation root depth	m	d_R

Tab 2: Vegetation parameters required by UTOPIA

Table 2 reports the list of parameters for the vegetation directly required by UTOPIA. These parameters can be initialized in three ways:

- Giving the values for each parameter (these values are initialised in the parameter file);
- Taking most of the values from the global dataset of Wilson and Henderson-Sellers (1985): in this case, only vegetation code is required;
- Taking most of the values from Ecoclimap database (Masson et al. (2003)).

These methods will be shortly described here.

10.1.1 Direct initialization

This is the simplest method to initialize all vegetation parameters. All parameters are kept fixed during the simulation and are initialized by reading the value in the parameter file.

10.1.2 The WH85 global database

1 – Crop/mixed farming	2 – Short grass
3 – Evergreen needleleaf tree	4 – Deciduous needleleaf tree
5 – Deciduous broadleaf tree	6 – Evergreen broadleaf tree
7 – Tall grass	8 – Desert
9 – Tundra	10 – Irrigated crop
11 – Semi-desert	12 – Ice cap/glacier
13 – Bog or marsh	14 – Inland water
15 – Ocean	16 – Evergreen shrub
17 – Deciduous shrub	18 – Mixed woodland
19 – Settlement	20 – Dense settlement
21 – Po Valley (SPC)	22 – Grugliasco
23 – Siberia	

Tab 3: List of vegetation codes currently inserted in UTOPIA

Using this method, the following variables are initialized according with a subset of the the database created using integrated data sources including the FAO/UNESCO Soil Map of the World, Oxford Regional Economic Atlas of the USSR and Eastern Europe, and Central Asia and East European map sheets. All values are depending on vegetation code, which is a code who identifies the main vegetation types in the world.

The current dataset used in UTOPIA is an extension of the Land Cover/Vegetation type taken from Dickinson et al. (1986). The original table contained only the first 18 fields, while the subsequent ones were added in successive times (see Tab. 3).

Two subroutines in UTOPIA are dedicated to the archives of the parameters inherent to the vegetation: VEGPAR_FIXED and VEGPAR_VAR. The former is dedicated to the

parameter that do not vary during the simulation (the vegetation height $h_f[m]$, the root depth $d_R[m]$, the typical leaf dimension $d_f[m]$, the shortwave albedo α_f , the emissivity ϵ_f , the Jacquemin and Noilhan (1990) parameter R_{gl} and the height of vegetation $h_f[m]$), the latter to the others (the vegetation cover f_v and the leaf area index *LAI*). According to vegetation types, the values of the variables are reported in table 4.

The root depth d_R is calculated as:

$$d_R = \begin{cases} \frac{h_f}{2} & if\ h_f \geq 0.2\,m \\ 0.1\,m & if\ h_f < 0.2\,m \end{cases}$$

The characteristic dimension of the leaves in the direction of wind flow, d_0 , is calculated, as in Dickinson (1984), as the inverse of the square value of d_f , which is tabulated according with vegetation type (see section 10.1.2):

$$d_0 = 1/d_f^2$$

The vegetation emissivity ϵ_f is evaluated using the longwave albedo $\alpha_{f,lw}$:

$$\epsilon_f = 1 - \alpha_{f,lw}$$

Which derives from the energy conservation equation $\epsilon + \alpha + \tau = 1$ where τ is the transmissivity and, in the wavelength interval considered by UTOPIA, can be considered equal to one.

The subroutine VEGPAR_VAR initializes the variables whose values depend on the annual cycle, parameterized in function of the root zone mean temperature T_s according with the relation:

$$f(T_s) = 1 - [1 - 0.0016(T_{opt} - T_s)^2] \tag{10.1}$$

Vegetation code Variable	1	2	3	4	5	6	7	8	9	10	11	12
$\alpha_{f,lw}$	0.05	0.04	0.03	0.05	0.05	0.05	0.04	0.14	0.05	0.15	0.04	0.18
α_f	0.20	0.26	0.10	0.10	0.20	0.15	0.16	0.30	0.20	0.18	0.25	0.40
h_f	0.8	0.5	10.	10.	8.0	20.	1.0	0.5	0.4	0.6	1.0	0.1
R_{gl}	100	100	30	30	30	30	100	100	100	100	100	100
r_{min}	120	200	200	200	200	150	200	200	200	200	200	200
d_f	10.	5.0	5.0	5.0	5.0	5.0	5.0	5.0	5.0	5.0	5.0	5.0
$f_{v,\mathrm{sum}}$	0.85	0.80	0.80	0.80	0.80	0.90	0.80	0.00	0.60	0.80	0.35	0.00
Δf_v	0.60	0.10	0.10	0.30	0.30	0.50	0.30	0.00	0.20	0.60	0.10	0.00
LAI_{min}	6.0	2.0	6.0	6.0	6.0	6.0	6.0	0.0	6.0	6.0	6.0	0.0
Δ_{LAI}	5.5	1.5	1.0	5.0	5.0	1.0	5.5	0.0	5.5	5.5	5.5	0.0

Vegetation code Variable	13	14	15	16	17	18	19	20	21	22	23
$\alpha_{f,lw}$	0.02	0.01	0.01	0.03	0.03	0.04	0.03	0.02	0.04	0.04	0.04
α_f	0.12	0.14	0.14	0.10	0.20	0.18	0.16	0.17	0.28	0.20	0.25
h_f	0.30	.004	.004	1.00	1.00	8.00	5.00	10.0	0.05	2.00	0.085
R_{gl}	100.	100.	100.	60.	60.	60.	100.	100.	100.	100.	100.
r_{min}	200.	200.	200.	200.	200.	200.	200.	200.	100.	50.	100
d_f	5.0	5.0	5.0	5.0	5.0	5.0	5.0	5.0	5.0	10.0	5.0
$f_{v,\mathrm{sum}}$	0.80	0.00	0.00	0.80	0.80	0.80	0.10	0.00	1.00	0.80	0.00
Δf_v	0.40	0.00	0.00	0.20	0.30	0.20	0.08	0.00	0.20	0.40	0.00
LAI_{min}	6.0	0.0	0.0	6.0	6.0	6.0	6.0	0.0	2.0	6.0	0.0
Δ_{LAI}	5.5	0.0	0.0	1.0	5.0	3.0	3.0	0.0	1.5	5.5	0.0

Tab 4: Distribution of vegetation parameters according with their codes (From Dickinson et al., 1986)

Where both arguments in the brackets must be positive or null, and where T_{opt} is the optimum temperature of vegetation, already introduced for eq. 4.6. In fig. 10.1 is reported

an example of this variation, for the case $T_{opt}=298.15\,K$, which is the most common value.

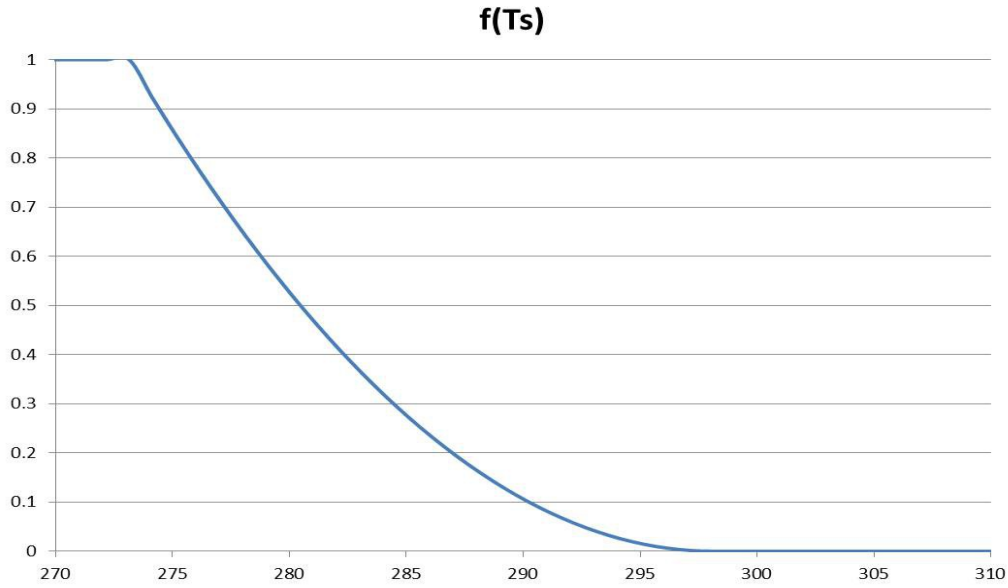

Figure 10.1: Behavior of the function f(Ts) (see eq. 10.1).

The vegetation cover f_v is expressed as:

$$f_v=\begin{Bmatrix} f_{v,\mathrm{sum}} & if\ T_s>298.15 \\ f_{v,\mathrm{sum}}-\Delta f_v & if\ T_s\le 273.15 \\ f_{v,\mathrm{sum}}-\Delta f_v\ \ f(T_s) & if\ 273.15<T_s\le 298.15 \end{Bmatrix}$$

Where $f_{v,\mathrm{sum}}$ represents the maximum summer value and Δf_v the difference between the (summer) maximum and the (winter) minimum values: thus vegetation cover varies between $f_{v,\mathrm{sum}}-\Delta f_v$ and $f_{v,\mathrm{sum}}$.

Finally, the Leaf Area Index (*LAI*) is .parameterized as:

$$LAI=LAI_{min}+\Delta_{LAI}f(T_s)$$

Where LAI_{min} is the (winter) minimum and Δ_{LAI} the (summer) increment, the max value being $LAI_{min}+\Delta_{LAI}$. All values of coefficients are reported in Tab. 4.

10.1.3 The Ecoclimap database

Although some complete datasets of surface parameters, like that above mentioned of Wilson and Henderson-Sellers (1985), which has a resolution of 1°, or the ISLSCP-2 (International Satellite Land Surface Climatology Project), obtained combining observations from satellite in period 1982-1990, are already available, nevertheless the increment of the regional climatic model studies and the increasingly greater resolution required for representing the smaller-scale phenomena need an accuracy greater and greater in the determination of surface parameter values.

Ecoclimap is a global dataset (Masson et al. (2003)) with a resolution of 1 Km^2, created with the aim to be used for the surface parameter initialisation in meteorological and climatic models. This database was constructed by mapping land cover at a resolution of 1 Km^2 using some global databases and world maps (Hansen et al. (2000); Loveland et al. (2000)). The ground cover types were combined with global climatic maps and with the NDVI (Normalized Difference Vegetation Index) index, deduced by NOAA satellite observations. Additional information for Europe was that coming from the projects FIRS (Forest Information from Remote Sensing, CORINE (COoRdination of INformation on the Environment) and PELCOM (Pan-European Land Cover Monitoring). In this way, 125 ecosystems in the extra-European world, and 90 ecosystems in Europe, were found.

It was decided to use the database Ecoclimap in order to allow, in some cases, a more correct initialization of the vegetation and soil surface parameters in UTOPIA. The parameters independent of the annual cycle (percentage of clay and sand in the ground, minimal stomata resistance and root depth) were defined at the beginning of the

simulation. The other parameters (surface emissivity, leaf area index, vegetation cover, vegetation albedo, and roughness length), varying in the course of the year, depend on the date.

It was necessary to introduce in UTOPIA some modifications in order to allow the calculation of some Ecoclimap parameters, because they do not have a direct correspondence with the UTOPIA ones.

As far as the surface emissivity is concerned, UTOPIA distinguishes between vegetation and bare soil emissivity. In the previous parameterisation, the latter was independent of the annual cycle, while the former was calculated according to the soil moisture and type. In the actual parameterisation, total emissivity is extracted from Ecoclimap: being the soil component unchanged, the vegetation component is calculated from the above two values by inverting the weighting averaging procedure:

$$\epsilon_f = \frac{\epsilon_{tot}^{Eco} - (1 - f_v)\epsilon_g}{f_v}$$

In this formula, the snow component is not considered, as albedo in Ecoclimap is computed only for the soil surface (including eventual vegetation): see option SNOW_ALBEDO in next paragraph.

To use Ecoclimap with UTOPIA, it is necessary first to create externally the database. Then, a specific subset of coefficients contained in the external function 'ecoclimap_constant.f90' must be set. If this database will not be used, it is sufficient to include a standard version of the function, provided with the software, as it is required for the compilation of the model. However, this function will not be called.

The following options are suggested for the creation of our database:

- NSCALE (database resolution) equal to 5; the original Ecoclimap database has a resolution of 30” in latitude and longitude, which means approximately 1 km at the latitude of 45°. It is possible to choose the resolution according with the scopes of the work. Higher is the resolution, higher the computation time required to generate the database. NSCALE allows to choice the desired resolution: NSCALE=5 means 5 times the Ecoclimap resolution, i.e. 5 x 30”=150”=2’30” (approximately 5 km at 45°). For the best resolution, set NSCALE=1.
- NTILE (number of tiles) must be set equal to 1, as UTOPIA do not uses tiles.
- NTIME (time resolution) shall be set equal to 36, which means decadal database. The database could be decadal or monthly.
- ZMINLON, ZMAXLON, ZMINLAT, ZMAXLAT (limits of the output box, in degrees) must be selected according with the study zone
- SNOW_ALBEDO (flag to choose albedo on permanent snow and ice) must be set equal to FALSE, as in UTOPIA there is a part of code dealing with the snow albedo. In this case, albedo is computed only for the soil surface, neglecting the fractional part of coverage of permanent snow soil albedo even if there is permanent snow in the grid mesh.

The variables extracted from Ecoclimap are:

- bare soil albedo α_{sd} ;

- vegetation albedo α_f ;
- root depth d_R [m];
- total soil depth d_{TOT} [m]: this variable is actually not used in UTOPIA;
- minimum stomatal resistance r_{min} ;
- sand and clay fractions, from which it is possible to determine the soil type, and then indirectly the soil parameters, using the routines SOIL_TYPE1 and SELECT_SOIL, or to deduce directly the soil parameters, using the routine SAXTON.

10.2. THE DATASET FOR THE SOIL PARAMETERS

There are two methods in UTOPIA to evaluate soil parameters. The first one consists in giving in input to UTOPIA the soil code type, while the second one consists in giving directly the percentage of sand, clay, silt and organic matter of the soil.

In the first method, soil parameters are taken from an extension of the Clapp and Hornberger (1978) table, also using Cosby et al. (1984) paper. The parameters are classified by soil type code, an index that needs to be specified externally. UTOPIA reads the soil type code from the parameter file.

The subroutine SELECT_SOIL assigns the values to soil parameters according with soil type. The variables are: $\eta_s[m^3_{void}\, m^{-3}_{soil}]$ (porosity), $\psi_s[m]$ (saturated moisture potential), $K_{\eta s}[m\, s^{-1}]$ (saturated hydraulic conductivity), b (the exponent for the calculation of non-saturated variables), $\eta_{wi}[m^3_{void}\, m^{-3}_{soil}]$ (the permanent wilting point, in

unit of volumetric water content), $(\rho c)_s [J\,K^{-1}\,m^{-3}]$ (the dry soil thermal capacity per unit of volume) and $q_{fc}[m^3_{water}\,m^{-3}_{soil}]$ (the field capacity, in units of saturation ratio).

Soil code type	Soil type
1	Sand
2	Loamy sand
3	Sandy loam
4	Silt loam
5	Loam
6	Sandy clay loam
7	Silty clay loam
8	Clay loam
9	Sandy clay
10	Silty clay
11	Clay
12	Peat
13	Ice
14	Very pure sand (Niger, Grugliasco)

Tab 5: Soil code types

Concerning the soil types (Tab. 5), UTOPIA considers 14 types of soil textures: the values of the parameters for the first 12 types are taken from Clapp and Hornberger (1978), while the last two were added in Qian et al. (2001). The types of soil are determined from the percentages of sand, silt and clay furnished by Ecoclimap database through the USDA-NCRS (1997) soil triangle (Fig. 10.2).

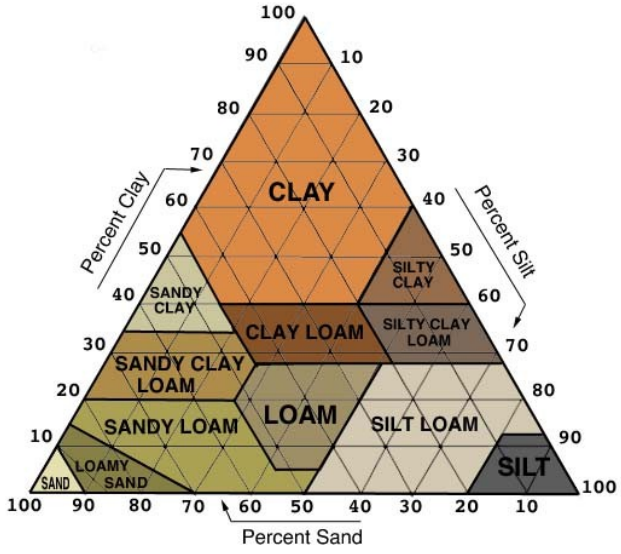

Figure 10.2: he USDA-NCRS (1997) soil textural database

The field capacity q_{fc} is defined as the soil moisture threshold above which the gravitational drainage due to the hydraulic conductivity is able to remove significantly water from the soil. According with Dingman (1994), the soil moisture threshold has been defined as fixed for all soil in terms of soil moisture potential, and equal to $\psi_{fc} = -3.4\,m$. Thus, field capacity in terms of saturation ratio is defined as:

$$q_{fc} = \left[\frac{\psi_s}{\psi_{fc}}\right]^{(1/b)}$$

Values of the parameters are reported into Tab. 6.

Code Var	1	2	3	4	5	6	7
b	4.05	4.38	4.90	5.30	5.39	7.12	7.75
$K_{\eta s}[dm^2 s^{-1}]$	.01760	.01563	.00341	.00072	.00070	.00063	.00017
$\eta_s[m^3_{void}\, m^{-3}_{soil}]$	.395	.410	.435	.485	.451	.420	.477
$\eta_{wi}[m^3_{void}\, m^{-3}_{soil}]$	.0677	.0750	.1142	.1794	.1547	.1749	.2181
$\psi_s[cm]$	-12.1	-9.0	-21.8	-78.6	-47.8	-29.9	-35.6
$(\rho c)[\mu J\, m^{-3} K^{-1}]$	1.465	1.407	1.344	1.273	1.214	1.177	1.319

Code Var	8	9	10	11	12	13	14
b	8.52	10.40	10.40	11.40	7.75	3.20	2.00
$K_{\eta s}[dm^2 s^{-1}]$	.00025	.00022	.00010	.00013	.00080	.03179	0.00555
$\eta_s[m^3_{void}\, m^{-3}_{soil}]$	.476	.426	.492	.482	.863	.355	.4
$\eta_{wi}[m^3_{void}\, m^{-3}_{soil}]$	.2498	.2193	.2832	.2864	.3947	.0212	.0677
$\psi_s[cm]$	-63.0	-15.3	-49.0	-40.5	-35.6	-4.8	-18.
$(\rho c)[\mu J\, m^{-3} K^{-1}]$	1.227	1.177	1.151	1.088	2.094	1.911	1.465

Tab 6: Values of soil parameters according with soil type.

11. Photosynthesis and carbon fixation

In this section, the parameterization of single leaf photosynthesis and respiration implemented in UTOPIA is described in detail. For a more clear description of the argument, and a historical overview on the parameterizations, the reader is referred to Cerenzia (2012). The approach used is the biochemical one, e.g. the more complete one. In this approach, photosynthesis is represented as the slowest among three biochemical processes. Let's make some basic definitions.

11.1. PRIMARY PRODUCTION AND CARBON ASSIMILATION

The Gross Primary Production, GPP, is the total amount of carbon fixed by photosynthesis or, in other words, the amount of carbon sequestered. It is a gross value, because it does not account for the carbon released to environment by the plant respiration processes. To obtain the Net Primary Production, NPP, e.g. the final amount of carbon assimilated, it is necessary to subtract by GPP the total amount of respiration of the plant (dark respiration), which involves leaves, stem and root maintenance and the carbon consumption for plant growth:

$$NPP = GPP - R_{growth} - R_{maintenance}$$

Where:

$$R_{maintenance} = R_{leaf} + R_{stem} + R_{root}$$

In terrestrial ecosystems, GPP and NPP are expressed in units of mass of carbon fixed per unit area and time (so physically they are fluxes). The unit of measurement most often used is $[g_C\, m^{-2} yr^{-1}]$.

Also for the rate of carbon sequestered there is a similar distinction. Let's call $A[\mu mol_C m^{-2} s^{-1}]$ the speed at which carbon is assimilated by photosynthesis. This term includes the carbon released to environment through the respiration. The variable that expresses this difference is A_{net} , obtained subtracting from the gross assimilation rate A the respiration maintenance rate of the leaves R_d :

$$A_{net} = A - R_d \tag{11.1}$$

However, this variable is only a partial result, because it do not takes account of the respiration due to stem and root maintenance and the carbon consumption for plant growth. These last terms are usually estimated from the GPP value. Therefore, if the parameterization aim is to produce an estimate of the total amount fixed in plants, a rescale procedure from A units to GPP units is necessary (see section 11.7.). In the biochemical approach, the photosynthesis is always expressed in terms of the variable A , called ***rate of carbon assimilation*** (or simply ***assimilation***), both at leaf and at canopy level.

11.1. LIMITING FACTORS FOR THE PHOTOSYNTHESIC RATE: C3 PLANTS

The gross rate of carbon assimilation, A , in C3 photosynthesis, is the slowest among the three biochemical processes:

- the Rubisco carboxylation rate in Calvin cycle (A_v) ;
- the RuBP regeneration rate in Calvin cycle (strongly related to the speed of the electron transport chain) (A_j) ;
- the Triose Phosphate utilization rate (A_c) .

The prevailing environmental conditions determine which is the smaller term in photosynthesic mechanism. In the subsequent sections, the three limiting factors for C3 plants will be described in detail.

11.1.1. The Rubisco-limited photosynthesis

This limiting factor is due to the speed at which carbon dioxide is bounded at RuBP in the first section of Calvin cycle. It depends therefore essentially by the Rubisco's kinetic. The possibility that this enzyme catalyzes both carboxylation and oxygenation of RuBP determines a competition of these two processes. This phenomenon is described by the Michaelis-Menten kinetics for an enzyme-catalyzed reaction between a substrate, CO_2 , and a competitive inhibitor, O_2 . In this case, the equation describing Rubisco-limited photosynthesis (Farquhar et al. (1980)) is:

$$A_v = \frac{V_{max}(C_i - \Gamma^*)}{C_i + K_c\left(1 + \frac{O_i}{K_o}\right)}$$

Where V_{max} is the maximum rate of Rubisco activity, C_i and O_i are the intercellular concentrations of CO_2 and O_2 , respectively, K_c and K_o are the

Michaelis-Menten coefficients of Rubisco activity for CO_2 and O_2, respectively, and Γ^* is the CO_2 compensation point in the absence of mitochondrial respiration.

This formulation is based on an historical assumption. It hypothesizes that the difference between C_i, the carbon dioxide concentration in the intercellular spaces, and the concentration in the (chloroplast) stroma, where carboxylation occurs, is negligible (Farquhar and Sharkey (1982)). On the contrary, some authors have argued that this term is significant, and might vary with temperature (Makino et al. (1999)), species and growth conditions. In literature, however, the proper data for every PFT are not available, then the formulation will not be used in UTOPIA.

Since all Rubisco kinetic parameters (K_c, K_o, Γ^*, and V_{max}) are temperature dependent, then temperature responses incorporated into the model are critical for model accuracy (von Caemmerer (2000)). However, K_c, K_o, and Γ^* are thought to be intrinsic properties of the Rubisco enzyme and are generally conserved among species, while it is not the same for V_{max}.

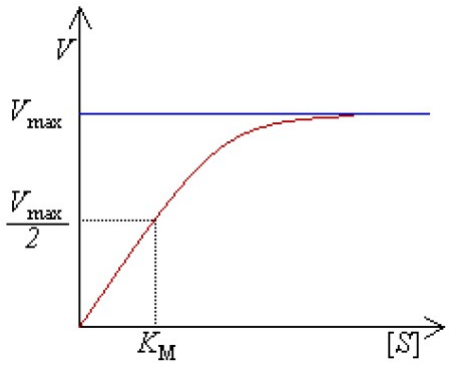

Figure 11.1: Speed of a non competitive reaction as a function of the substrate concentration [S]. V_{max} is the maximum reaction rate, while K_M is the Michaelis-Menten coefficient of the reaction activity. Image source: www.knowledgerush.com/kr/encyclopedia/Enzyme

11.1.1.1. Michaelis-Menten coefficients of Rubisco activity

In general, a Michaelis-Menten coefficient K_M of a reaction activity represents the substrate concentration at which the reaction rate is half of the maximum one (see fig. 11.1). The Rubisco carboxylation is a particular case of reaction because it expresses the competition between the two possible substrates, CO_2 and O_2 . Thus, for each gas exists a Michaelis-Menten coefficient, $K_c[\mu mol\, mol^{-1}]$ and $K_o[mmol\, mol^{-1}]$, respectively, which represent the CO_2 and O_2 concentrations at which the Rubisco carboxylation rate is half of V_{max} .

Both of them depend on leaf temperature: in literature, this relation has been described by different temperature function (Q_{10} , polynomial, exponential or normal).

Farquhar et al. (1980), hereafter F80, suggested the simpliest general relation:

$$K_M(T_f) = K_M(298\mathrm{K})\, Q_{10}^{\frac{T_f - 298\mathrm{K}}{10}} \tag{11.2}$$

Using the Q_{10} function and adapting the original relation in the simple empirical model developed by van 't Hoff (1884). In this relation, $K_M(298\mathrm{K})$ is the value of the parameter at the canopy temperature (T_f) of 298K, and assumes the values $K_c(298\mathrm{K}) = 30\,\mu mol\, mol^{-1}$ and $K_o(298\mathrm{K}) = 30\, mmol\, mol^{-1}$, while $T_{canopy}[K]$ is the canopy surface temperature. The factor Q_{10} is a nondimensional coefficient that represents the increase in reaction rate for every 10K rise in temperature, and assumes the values 2.1 for K_c and 1.2 for K_o . Finally, units are: $K_c(298\mathrm{K})[\mu mol\, mol^{-1}]$ and $K_o[mmol\, mol^{-1}]$.

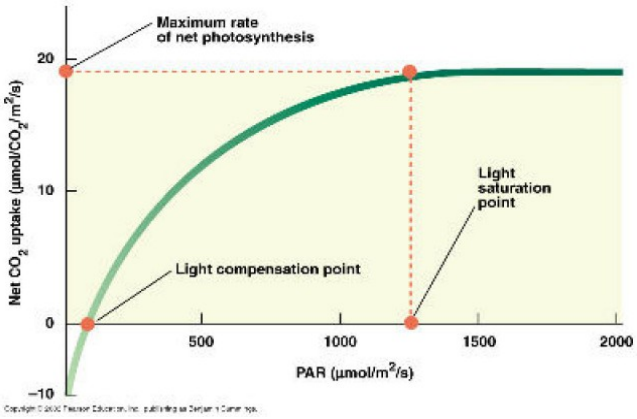

Figure 11.2: The rate of photosynthesis is plotted as a function of the PAR flux density. Note that a negative net CO_2 uptake indicates a loss of carbon due to the respiration. The light saturation point will be descripted subsequently. Image source: Pearson Education, Inc.

A more complex relationship, suggested some years later by Arrhenius (1889), is an exponential equation, which takes account explicitly of the reaction activation energy (that is the minimum energy needed to create the chemical reaction). In this instance, the reaction considered is the Rubisco carboxylation:

$$K_M(T_f) = K_M(298\text{K}) \exp^{\frac{H_a(T_f - 298\text{K})}{298 R T_f}} \tag{11.3}$$

Where $H_a[J\,mol^{-1}]$ is the enzyme activation energy, and $R = 8.314[J\,mol^{-1}K^{-1}]$ is the universal gas constant. Many different values were proposed for H_a, $K_c(298\text{K})$ and $K_o(298\text{K})$, but in general they are derived from *in-vitro* measures. On the contrary, Bernacchi etal. (2001), hereafter B01, obtained their values $H_a(K_c) = 74930$, $H_a(K_c) = 36380$, $K_c(298\text{K}) = 404.9\,\mu mol\,mol^{-1}$ and $K_o(298\text{K}) = 278.4\,mmol\,mol^{-1}$ from in-vivo measurement of transgenic tobacco (with Rubisco content depressed to about 10% of wild type concentration, without any

affection of the enzyme activase). For this reason these parameters values have to be preferred rather than the previous ones.

11.1.1.2. The compensation point

The compensation point $\Gamma^*[\mu mol\, mol^{-1}]$ is the amount of radiation at which the rate of photosynthesis exactly matches the rate of respiration. Therefore, in assimilation terms, at the compensation point, the net carbon dioxide assimilation is zero (see fig. 11.2). Also in this case, there are several parameterizations. In the simplest one (F80), Γ^* is related to K_c and K_o and to the maximum oxygenation activity of Rubisco:

$$\Gamma^* = 0.21 \frac{K_c}{2K_o} O_2$$

While in the most complex one (B01) is described using the same temperature dependence as Michaelis-Menten coefficients of Rubisco activity:

$$\Gamma^*(T_f) = \Gamma^*(298\mathrm{K}) \exp^{\frac{H_g(T_f - 298\mathrm{K})}{298\, R\, T_f}}$$

Where $\Gamma^*(298\mathrm{K}) = 42.74\, \mu mol\, mol^{-1}$ and $H_g = 37830$.

11.1.1.3. Maximum rate of Rubisco carboxylation

$V_{max}[\mu mol\, m^{-2} s^{-1}]$ is the key parameter of the process and is also the most complex to estimate. It varies among species, plants and leaves within a plant, even at a standard temperature (Wullschleger (1993)), and has a complex temperature dependence. V_{max} depends on the total number of Rubisco active sites at a given temperature, and thus on the nitrogen leaf content. However, in UTOPIA it is not possible to include an explicit dependece on the nitrogen leaf concentration, because the nitrogen cycle is not yet

included in the model). The number of Rubisco active sites (and carboxylation events) increases with temperature until an optimum temperature T_{opt}, which varies between plants, but in general is in the range 35-41 °C. Beyond this threshold, the rate of Rubisco carboxylation decreases because of two main reasons. Firstly, at high temperatures the affinity of O_2 relative to CO_2 binding to RuBP in the Rubisco active sites increases rapidly: this fact causes a relative increase of frequencies of oxygenation events. The second reason is that the enzyme loses activity at temperatures higher than the thermal optimum. This happens for two reasons too: from one hand, a more rapid deactivation of Rubisco caused by a faster rate of dead-end product formation;on the other hand, a slower re-activation of Rubisco by activase (Salvucci and Crafts-Brandner (2004)).

V_{max} behaviour as a function of temperature, in particular the Rubisco deactivation, is however currently a focus of debate (Bernacchi et al. (2009)). Among the published datasets, examples exist where the decrease in Rubisco activity is not present. In many cases, this is simply due to the fact that measurements had stopped at temperature lower than the optimum temperature, and that peak value close to 40 °C are statistically difficult to estimate (Medlyn et al. (2002)). In some cases, furthermore, the lack of Rubisco deactivation is explained by the particular experimental conditions (Bernacchi et al. (2002), Bernacchi et al. (2003)).

In the V_{max} parameterizations, the number of Rubisco active sites is set by imposing a measured value of V_{max} at a standard reference temperature. A function normalized to unity at the reference temperature will allow V_{max} values to be determined over a wide temperature range.

In the F80 photosynthesis parameterization, the reference temperature was set to 298K and, moving away from this value, the parameterization accuracy was decreasing. For this reason, to simulate the enzyme deactivation at high temperature, it was suggested a correction which introduces a gradual temperature inhibition at increasing temperatures (Collatz et al. (1991)):

$$V_{max}(T_f) = V_{max}(298\text{K}) \left\{ \frac{1}{1+\exp^{\frac{-a+bT_f}{RT_f}}} \right\} Q_{10}^{\frac{T_f-298\text{K}}{10}} \tag{11.4}$$

With $V_{max}(298\text{K}) = 200\,\mu mol\,m^{-2}\,s^{-1}$ and $Q_{10} = 2.4$, and where a and b are coefficients, whose numerical values are (Oleson et al. (2010)): $a = 220000\,J\,mol^{-1}$ and $b = 710\,J\,mol^{-1}\,K^{-1}$.

Over the years, many other functions have been suggested, but all of these equations are just alternative expressions of two basic functions. Among the others, we may report the modified Arrhenius function (IUPAC (1997), Medlyn et al. (2002)) that, differently from the original function of Arrhenius (1889), takes into account of the decrease in the enzyme activity at high temperature:

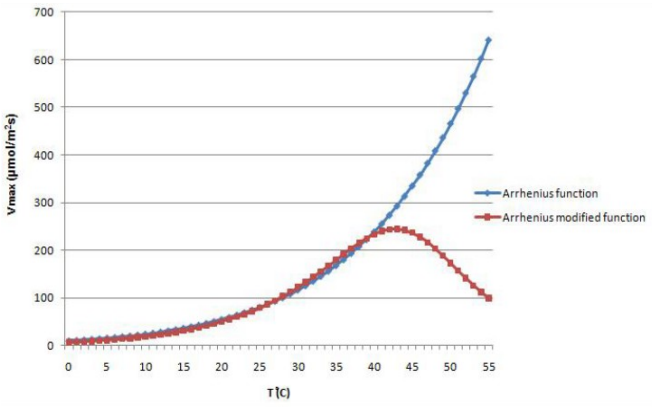

Figure 11.3: Arrhenius and Arrhenius modified function plotted using the coefficients values of a Sessile Oak tree Quercus petraea. Source: Cerenzia (2012), p. 38.

$$V_{max}(T_f) = V_{max}(T_{opt}) \frac{H_d \exp\left[H_a \frac{(T_f - T_{opt})}{T_f R T_{opt}}\right]}{H_d - H_a \left\{1 - \exp\left[H_d \frac{(T_f - T_{opt})}{T_f R T_{opt}}\right]\right\}} \quad (11.5)$$

Where T_{opt} is the optimum temperature [K], expressed as:

$$T_{opt} = \frac{H_d}{\Delta S - R \ln\left[\frac{H_a}{H_d - H_a}\right]}$$

In the two above equations, $H_d [J\,mol^{-1}]$ is the decrease rate of the function above the optimum temperature, $\Delta S [J\,mol^{-1}\,K^{-1}]$ is an entropy factor, and $V_{max}(T_{opt}) [\mu mol\,m^{-2}\,s^{-1}]$ is the value of V_{max} at the temperature optimum.

The formulation reported above limits the growth of the carboxylation rate at increasing temperatures, exponential in the original equation of Arrhenius (1889), showing a peak (see fig. 11.3) that, according with the review reported in Medlyn et al. (2002), fits significantly better the data.

The difficulty of this parameterization is to find the necessary coefficients (6) for every vegetation type.

11.1.2. RuBP–limited photosynthesis

The RuBP molecule is used and regenerated in each Calvin's cycle. The regeneration process requires energy in the form of the energy-carrying molecules ATP and NADPH. They are produced in the first step of the photosynthesis, the light-dependent phase, through the electron transport chain. RuBP regeneration rate is then controlled by the

speed at which the radiative energy is converted into energy-carrying molecules, or otherwise by the electron transport rate.

Over the years, two hypotheses have been proposed to describe this dependence. The older one was suggested by Farquhar and Sharkey (1982):

$$A_j = \phi Q \frac{(C_i - \Gamma^*)}{4(C_i + 2\Gamma^*)} \quad (11.6)$$

Where:

- $\Gamma^*[\mu mol\, mol^{-1}]$ is the CO_2 compensation point and $C_i[\mu mol\, mol^{-1}]$ the intercellular carbon dioxide concentration, already seen in the Rubisco-limited rate;
- $Q[\mu mol_{photons}\, m^{-2} s^{-1}]$ is the absorbed incident photosynthetically active photon flux density, obtained by the equation:

  $Q = 4.5\, 0.4\, R_{sfd}(1 - a_f)$ (3.14)

  where $R_{sfd}[W\, m^{-2}]$ (see section 3.1.), the shortwave radiation incident on the leaf (or on the canopy), is multiplied by 0.4 because, in average, only some 40% of incident radiation is photosynthetically active. The first coefficient, 4.5, is the factor needed to transform the units from $W\, m^{-2}$ to $\mu mol_{photon}\, m^{-2} s^{-1}$ (Murthy (2002)).
- The variable $\phi[\mu mol_{CO2}\ \mu mol^{-1}_{photon}]$ represents the photosynthetic quantum yield, i.e. a measure of the process efficiency. More precisely, it represents the initial slope of the radiation response curve of leaf photosynthesis (eq. 11.2). In C3 plants, the quantum yield varies little among species widely different. However, many published studies contradict this conclusion, reporting quantum yields measurements values with 30% difference, between different species, producing thus some confusion. Comparative studies (Singsaas et al. (2001); Skillman (2009)) had demonstred that this variability is actually due

to particular measurement conditions and/or experiments techniques, that alterate the final results.

The value used in UTOPIA is $\phi = 0.06\,\mu mol_{CO2}\,\mu mol_{photon}^{-1}$ for C3 plants, which approximates the most frequent value measured in past researches. From Oleson et al. (2010).

Theoretically, in C3 plants, the maximum photosynthetic quantum yield is $\phi_{max,C3} = 0.125\,mol_{CO2}\,mol_{photon}^{-1}$, meaning that 8 moles of photons are required to reduce 1 mole of CO_2. This maximum is reached in the absence of photorespiration, which is the major sink of electron transport efficiency and can cause a variation in quantum yield of 30%.

In recent works (Medlyn et al. (2002); Bonan (2002)), a new hypothesis has been used to express the RuBP-limited photosynthesis, in which it is explicitly considered the electron transport rate by introducing the the potential of the whole electron transport chain $J\,[\mu mol\,m^{-2}\,s^{-1}]$ as:

$$A_j = J\,\frac{(C_i - \Gamma^*)}{4(C_i + 2\Gamma^*)}$$

Where J is evaluated as the smallest solution of the algebric 2nd degree equation:

$$\theta J^2 - (\alpha Q + J_{max})J + \alpha Q\,J_{max} = 0 \qquad (11.7)$$

i.e.:

$$J = \frac{(\alpha Q + J_{max}) - \sqrt{(\alpha Q + J_{max})^2 - 4\alpha Q\theta}}{2\theta}$$

Where:

- $\alpha\,[mol_{electron}\,mol_{photon}^{-1}]$ is the quantum yield of the electron transport. It is expressed in mol of electrons transported per incident light quanta and its

value, as ϕ, is quite constant for different plants: $\alpha = 0.385\, mol_{electron}\, mol^{-1}_{photon}$ (Bonan (2002)). The product of α with $\phi_{PSII,max}$, the maximum quantum yield for stable charge separation of Photosystem II, is proportional to the initial slope of the electron transport curve as a function of radiation.

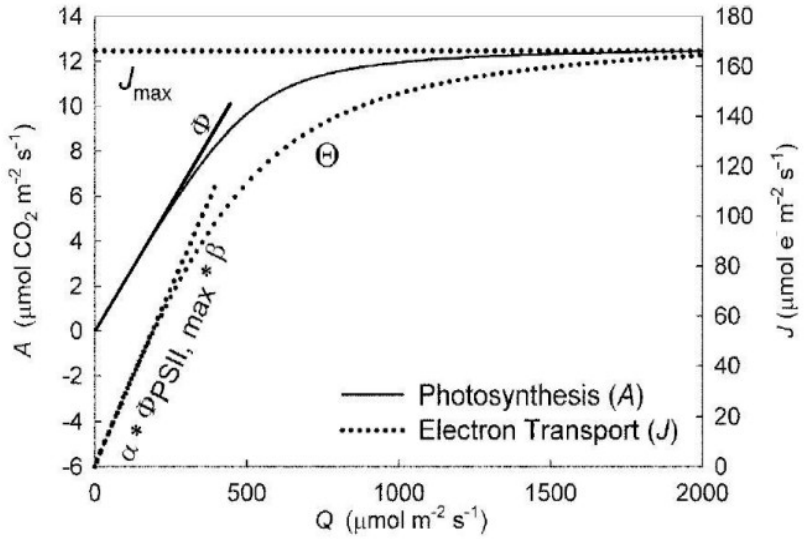

Figure 11.4: Parameters required for modeling RuBP-limited photosynthesis according to Collatz model (1991), solid line, and to Bonan (2002), dashed line, based on the response of electron transport to incident photon flux. β is a constant (Bernacchi et al. (2009)).

- $\theta[non-dimensional]$ is the convexity of the transition between the initial slope and the plateau of the hyperbola (see fig. 11.4). Different modelers have proposed slightly different values for θ. In UTOPIA, the value $\theta = 0.7$ has been chosen as suggested by Bonan (2002), for homogeneity with α.
- $J_{max}[\mu mol_{\text{electrons}}\, m^{-2}\, s^{-1}]$ is the maximum rate of electron transport. Like V_{max}, it can be highly variable among C3 species (Wullschleger (1993)), and for growth conditions; in particular, it depends on the temperature range in which the plant lived. As for V_{max}, the function of Arrhenius (1889) (not shown) and the Arrhenius modified function (IUPAC (1997), eq. 11.8) are the most used formulations to describe the relationship, and, as in the previous

case, the peaked function is preferable in presence of proper coefficient values:

$$J_{max}(T_f) = J_{max}(T_{opt}) \frac{H_d \exp\left[H_a \frac{(T_f - T_{opt})}{T_f R T_{opt}}\right]}{H_d - H_a\left\{1 - \exp\left[H_d \frac{(T_f - T_{opt})}{T_f R T_{opt}}\right]\right\}} \tag{11.8}$$

Where $J_{max}(T_{opt})$ and T_{opt} for J_{max} are determined fitting several experimental dataset, collected on plants grown in different environmental conditions. The optimal temperature for J_{max} is generally in the range 30-38 °C, with no clear pattern among species as visualized in fig. 11.5.

Furthermore, in confirmation of the relationship between J_{max} and V_{max}, it was demonstrated by Wullschleger (1993) that their ratio at 25 °C is quite constant among species, althouth it does vary with temperature in proportion to the ratio of the temperature sensitivities of the components. Therefore, since V_{max} depends on the total amount of the enzyme Rubisco, which in turn depends on the nitrogen leaf concentration, also J_{max} is related to the nitrogen located in the leaf.

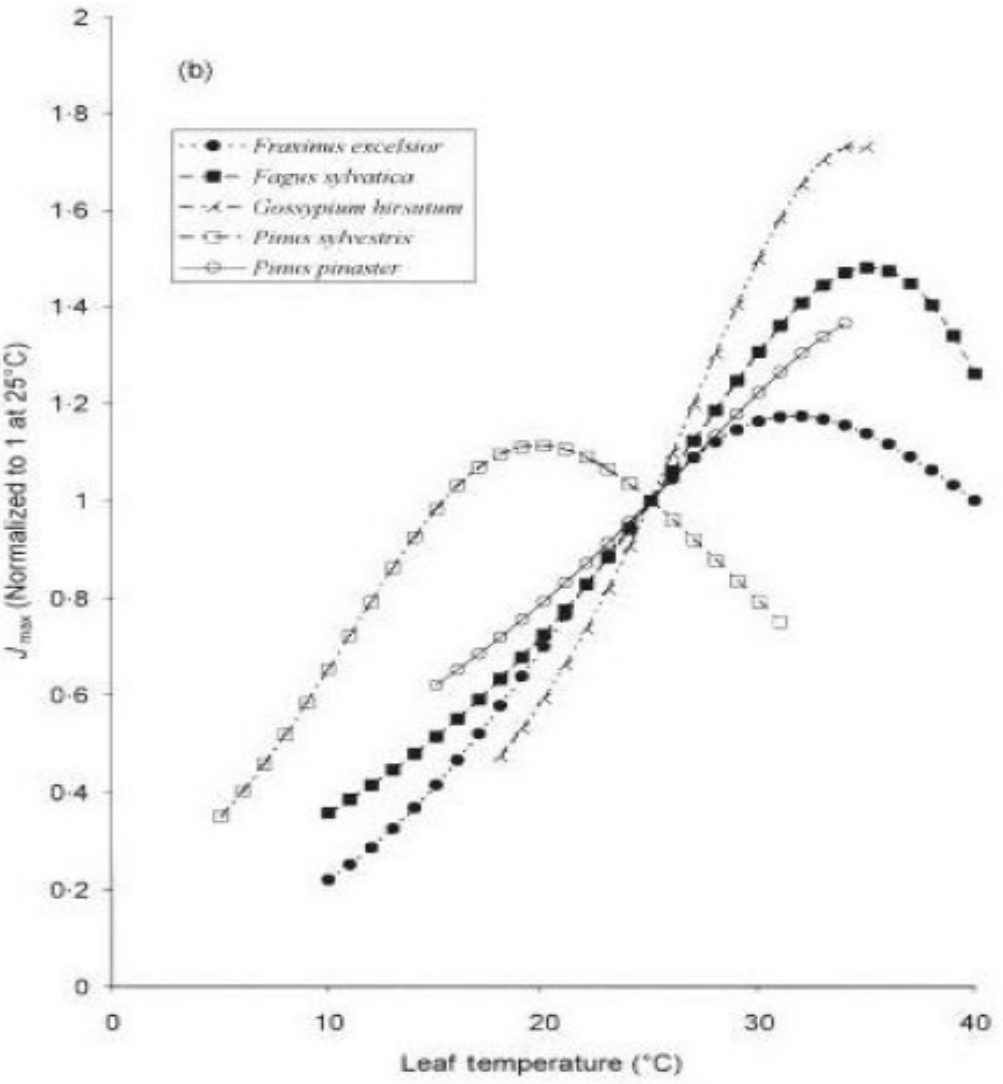

Figure 11.5: Sample responses of J_{max} to leaf temperature. Value are normalized to 1 at 25 °C. From Medlyn et al. (2002).

As visualized from fig. 11.4, the relative importance of these parameters ($\phi_{PSII,max}$, θ and J_{max}) varies with Q : RuBP-limited photosynthesis is more dependent on $\phi_{PSII,max}$ at lower Q , on θ at moderate Q , and on J_{max} at higher Q . While the temperature responses of these parameters are critical to modeling accurately RuBP-limited photosynthesis, $\varphi_{PSII,max}$, and to a lesser extent θ , is more critical at lower Q where photosynthetic rates are low. Thus, the model is generally less sensitive to

errors in these two parameters than those in J_{max} , associated with high photosynthetic rates (Bernacchi et al. (2009)).

11.1.3. Triose Phosphate Utilization-limited photosynthesis

Triose Phosphate is the product of Calvin's cycle; after its creation, it is mainly converted into starch in chloroplast or exported and metabolized to sucrose. If this sugar phosphate is producted at rates higher than it is consumed, then a lack of inorganic phosphate, necessary for the production in the cycle, occurs. This limitation is difficult to detect, but this process is only relevant at very high values of CO_2 concentration low O_2 high irradiance and/or low temperatures: practically, when the two other limiting factors do not act. TPU-limiting factor is parameterized in all models as:

$$A_c = \frac{V_{max}}{2}$$

11.2. LIMITING FACTORS FOR THE PHOTOSYNTHESIC RATE: C4 PLANTS

As for C3 plants, the rate of carbon assimilation also in the C4 simplified model is evaluated as the minimum of three biochemical limiting factors. The first two are the Rubisco and the RuBP limiting rates, while the third one concerns the PEP-carboxylase rate of carboxylation, i.e. the speed at which the enzyme PEP-carboxylase, catalyzes the binding between CO_2 and PEPmolecules, in the cycle preliminary at the Calvin cycle.

11.2.1. RuBP-limited photosynthesis

At rate limited by radiation intensities, the efficiency of CO_2 assimilation, with respect to absorbed light (quantum yield of photosynthesis, φ) determines the rate of

photosynthesis. As for the C3 plants, empirical measurements indicate that the photosynthesis quantum yield is constant for C4 plants over a wide range of conditions (Ehleringer and Björkman (1977); Ehleringer and Pearcy (1983)). Its maximum ($\phi_{max,C4} = 0.067\, mol_{CO2}\, mol^{-1}_{photon}$) is lower than the one of the C3 pathway ($\phi_{max,C3} = 0.125\, mol_{CO2}\, mol^{-1}_{photon}$), although the photorespiration, which is the biggest cause of efficiency loss in C3 plants, is almost absent in C4 pathway. That is mostly due to the greater energy requirement, caused by the initial PEP pump.

The value used in UTOPIA is the one proposed in the CLM, for homogeneity with the one used in C3 plants: $\phi = 0.04\, mol_{CO2}\, mol^{-1}_{photon}$.

The equation which describes the radiation limiting rate, in this case, is suggested by Collatz et al. (1992):

$$A_j = \phi Q$$

This equation is valid under the condition that the CO_2 concentration in the bundle sheath cells is sufficiently high to suppress photorespiration.

11.2.2. PEP carboxylase-limited photosynthesis

PEP carboxylase-limited photosynthesis represents the limitation due to therate of PEP carboxylation in the mesophill cells. This term is relevant at low CO_2 internal concentration, where the photosynthetic rate typically shows a linear increase from the compensation point Γ^* (no molecules of carbon dioxide) to a saturation rate, which occurs at an intercellular CO_2 concentration of about 100 ppm (or a CO_2 partial pressure of 10 Pa). The equation that describes this process is:

$$A_c = \frac{f V_{max} C_i}{p_a}$$

Where V_{max} is, in general, assumed constant: as example, for corn plants $V_{max} = 39\ \mu mol\, m^{-2} s^{-1}$ (Collatz et al. (1992)). $C_i[Pa]$ is the intercellular partial pressure of carbon dioxide and $p_a[Pa]$ represents the atmospheric pressure.

Finally, concerning f, which is a non dimensional coefficient, different authors suggested different values: in literature, it is found the value $f = 18000$, while Sellers et al. (1996) used $f = 20000$. These values cause C4 photosynthesis to saturate at low values of ambient CO_2 concentration (Oleson et al. (2010)). For this reason, in the CLM it is proposed to utilize $f = 18000$, which results in saturation at about $C_a = 400\ ppm$.

11.2.3. Rubisco-limited photosynthesis

Empirical observations have shown that the rate of Rubisco carboxylation is a limiting factor only under conditions of high radiation and high CO_2 internal concentration. The high CO_2 concentration in the bundle sheath chloroplasts is close to saturation for Rubisco, and the rate under which these conditions approach is:

$$A_c = V_{max}$$

Summarizing, at low CO_2 concentration the rate of carbon assimilation is limited by A_c, then A reached the saturation rate and it assumes a constant value equal to A_j or A_v, depending if radiation intensities are or not a limiting factor.

11.3. GROSS AND NET RATE OF ASSIMILATION

As already said before, the net rate of carbon assimilation (A_{net}) is derived from the gross rate (A), subtracting the mitochondrial respiration (R_d) (see section 11.3.1. and eq. 11.1). The gross rate A can be calculated as the minimumof the threlimiting factors previously described:

$$A = MIN\left(A_v, A_j, A_c\right)$$

The limiting factors to photosynthesis in both pathways can be summarized as:

$$A_v = \begin{cases} \dfrac{V_{max}\left(C_i - \Gamma^*\right)}{C_i + K_c\left(1 + \dfrac{O_i}{K_o}\right)} & if\ C_3\ plant \\ V_{max} & if\ C_4\ plant \end{cases}$$

$$A_j = \begin{cases} \left(\phi Q, \text{or } J\right)\dfrac{\left(C_i - \Gamma^*\right)}{4\left(C_i + \Gamma^*\right)} & if\ C_3\ plant \\ V_{max} & if\ C_4\ plant \end{cases}$$

$$A_c = \begin{cases} \dfrac{V_{max}}{2} & if\ C_3\ plant \\ \dfrac{f\,V_{max}\,C_i}{P_{atm}} & if\ C_4\ plant \end{cases}$$

To introduce a more gradual transition from one limitation to another and to allow for some co-limitation between them, many authors (Kirschbaum and Farquhar, 1984; Collatz et al. (1991)) have proposed to use the smallest solution of the subsequent system of equations:

$$\begin{Bmatrix} \theta A_p - A_p(A_v + A_j) + A_v A_j = 0 \\ \beta A^2 - A(A_p + A_c) + A_p A_c = 0 \end{Bmatrix}$$

Where A and A_p are the unknowns; in particular, A_p is only an intermediate variable and represents the smoothed minimum between A_v and A_j . θ and β are empirical non dimensional constants, governing the sharpness of transition between the three limiting rates, and they are typically close to one. In UTOPIA, the values $\theta = 0.8$ and $\beta = 0.8$ have been used (Sellers et al. (1996)). However, the coupling of these quadratic equations with the photosynthesis parameterization implemented (and previuos described), produced anomalous results, even changing θ and β values. Therefore, in UTOPIA, it has been decided to use only eq. 11.1.

Actually, this is not a big problem at a canopy scale, because the co-limtation of factors has a little effect on photosynthesis modelization, since only a small fraction of leaves are near the transition to light saturation at any moment (De Pury and Farquhar (1997)).

11.3.1. Mitochondrial respiration

Mitochondrial respiration R_d is highly temperature dependent, and its optimum temperature, over short timescale (minutes to hours), occurs just below the temperature at which the thermal deactivation of enzyme occurs (generally above 42 °C: Bernacchi et al. (2009)). Historically, R_d is scaled to the maximum rate of Rubisco's carboxylation:

$$R_d = l V_{max}$$

Where l is a non-dimensional constant: $l = 0.015$ for C3 plants (Collatz et al. (1991)) and $l = 0.021$ for C4 plants (Collatz et al. (1992)).

Taking account also of respiration decrease at high temperature, the relationship becomes:

$$R_d = \frac{l V_{max}}{1 + \exp[1.3(T_f - 328.15)]}$$

11.4. CARBON FLUX AND STOMATAL CONDUCTANCE

11.4.1. Intercellular gases concentration

The evaluation of intercellular gas concentration is based on the gas diffusion process from external air to leaf surface and from leaf surface through stomata to intercellular space. The gases concentration flux could be considered, in a electric analogy, as the current between a potential difference. The gases concentration gradient between air, leaf surface and intercellular space guide the transport. Following the electric analogy, every step is characterized by a resistance: laminar leaf resistance and stomatal resistance, respectively. The resistances network is shown in fig. 11.6.

The parameterization usually proposed is:

$$C_s = C_a - 1.37 r_b A_{net} P_a \tag{11.9}$$

$$C_i = C_s - 1.64 r_s A_{net} P_a$$

Where C_a , C_s and C_i are the carbon dioxide concentrations in ambient air, at the leaf surface and in the intercellular space, respectively. Traditionally, they are expressed as partial pressure, instead of concentrations. This choice simplifies the global calculation of the model. To convert units, it is used the equation:

$$C_i[Pa] = C_i[ppm \text{ or } \mu mol\, mol^{-1}]\, P_{atm}\, 10^{-6}$$

Where $P_a[Pa]$ is the atmospheric pressure.

Further, A_{net} is the net rate of carbon assimilation and r_b and r_s are the boundary layer and stomatal resistance for water vapor, respectively. The numerical coefficients account for different diffusivities between H_2O and CO_2 in the leaf boundary layer and stomatal pores. The oxygen concentration is assumed constant in the ambient air, at the leaf surface and in the intercellular space, and is fixed at $O_2 = 20.9\, kPa$.

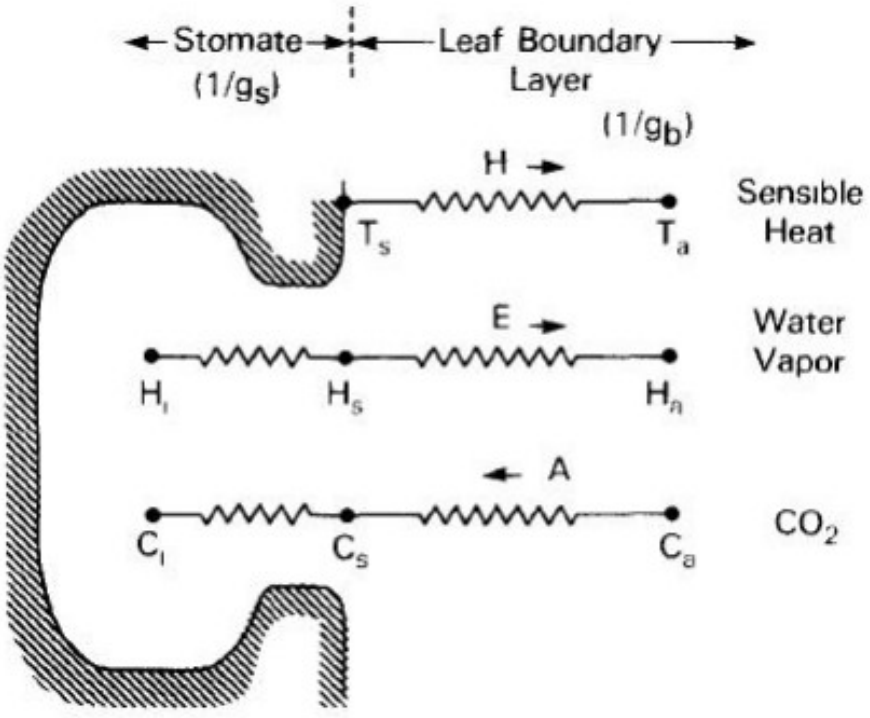

Figure 11.6: Heat, CO_2 and water vapor fluxes at the leaf surface interface. The subscripts a, s and i, refer to ambient air, leaf surface and leaf, respectively. From Sellers et al. (1992)

11.4.2. Laminar leaf and stomatal resistances

Laminar leaf resistance r_b beneath canopy represents the resistance to water vapor mass transport in the region just above the leaf surface. In UTOPIA, it is evaluated using eq. (4.1). The stomatal resistance r_f is due instead to the stomata opening/closure, and is not easy to estimate. It depends on many different environmental factors: the water vapor deficit, the air temperature, the incident solar radiation, the soil humidity in the root zone, the photosynthetic rate, and the carbon dioxide concentration in ambient air. UTOPIA has one parameterization for r_f (eq. 4.2), that follows Running and Hunt (1982), which in turn derives from Jarvis (1976). In this empirical expression, the effects of the environmental factors, which influence stomata opening, are modeled by multiplicative factors of the minimum value of stomatal resistance $r_{s,\min}[sm^{-1}]$.

In the formula currently implemented in UTOPIA, the five F_i factors account for the dependence on solar radiation, soil moisture in the root zone, atmospheric water vapor deficit, air temperature, and CO_2 concentration (see section 4.7. and eqq. 4.3-4.7). The hypothesis behind this approach is that the response to each environmental factor is independent of the others.The main criticism formulated against this models is that the interactive effects between these environmental factors are not taken into account, although such interactions were shown and reported in literature (Tardieu et al., 1996). Futhermore, although successfully tested in numerous circumstances, multiplicative or limiting factor-based model is essentially empirical and require a new

parameterization for each new environmental condition. This is another drawback likely resulting from the assumption that environmental factors have independent effects.

Another approach to rs parameterization, which eliminates these problems, is built on the relationship existing between r_f and the photosynthesic rate.

The first and most commonly used model developing this approach is that of Ball et al. (1987). In this model, the stomatal resistance r_s depends on the net photosynthesis rate, the air relative humidity at the leaf surface (H_r) and the CO_2 concentration on the leaf surface (C_s):

$$\frac{1}{r_s} = m \frac{A_{net}}{C_s} H_r P_{atm} + b \tag{11.10}$$

Here the symbol of the stomatal resistance is r_s because it is expressed in molar units $[m^2 s\, \mu mol^{-1}]$. In this equation, m is a non dimensional plant functional type parameter and b $[m^2 s\, \mu mol^{-1}]$ is the minimum stomatal conductance when $A_{net} = 0$. Typical values are $m = 9$ for C3 plants and $m = 4$ for C4 plants (Collatz et al. (1991), Collatz et al. (1992); Sellers et al. (1996)). More precisely, Sellers et al. (1996) suggested to set b in order to have $r_s = 10000\, m^2 s\, \mu mol^{-1}$ for C3 plants and $r_s = 40000\, m^2 s\, \mu mol^{-1}$ for C4 plants, but in UTOPIA b has been chosen in order to give a maximum stomatal resistance $r_{s,\max} = 20000\, s\, m^{-1}$, following Oleson et al. (2010).

Because C_s , in the previous equations, is unknown, Ball's model must be coupled to the model of photosynthetic assimilation. In this way, a system of three equations

(11.1, 11.9, and 11.11) and three unknowns (r_s , A_{net} and C_s) is obtained, which can be solved numerically. The solution of a system of equations requires an iterative solution method, which requires in turn a major compute time and power confronted with the solution of the eq. 4.2. This is the main criticism formulated against this approach, but on the other hand the result accuracy improves (Arora (2002); Damour et al. (2010)). This coupled model was proposed for the first time by Collatz et al. (1991), and subsequently implemented by Sellers et al. (1996)in a global climate model.

Actually in this model, following the approach used in CLM model (Oleson et al. (2010)). in eq. 11.10, the gross rate of photosynthesis (A) is used instead of the net one (A_{net}). Thus:

$$\frac{1}{r_s} = m \frac{A}{C_s} H_r P_a + b \tag{11.11}$$

Furthermore, as in the CLM, the equation 11.11 is associated to the equation of transpiration flux:

$$e_f = \frac{e'_a r_s + e_s(T_f) r_b}{r_b + r_s} \tag{11.12}$$

Where $e_f[Pa]$, the vapor pressure at leaf surface, is the weighted mean (with the appropriate resistances as weights) of $e_s(T_f)[Pa]$ (the saturation vapor pressure evaluated at the leaf temperature) and $e'_a = max[min(e_{af}, e_s(T_f)), e_{min}][Pa]$ is the vapor pressure of air, evaluated as the minimum value between the air vapor pressure within canopy e_{af} and $e_s(T_f)[Pa]$. The lower limit e_{min} is used to prevent

numerical instability in the iterative stomatal resistance calculation, and has been set to $e_{min}=0.25\,e_s(T_f)[Pa]$ for C3 plants and $e_{min}=0.40\,e_s(T_f)[Pa]$ for C4 plants, because C4 plants are not as sensitive to vapor pressure as C3 plants.

Substituting equation 11.12 in 11.11, a quadratic equation is obtained, in which r_s is expressed as a function of A, the gross rate of photosynthesis:

$$\left[\frac{m\,A\,P_a\,e'_a}{c_s\,e_s(T_f)}+b\right]r_s^2+\left[\frac{m\,A\,P_a\,r_b}{c_s}+b\,r_b-1\right]r_s-r_b=0 \qquad (11.13)$$

Stomatal resistance r_s is the largest of the two solutions of this equation.

11.4.2.1. The stomatal resistance in the presence of water stress

A defect of this parameterization is that it does not include any dependence on soil water content. A simple approach to integrate the effects of water stress in the r_s equation (eq. 11.13) consists in introducing a response function to soil water content as a multiplicative factor of r_s. Many equations have been proposed to describe the process: in some cases it is expressed as a function of the soil humidity, while in other cases the process is parametrized as a function of the air vapor pressure deficit, i.e. the difference between the actual amount of moisture in the air and its maximum value at saturation.

In UTOPIA the former approach has been choosen, because UTOPIA calculates all the information about the soil moisture content. The equation used is the empirical function

F_2 (eq. 4.4), already introduced in the alternative parametrization of canopy resistance (eq. 4.2). In this way:

$$r'_f = \frac{r_s}{F_2}$$

Finally, canopy resistance values can be converted from $r'_f[s\,m^2\,\mu mol^{-1}]$ units to $r_f[s\,m^{-1}]$ as:

$$r_f = 10^{-9} R \frac{\theta_{af}}{P_a} r'_f$$

Where $\theta_{af}[K]$ is the potential temperature in the air within canopy.

11.5. THE TWO PARAMETERIZATIONS IMPLEMENTED

Two different parameterizations for the quantities K_c, K_o, Γ^*, V_{max}, and J have been considered.

The simplest refers to the papers of Farquhar et al. (1980) and Collatz et al. (1991), later improved by Oleson et al. (2010), and is indicated in UTOPIA as **F80**. This method is considered simpler than the other one because it uses the Q_{10} parameterization to evaluate the quantities K_c, K_o, Γ^*, and V_{max} (eqs. 11.2-11.4) and assumes a linear dependence on the radiation to calculate A_j (eq. 11.6). Despite its simplicity, this parameterization is still the one most commonly used. This parameterization allows to differentiate between different plant functional types (PFT) by modifying the coefficient $V_{max}(298\mathrm{K})$, ϕ and m (tabulated in table 3.9).

The term $V_{max}(298\mathrm{K})$ (as defined by Thornton and Zimmermann (2007)) is scaled to account for nitrogen limitation (Oleson et al. (2010)). The CLM parameterizations have been used for calculating the terms ϕ and m. Furthermore, the coefficients values for the following plant functional types, corresponding to LVEG = 2, 3, 4, 5, 6, 16, and 17, have been set equal to those corresponding to temperate plants.

LVEG	Pathway	C3			C4		
		$V_{max}(298\mathrm{K}$	ϕ	m	$V_{max}(298\mathrm{K})$	ϕ	m
		$[m^2 s\,\mu mol^-$	$[mol\,mol^-$	[-]	$[m^2 s\,\mu mol^{-1}$	$[mol\,mol^-$	[-]
1	Crop/mixed farming	35	0.06	9	35	0.04	5
2	Short grass	31	0.06	9	33	0.04	5
3	Evergreen needleleaf tree	44	0.06	6			
4	Deciduous needleleaf tree	45	0.06	6			
5	Deciduous broadleaf tree	33	0.06	9			
6	Evergreen broadleaf tree	51	0.06	9			
7	Tall grass	31	0.06	9	33	0.04	5
9	Tundra	31	0.06	9			
10	Irrigated crop	35	0.06	5	33	0.04	9
13	Bog/marsh	31	0.06	9			
16	Evergreen shrub	44	0.06	9			
17	Deciduous shrub	31	0.06	9			
18	Mixed woodland	33	0.06	9			
19	Settlement (*)	33	0.06	9			
21	Po-Valley (*)	33	0.06	9			
22	Grugliasco (*)	33	0.06	9			
23	Siberia (*)	33	0.06	9			
24	Grass reference crop (*)	33	0.06	9			
25	Hazel	33	0.06	9			
26	Vineyard	33	0.06	9			

Tab 7: Coefficients used in the old model parameterization.

(*) indicates that these LVEG coefficients are inserted only for completeness, but their values are fictitious, thus they will not be used in the model.

The most complex parametrization considered, instead, uses the equations shown in Medlyn et al. (2002), and in UTOPIA is referenced to as **M02**. K_c , K_o , and Γ^* are described with an exponential function (eq. 11.3), while the A_j dependence on the radiation is expressed by J through an empirical hyperbolic function of adsorbed photon flux and the efficiency of photon use (eq. 11.7).

LVEG	Pathway	C3				C4			
		$V_{max}(298\mathrm{K})$	T_{opt}	H_a	H_d	$V_{max}(298\mathrm{K}$	T_{opt}	H_a	H_d
		$[m^2 s\,\mu mol^{-1}]$	$[^\circ C]$	$[kJ\ mol^{-1}]$		$[m^2 s\,\mu mol$	$[^\circ C$	$[kJ\ mol^{-1}]$	
1	Crop/mixed farming	338.38	41.24	92.94	200				
2	Short grass								
3	Evergreen needleleaf tree	174.75	38.57	63.55	200				
4	Deciduous needleleaf tree								
5	Deciduous broadleaf tree	206.86	40.37	72.1	200				
6	Evergreen broadleaf tree	175.81	37.83	60.79	200				
7	Tall grass								
9	Tundra								
10	Irrigated crop	338.38	39	72.1	200				
13	Bog/marsh								
16	Evergreen shrub								
17	Deciduous shrub								
18	Mixed woodland	206.86	40.37	72.1	200				
19	Settlement (*)								
21	Po-Valley (*)								
22	Grugliasco (*)								
23	Siberia (*)								
24	Grass reference crop (*)								
25	Hazel	206.86	40.37	72.1	200				
26	Vineyard	206.86	40.37	72.1	200				

Tab 8: Coefficients related to Rubisco carboxylation used in the new model parameterization.

(*) indicates that these LVEG coefficients are inserted only for completeness, but their values are fictitious, thus they will not be used in the model;

(◦) indicates that these LVEG coefficients are equal to those of LVEG=5.

LVEG	Pathway	C3				C4			
		$J_{max}(T_{opt})$	T_{opt}	H_a	H_d	$J_{max}(T_{opt})$	T_{opt}	H_a	H_d
		$[m^2 s\,\mu mol^-$	$[^\circ C]$	$[kJ\ mol^{-1}]$		$[m^2 s\,\mu mol^-$	$[^\circ C$	$[kJ\ mol^{-1}]$	
1	Crop/mixed farming	275.07	36.3	82.99	156.88				
2	Short grass								
3	Evergreen needleleaf tree	153.14	31.01	51.85	191.32				
4	Deciduous needleleaf tree								
5	Deciduous broadleaf tree	161.67	33.43	54.2	188.79				
6	Evergreen broadleaf tree	175.13	32.19	43.79	200				
7	Tall grass								
9	Tundra								
10	Irrigated crop	275.07	36.3	82.99	156.88				
13	Bog/marsh								
16	Evergreen shrub								
17	Deciduous shrub								
18	Mixed woodland	161.67	33.43	54.2	188.79				
19	Settlement (*)								
21	Po-Valley (*)								
22	Grugliasco (*)								
23	Siberia (*)								
24	Grass reference crop (*)								
25	Hazel	161.67	33.43	54.2	188.79				
26	Vineyard	161.67	33.43	54.2	188.79				

Tab 9: Coefficients related to the electron transport used in the new model parameterization.

(*) indicates that these LVEG coefficients are inserted only for completeness, but their values are fictitious, thus they will not be used in the model;

(◦) indicates that these LVEG coefficients are equal to those of LVEG=5.

Finally V_{max} and J_{max} are expressed using the Arrhenius modified function (IUPAC (1997), eqs. 11.5 and 11.8). The defect of this parameterization is the great number of coefficients required in these equations, which varies for every PFT. Using

experimental data from many researches, it could be possible to evaluate all these coefficients, but this difficult work has been done only for some PFTs, and in particular for crop C3 species, evergreen needle leaf trees, and broadleaf deciduous trees (Medlyn et al. (2002)). Unfortunately, for all the others PFTs, the necessary coefficients have not been found; therefore, for these PFTs, it is possible to use only the F80 parameterization. The coefficients used are tabulated in figs. 3.10 and 3.11, from M02.

The simplest refers to the papers of Farquhar et al. (1980) and Collatz et al. (1991), later improved by Oleson et al. (2010), and is indicated in UTOPIA as **F80**.

This method is considered simpler than the other one because it uses the Q_{10} parameterization to evaluate the quantities K_c, K_o, Γ^*, and V_{max} (eqs. 11.2-11.4) and assumes a linear dependence on the radiation to calculate A_j (eq. 11.6).

Despite its simplicity, this parameterization is still the one most commonly used. This parameterization allows to differentiate between different plant functional types (PFT) by modifying the coefficient $V_{max}(298\text{K})$, ϕ and m (tabulated in table 3.9).

The term $V_{max}(298\text{K})$ (as defined by Thornton and Zimmermann (2007)) is scaled to account for nitrogen limitation (Sellers et al. (1996)). The CLM parameterizations have been used for calculating the terms ϕ and m. Furthermore, the coefficients values for the following plant functional types, corresponding to LVEG = 2, 3, 4, 5, 6, 16, and 17, have been set equal to those corresponding to temperate plants.

The most complex parameterization considered, instead, uses the equations shown in Medlyn et al. (2002), and in UTOPIA is referenced to as **M02**. According with this parameterization, K_c, K_o, and Γ^* are described with an exponential function

(eq. 11.3), while the A_j dependence on the radiation is expressed by J through an empirical hyperbolic function of adsorbed photon flux and the efficiency of photon use (eq. 11.7). Finally V_{max} and J_{max} are expressed using the Arrhenius modified function (IUPAC (1997), eqs. 11.5 and 11.8). The defect of this parameterization is the great number of coefficients required in these equations, which varies for every PFT. Using experimental data from many researches, it could be possible to evaluate all these coefficients, but this difficult work has been done only for some PFTs, and in particular for crop C3 species, evergreen needle leaf trees, and broadleaf deciduous trees (Medlyn et al. (2002)). Unfortunately, for all the others PFTs, the necessary coefficients have not been found; therefore, for these PFTs, it is possible to use only the F80 parametrization. The coefficients used are tabulated in figs. 3.10 and 3.11, from M02.

11.6. MODEL NUMERICAL IMPLEMENTATION

The system of equations (11.1, 11.9, 11.11 and 11.12) represents the stomatal photosynthesis coupled model, which permits to compute A_{net}. The solution of the system needs the use of an iterative method. The phases of the calculation procedure can be summarized as follows:

- **i.** evaluation of a first estimate of the intercellular carbon concentration C_i, which is, generally, fixed at 70% of environmental carbon dioxide concentration (C_a) in C3 plants and at 40% in C4 plants (Collatz et al. (1991); Collatz et al. (1992));
- **ii.** using this value, evaluation of A, A_{net} (eq. 11.1) and r_s (eq. 11.11);
- **iii.** using the A_{net} and r_s values just computed, evaluation of a new estimate of C_i, called for simplicity C'_i (eq. 11.9);

iv. at this point, if C'_i estimate differs from C_i by less than a fixed threshold, then the final net rate of carbon assimilation has been found and it is equal to the A_{net} just computed in the last iteration; otherwise, the new (C'_i) is reintroduced in the

v. calculation, substituting the old one at step (i), and a new iteration starts.

The number of iterations needed for obtaining the final result in UTOPIA is normally lower than 30, using the bisection method, that has been proved to be the more stable and converging method.

11.7. SCALING UP PHOTOSYNTHESIS FROM LEAF TO CANOPY

The model developed in the previous chapter simulates the rates at which carbon is assimilated (A) and consumed (R_d) in a single leaf. More precisely, since the model is done in big-leaf approximation, if the leaf area index (LAI) is equal to 1 (LAI) represents the leaves area per ground area unit), it assigns the assimilation and respiration rates of a single leaf to the whole canopy, . Otherwise, the association is done just multiplying the assimilation and respiration rates of a single leaf by the canopy LAI :

$$(A_{net})_f = (A_{net})_{leaf} LAI \tag{11.14}$$

However the eq. 11.14 is too rough: in a plant, not all leaves are exposed to the same environmental conditions and, furthermore, leaves in the same plant have different photosynthetic capacities; therefore, carbon assimilation and respiration rates of leaves within canopy are not the same.

The scaling-up from leaf to canopy should taking into account also these features. It was demonstrated by Farquhar (1989) that the equations describing whole-leaf photosynthesis would have the same form as for individual chloroplasts across a leaf, provided that:

- **i.** the distribution of chloroplast photosynthetic capacity is in proportion to the profile of absorbed radiation;
- **ii.** the shape of the response to radiation is identical in all leaf layers.

This can also be extended to canopies, as argued by Sellers et al. (1992). Substantially, if the distribution of the photosynthetic capacity between leaves is proportional to the profile of absorbed radiation, then the equations describing leaf photosynthesis would also represent canopy photosynthesis.

This hypothesis was confirmed by several studies on within-canopy profiles of leaf properties of a great number of species (Hirose and Werger (1987); Sadras et al. (1993); Anten et al. (1995)). In particular, these authors focused on the within-canopy nitrogen concentration profiles, because the biochemical photosynthetic capacity is strongly related to the leaf nitrogen concentration (see fig. 11.7).

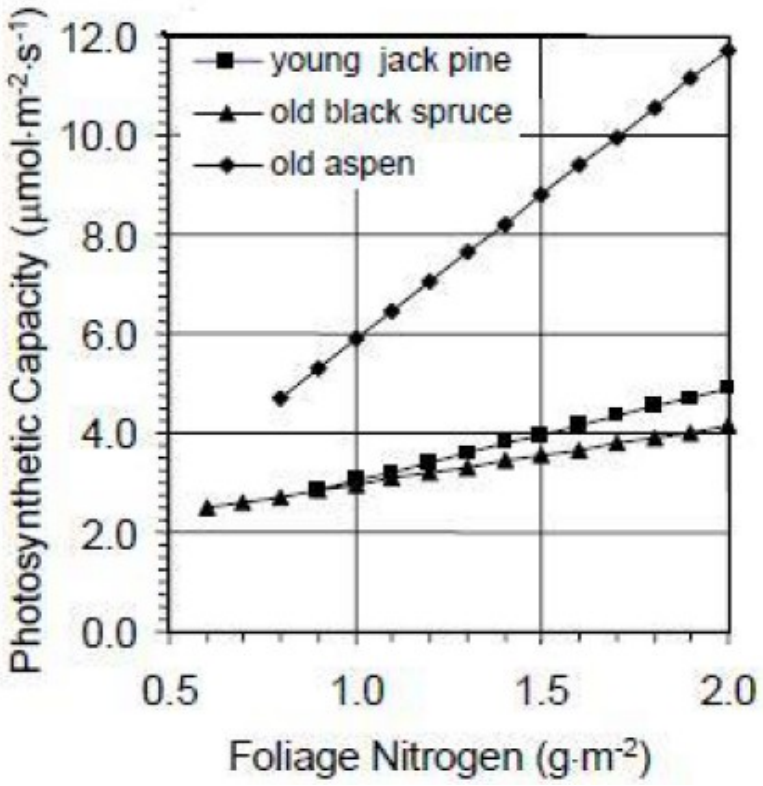

Figure 11.7: Measured photosynthetic capacity shows a direct proportionality with the canopy nitrogen amount for different trees species. Jack pine and black spruce are needleleaf evergreen trees, while aspen is a broadleaf tree. From Bonan (2002).

In fact, the biochemical photosynthetic capacity consists mainly in the electron-transport and in the carboxylation capacities. In turn, they depend on the amount of chloroplasts and Rubisco enzymes in the leaf, respectively. Both chlorophyll and Rubisco concentrations require nitrogen. Therefore, the presence of nitrogen in a leaf is an index of its biochemical photosynthetic capacity. Nitrogen leaf amount is energetically expensive to be maintained by the plant. Then, the plant displaces it between the leaves in order to minimize losses, maximizing carbon fixation. An optimal distribution of leaf nitrogen exists when any reallocation of nitrogen would decrease daily photosynthesis (De Pury and Farquhar (1997)).

Several studies on the within-canopy nitrogen concentration profiles highlighted that leaves adapt or acclimate to their radiation environment, such that a plant nitrogen contents may be distributed to maximize daily canopy photosynthesis (Field (1983); Hirose and Werger (1987)). This confirms that the nitrogen profiles are useful to describe the photosynthetic activity within a plant.

These studies also showed that the optimal distribution of nitrogen occurs when the nitrogen is distributed in proportion to the distribution of absorbed radiation in the canopy, averaged over the previous several days or a week, i.e. the time in which leaves are able to modify their nitrogen content.

Summarizing, the time-integrated distribution of absorbed radiation in the canopy causes a proportional distribution of nitrogen in the leaves (and of photosynthetic capacity), led by the plant in order to maximize photosynthesis.

In this way, it is then possible to scale up the photosynthetic activity from leaf to canopy, as previously outlined. This operation consists, firstly, in the integration of the vertical profile of PAR along the height of the canopy: in this way, a factor indicating the average radiation that reaches the leaves over the whole canopy is obtained. Then, using this factor, the incident PAR at the top of the canopy can be scaled to obtain the canopy-averaged value. Photosynthesis and respiration estimated at the top of the canopy can thus similarly be scaled to obtain the total canopy values (Arora (2002)).

The simpler way to describe the radiation profile through canopies, in a big-leaf model, is by using the Beer's law (Monsi and Saeki (1953)). It states that the decrease of the PAR flux density, Q, through a path z in the canopy is a function of Q

itself, of the radiation extinction coefficient, k (see sect. 11.2.1.), and of the leaf area of each canopy layer, $l(z)$:

$$\frac{dQ}{dz} = -k\, l(z)\, Q$$

After several passages (Cerenzia (2012)), the total absorbed PAR Q_T that reaches the entire canopy can be calculated as:

$$Q_T = \frac{Q_0}{k}\left[1 - \exp(-k\, LAI)\right] = Q_0 f_Q \tag{11.15}$$

Finally, multiplying the values of $(A_{net})_{leaf}$, obtained for a single leaf, by the factor f_Q , it is possible to obtain the net rate of carbon assimilation averaged on the entire canopy, taking into account that canopy surface exposed to solar beam is not a plane surface and that the radiation within the canopy is exponentially attenuated:

$$(A_{net})_{canopy} = (A_{net})_{leaf} f_Q$$

The coefficient k in eq. 11.15, e.g. the PAR extinction coefficient through canopy, depends, among other factors, on the vegetation species and density, on the Sun zenithal angle and on the leaf angle distribution. The angle at which the solar beam strikes a leaf is particularly important: the greatest radiation per unit surface area is received when the radiation is perpendicular to a surface, while, at oblique angles, less radiation impinges on a surface. The angle at which solar radiation strikes a leaf depends also on leaf orientation besides on solar zenith angle. Some leaves are oriented horizontally, while others are vertical (it depends on the plant species). However, in the most part of cases,

leaves are oriented randomly, so that there is an equal probability of orientation in any direction (Bonan (2002)).

Summarizing (for more detail see Cerenzia (2012)), under the condition of spherical leaves angle distribution, k can be defined as the ratio between a geometric coefficient, $G = 0.5$, and the sine of the solar elevation angle, β (Goudriaan (1977)):

$$k = \frac{0.5}{\sin \beta}$$

12. Useful formulations

12.1. SOIL INTERPOLATIONS

The problem of how to calculate the mean value at the interface between two different soil levels is very important, in particular for physical quantities extremely variable as the hydraulic conductivity or the soil matric potential (Wetzel et al. (1996)). The latter is the pressure required to remove water from a surface, due to the adhesion of molecules to a surface. It represents the potential energy needed to extract water against capillarity. The hydraulic conductivity accounts for the influence of gravitational drainage in soil.

According to Clapp and Hornberger (1978), the hydraulic conductivity K_η and the soil matrix potential ψ vary with soil moisture content η and soil texture according with equations:

$$K_\eta = K_{\eta s} q^{2b+3}$$

$$\psi = \psi_s q^{-b} \tag{12.1}$$

Where $q = \eta / \eta_s$ is the saturation ratio. The hydraulic diffusivity is given by:

$$D_{l\eta} = K_\eta \frac{\partial \psi}{\partial \eta}$$

And the other parameters have already been previously defined.

Soil thermal capacity is defined as the average between the thermal capacity of its constitutents (dry bare soil, soil water and air), using as weights the current soil water content and porosity:

$$(\rho c)=(\rho c)_{dry}(1-\eta_s)+(\rho c)_w \eta_s+(\rho c)_a(\eta_s-\eta) \qquad (12.2)$$

Where the part relative to the atmospheric heat capacity (proportional to (η_s-η), is normally neglected as much smaller (three order of magnitude lower than the others).

Since soil can also contain roots, in UTOPIA the soil thermal capacity associated to *i-th* soil layer has been recalculated as:

$$(\rho c \Delta z)_i=[1-(RP_{total})_i]\{[1-(\eta_s)_i]((\rho c)_{dry})_i + (\eta)_i(\rho c)_w\}+(RP_{total})_i 23023\, LAI$$

The first term refers to the fraction of soil not occupied by the roots and is function of the thermal capacity of dry soil $(\rho c)_{dry}$ and of that of the water

$(\rho c)_w=4.186\ 10^6 J\, m^{-3} K^{-1}$ according with eq. (12.2). The last term refers instead to the roots.

The soil thermal conductivity $k_T[W\, m^{-1} K^{-1}]$ has been calculated according with Pielke (1984) as:

$$k_T=420\exp(-P_f-2.7) \qquad with \qquad P_f=\log(-100\,\psi_1) \qquad (12.3)$$

Where the suffix "*1*"refers to the first (uppermost) soil layer. Concerning the value of k_T at the interface between the *i-th* and *(i+1)-th* soil layers, eq. (12.3) has been used, where the value of ψ has been evaluated using eq. at the "*i,i+1*" interface has been obtaines by eq. (12.1) and the interfacial values of ψ_s, b and q , i.e. $(\psi_s)_{i,i+1}, (b)_{i,i+1}$ and $(q)_{i,i+1}$, have been obtained using the following averaging function, here given for the generic variable ξ :

$$(\xi)_{i,i+1}=\frac{\xi_i}{d_i}+\frac{\xi_{i+1}}{d_{i+1}}$$

The mean values of the hydraulic conductivity (both unsaturated and saturated) at the "*i,i+1*" interface have been calculated using the following averaging function:

$$(\xi)_{i,i+1}=\exp\left(\ln\xi_i+\frac{\ln\xi_{i+1}-\ln\xi_i}{d_{i+1}+d_i}\right)$$

According with Wetzel et al. (1996), the soil heat flux at the "*i,i+1*" interface $(F_{so})_{i,i+1}[W\,m^{-2}]$ is given by:

$$(F_{so})_{i,i+1}=-2(k_T)_{i,i+1}\frac{T_{i+1}-T_i}{d_i+d_{i+1}}$$

Dew point temperature $T_d[^\circ C]$ is calculated as:

$$T_d=\frac{35.86\,A-273.15}{A-1}\qquad\qquad A=\frac{\ln(e/6.1078)}{17.269}$$

The non-saturated vapor pressure $e[hPa]$ is given by:

$$e=\frac{q_a\,p_a}{0.378\,q_a+0.622}$$

The specific humidity q $[kg_{water\,vapor}\,kg_{air}^{-1}]$ can be calculated approximately by the atmospheric pressure $p[hPa]$ and the partial water vapor pressure $e[hPa]$ as:

$$q=\frac{0.622\,e}{p-0.378\,e}\approx 0.622\frac{e}{p} \tag{12.4}$$

The relative humidity RH is calculated as the ratio of the actual and saturated water vapor pressures:

$$RH = 100 \frac{e}{e_s(T)}$$

Where the saturated vapor pressure $e_s(T)$ at the temperature T is given by:

$$e_s(T) = 6.1078 \quad \exp\left[\frac{17.269 \ (T - 273.15)}{T - 35.86}\right]$$

The variation of saturated specific humidity with the temperature can be calculated by inverting eq. (12.4) For the saturated values:

$$\frac{\partial q_s(T)}{\partial T} = \frac{17.269}{273.15 - 35.86} \frac{p \, q_s(T)}{[p - 0.378 e_s(T)](T - 35.86)^2}$$

The latent heat of evaporation and fusion are calculated using the following relation:

$$\lambda(T) = A - B(T - T_m) \quad [J kg^{-1}]$$

Where $A = 2.5 10^6 J kg^{-1}$ and $B = 2.39 10^3 J kg^{-1} K^{-1}$ for evaporation and $A = 2.824 10^6 J kg^{-1}$ and $B = 0.2 10^3 J kg^{-1} K^{-1}$ for evaporation and fusion, and $T_m = 273.15 K$ is the melting point of ice.

The dewpoint is calculated from the specific humidity q and the pressure p as:

$$T_d = \frac{\left[\frac{A_4}{A_2} \log\left(\frac{e}{A_1}\right) - A_3\right]}{\frac{1}{A_2} \log\left(\frac{e}{A_1}\right) - 1}$$

12.2. INITIALISATION OF SOIL TEMPERATURE AND MOISTURE

Frequently soil parameters are required in SVAT schemes or LAMs (Limited Area Models) in order to initialise the values at the beginning of the simulations. The soil

values are recognized as very important parameters able to affect in a substantial way the surface turbulent heat fluxes and, thus, the atmospheric stability. However, measurements of soil temperature and moisture on a global or mesoscale area are not available. There are some locations in which those data are measured, but they are too sparse and sometimes not representative of the surrounding area. The satellite images can be also used to provide the surface values of soil temperature and moisture, but they cannot provide the values for the deepest soil layers. For a simulation of medium-range weather forecast (7–10 days), the knowledge of parameters in the first 20–50 cm of soil is required. For this reason, in the recent years, the Meteorological Services are trying to find some methods to infer the values of soil parameters on a global or mesoscale region.

In this subsection, two simple methods were derived for the initialisation of soil temperature and moisture, respectively. These algorithms contained some empirical parameters to be determined through a calibration over the experimental site. Nevertheless, as the equations were based on physical processes, these methods could be generalised and used for many different sites.

For soil temperature, it is useful to remember that the equation accounting for the heat conduction is eq. (5.2), in which it is possible to define the soil thermal diffusivity as the ratio between the soil thermal conductivity and the heat capacity $\nu_T = k_T / (\rho c)_s$. Here, $T = T(z, t)$ is the soil temperature, z is vertical axis, defined positive when directed downward into soil. A solution of this equation can be found under the hypothesis of considering constant the soil thermal diffusivity ν_T and with the following boundary condition at the soil-atmosphere interface:

$$T(0,t) = T_0 + \Delta T \sin(\omega t + \phi)$$

Where T_0 is the average soil temperature in all soil layers during the period $\tau = \frac{2\pi}{\omega}$, with ω angular frequency, and where ΔT is the amplitude of the thermal wave during the period τ, and ϕ is the initial phase of the wave. The solution of heat conduction equation in this case is:

$$T(z,t) = T_0 + \Delta T \exp\left(-\frac{z}{D}\right) \sin\left(\omega t - \frac{z}{D} + \phi\right)$$

Where $D = \nu_T \tau$ is the depth of exponential decay for the temperature. Based on this analytical solution, in UTOPIA we propose the following empirical equation for the evaluation of soil temperature:

$$T_{emp}(z,t) = T_{air} + \Delta T_{exc} \exp\left(-\frac{z}{D}\right) \sin\left(\frac{2\pi J_{day}}{365} - \frac{z}{D} + \phi\right) \qquad (12.5)$$

The values needed for this calculation are: the daily mean air temperature at the z_a model level T_{air}, the observed yearly excursion of daily mean air temperature at z_a model level $\Delta T_{exc} = T_{July} - T_{January}$, and the Julian day of the year J_{day}.

Concerning soil moisture, in this case the propagation of moisture into soil obeys to eq. (7.1), that can be rewritten here in a simplified form neglecting the contribution of the water vapor:

$$\frac{\partial q}{\partial t} = \frac{1}{\eta_s} \frac{\partial}{\partial z}\left[K_\eta \frac{\partial}{\partial z}(z + \psi) \right] \qquad (12.6)$$

Where q is the saturation ratio, η_s the soil porosity, K_η the hydraulic conductivity, and ψ the moisture (soil matric) potential. Note also that the simplified eq. (12.6) does not consider the eventual input-output of water due to evapotranspiration and precipitation. An analytical solution of this equation cannot be derived due to the strong dependence of the hydraulic conductivity and moisture potential on soil moisture itself. Nevertheless, we must consider that:

- during normal conditions, surface soil shows larger soil moisture fluctuations than deepest soil, with a yearly cycle showing its minimum during the warmest months (when evaporation is generally larger) and conversely its maximum during the coldest months;
- deepest soil shows the lowest variations and its soil moisture content generally tend to approach the field capacity;
- excluding arid conditions, wintertime soil moisture approaches the field capacity also in surface layers;
- during very strong precipitation events, soil moisture can exceed temporarily the field capacity but, when rainfall ends, due to the very high hydraulic conductivity, soil moisture rapidly decreases to the field capacity;
- periods characterized by precipitations above the normal are generally also characterized by relative humidity values above the normal, and vice versa.

Based on these considerations, the following relationship has been derived, in analogy with eq. (12.5):

$$q_{emp} = q_{fc} - \left(q_{fc} - q_{wi}\right)\left(\frac{RH_{max} - RH_{air}}{RH_{max} - RH_{min}}\right)\exp\left(-\frac{z}{D}\right) \tag{12.7}$$

Where q_{emp} is the empirical initial soil moisture (expressed in units of saturation ratio $q = \eta/\eta_s$), q_{fc} is the field capacity and q_{wi} the wilting point (both expressed in units of saturation ratio), and RH_{min} and RH_{max} are the air relative humidity thresholds, while RH_{air} is the daily mean air relative humidity at the model level z_a (for numerical and physical reasons, the fraction inluding relative humidities must range between 0 and 1).

Eqq. (12.5) and (12.7) were tested over an Italian plain site against experimental observations (Cassardo et al. (2006)), using decadal mean values and the following parameters: $\Delta T_{exc} = 14\,^{\circ}C$ (taken from the climatology of the site), $D = 2.3\,m$ (typical for a loamy soil), $\phi = -1.64\,rad$, $q_{fc} = 0.761\; m^3_{water}\, m^{-3}_{void}$ and $q_{wi} = 0.343\; m^3_{water}\, m^{-3}_{void}$ (values typical of loamy soil), and $RH_{min} = 65$ and $RH_{max} = 90$. Generally speaking, there was a qualitatively good agreement, better for soil temperatures, even if some extreme values, particularly the minima, were sometimes not well captured by the two empirical equations.

13. Input/output

The following sections of this manual are technical notes useful to install, preprocess the input data, execute the UTOPIA and post-process its results.

13.1. INSTALLATION AND DIRECTORY MANAGEMENT

It is expected that UTOPIA is installed in a directory named ***utopia***. In that directory 3 main sub-directories will be created: ***model***, ***bin*** and ***par***. In the directory ***model***, there are the UTOPIA source code, all include files, eventual compilation scripts and post-processing codes. In the directory ***par***, there are the parameter files used by UTOPIA. Finally, in the directory ***bin***, the executable files will reside. The input data are stored in a separate input data directory, as well as the output files in a separate output data directory, which could eventually be two other subdirectories named ***input*** and ***output***, respectively.

In the ***input*** directory, input file must have the extension '.INT'. In the output directory, according with the user selection, the UTOPIA model creates some files with some of the following extensions: '.OUT'. These files contain, in the name, the following suffixes: '.INP' (some input data), '.THE' (data relative to the thermal budget), '.RAD' (radiation fluxes), '.HYD' (relative to the hydrologic budget), '.RUM' (other relevant data) and '.LAM' (in which the user can select which data to write). The user can select if to have all output files, or only '.LAM', or only the other five.

The source code for the 2013 version of UTOPIA is named utopia2013.f90. It is written in Fortran 90. Two other files (external routines) are needed for the compilation: the file eco_routines.f90, which contains the routines used to extract ECOCLIMAP data

(this file must be present even if Ecoclimap will not be used: in this case, a standard version of this routine is given) and the file calendario2000.f90, which contains some routines useful to manage date and time.

13.2. INPUT: INITIAL CONDITIONS

UTOPIA is a one-dimensional model and is expected to be run over a single grid point. In case of a run over a bi-dimensional domain, an external model driver or scripts must be created, in which the initial and boundary data could be properly managed during the sequential runs. Thus, let's describe in the following how the model works over a single point.

Initial data, which are expected to be given to the model only at the first stage of the simulation, are contained in a specific file called par file (FILEPA in the code), located in the directory '***./par***', that normally should be named 'utopia2013.par'. An example of file is reported into Table 12.

At the beginning of the file, the information about input and output data directories and about the file name are required. ***DIRIN*** is the input file directory (ex: /data/agro/dati/UTOPIA_2010/input/), while ***DIROU*** is the output file directory (ex: /data/agro/dati/UTOPIA_2010/output/). ***PREF*** is the name (without extension) of the input file.

Then there are the parameters driving the procedure which allows to stop the model at a certain time and restart it at the same time with another simulation (called "freezing"): in this case, the model write all values of all internal variables in a file whose extension is '.FRZ'; if this option is used, we must care to remove the .FRZ file if it is not needed). In

this section, ***LFREEZE*** is a logical variable that, if true, activates the storage of all UTOPIA variables at the end of the simulation and/or during the simulations according to the value of MIN_FREEZE. ***MIN_FREEZE***, if LFREEZE is true, represents the number of minutes between two successive storage of all UTOPIA variables in the file named XXXXX_TMP.FRZ, which is a temporary file and will be overwritten many times, in order that the last one will be available in case of simulation stop (ex: 10080). A value of LFREEZE equal to 1440, 10080 or 525600 indicate that the storage of all UTOPIA variable occur respectively even 1 day, 1 week or 1 year. Please remember that, if LFREEZE is true, UTOPIA creates in the output directory the freezing file and, at the beginning of the simulation, UTOPIA search for a file named XXXXX.FRZ. Thus, if the user do not want to restart a simulation from previously "frozen" data, it is necessary to delete freezing file before each simulation, or to set LFREEZE to .false. .

Next group of parameters are relative to input and output data. ***KDATA*** represents the number of observations (=input data) in 1 hour (ex: 2 means that the observations are available every 30 minutes; it is not suggested to run UTOPIA using input data which have less than two observations per hour, and UTOPIA is unable to use datasets with less than one datum per hour). It can be here remembered that the internal timestep of UTOPIA has nothing to do with the frequency of the observations, even if it is - in some way - related to it. The internal UTOPIA timestep, named ***DTSEC***, is calculated as:

$$DTSEC = \frac{60}{KDATA}\frac{60}{MITER}$$

Where ***MITER*** is a parameter which represents the number of calculations between the observations.

```
0
********** DIRIN, Directory path for input files:       ---->VERSION 2010<----
/data/agro/dati/UTOPIA2010/input/
********** DIROU, Directory path for output files:
/data/agro/dati/UTOPIA2010/output/
********** PREF, suffix for output files:
prova
********** Freezing parameters ! 1d=1440,1wk=10080,1y=525600
 F         10080
********** KDATA, n. of obs. in 1 h,NCODFILE, output file code(1=ref,2=ref+LAM,3=LAM,<0=unformatted), MITER n. of LSPM time steps among two
input records (if not read, is used the value setted in the code (=120))
 2 3 60
********** NNDD, n.of input data columns (+1 which is time section), thus IC, columns
 10
 2  3 -1 -1  4  5  7 -1  8  6
********** ILOGCOE, use Wilson-Hend.Sell archive, LVEG, veg.code,if not read SIGMAF,D0LSPM,AFFH,RMINLSPM,LAILSPM,HLSPM,EPSF,DRLSPM 0.80  0.04
0.18  200  6.00  0.60  0.85  0.30
 T   1
********** INP_SOIL, soil freezing? no freezing (0), Schrodin (1) + coupling (2), Viterbo (3) + coupling (4), Viterbo modified (5)
0
********** NSOILLSPM: number of soil layers
 8
********** Soil characteristics: NSO = soil layer type, TILSPM = initial soil temperature (K); QILSPM = initial soil moisture (-); DEP = soil
depth (m). Possibility to set the soil texture CLAY(%), SAND(%), OM(%) (organic matter) and the soil parameters ETAS, ETAFC, CAPPAETAS, BSOIL,
ETAWI, ROCI
 7   288.15     0.40     0.05      34.80     12.20      0.00   -999.99   -999.99   -999.99   -999.99   -999.99   -999.99
 7   288.15     0.48     0.10      34.80     12.20      0.00   -999.99   -999.99   -999.99   -999.99   -999.99   -999.99
 7   288.15     0.50     0.20      34.80     12.20      0.00   -999.99   -999.99   -999.99   -999.99   -999.99   -999.99
 7   288.15     0.63     0.40      34.80     12.20      0.00   -999.99   -999.99   -999.99   -999.99   -999.99   -999.99
 7   288.15     0.74     0.80      34.80     12.20      0.00   -999.99   -999.99   -999.99   -999.99   -999.99   -999.99
11   288.15     0.96     1.60    -999.99   -999.99   -999.99   -999.99   -999.99   -999.99   -999.99   -999.99   -999.99
11   288.15     0.98     3.20    -999.99   -999.99   -999.99   -999.99   -999.99   -999.99   -999.99   -999.99   -999.99
11   288.15     0.98     6.40    -999.99   -999.99   -999.99   -999.99   -999.99   -999.99   -999.99   -999.99   -999.99
********** ALBSD: bare soil albedo and surface, TORTUOS: tortuosity coefficient, C_DREN
 0.30   1000.  1.00
********** date (yy mm dd), time (hh mm), legal hour code, LUCTFLAG
 2004      10      6      18      00      0        T
********** station: ALON_INI = longitude, ALAT_INI = latitude, QUOTA = height, ZLSPM = station height, RRR = turbidity factor, ASLOPE, BSLOPE
= slope angle, ZVLSPM = anemometer           heigth
 -88.2410     41.8406     226.0000    2.4000      0.0000   0.0000  0.0000   3.7600
********** ECO_CHOICE, ECOCLIMAP database use?
 F
********** HSN, Initial snow height (m)
 0.000
L360DAYS_CALENDAR, T means that 360 days climatic calendar is used, ILOGALB,F means that soil albedo change, T means that soil albedo is
fixed, ILOGFUN, T means that haze      function is activated, F means not activated, LDATA, F means that date change day by day, T means that
date will be fixed, LVAP, T means that water vapor effects in the soil  will be taken into account, LTCAN_NEW: T means to use the new untested
canopy temperature scheme, F uses the old one
 F F T F T F
********** END DATA INPUT FOR THIS SITE
```

Tab 10: An example of PAR file.

If A is an observed variable, and if A_{NM} and A_{NEW} are the values corresponding to the instants t and $t+\Delta t$, respectively (where Δt is the time between two observations), the value of A in the J-th iteration on DTSEC is defined by the equation:

$$A = A_{NM} + (J-1)\frac{A_{NEW} - A_{NM}}{MITER}$$

The MITER value could be defined by the user in the '.par' file after NCODFILE (see Table 12). If MITER is not defined in the FILEPA, this variable assumes a default value set equal to 120. Normally, for every simulation, it is suggested to set MITER in order to have an optimum value of DTSEC=30 s.

NCODFILE is the output file code (see the routine DINAMIC_MEMORYOUT or section 13.4.for more details about the exact file content) and its absolute value can assume the following values:

- 0 means that UTOPIA does not produce any output (this is useful for see if the model can run without errors);
- 1 means that UTOPIA creates 5 output files with the following extensions:

  '.INP' (contains a subset of input data);

  '.RAD' (contains the components of radiative balance);

  '.THE' (contains the temperatures of atmosphere, vegetation and soil);

  '.HYD' (contains atmospheric and soil moisture and the components of the hydrological balance);

  '.RUM' (contains other parameters);
- 2 means that, in addition to the files relative to the code 1, also a file with the extension '.LAM' will be created. This file contains a list of parameters that can be selected by user in the file 'memoryout.config' in the par folder (for more details see 'dynamic_memoryout.pdf');
- 3 means that only the file with extension '.LAM' will be created;

  If the code is positive, the output file is created 'formatted', while if the code is negative, the output file is created as 'unformatted'. The suggested value for NCODFILE is 3.

The following part refers to the codification of input data (it contains the variables NNDD and IC), that will be detailed in the section 13.3..

The next parameters are related to the vegetation (if required) and to the eventual use of databases. The logical variable ***ILOGCOE***, if true, means that the integrated Wilson

and Henderson-Sellers (1985) archive of vegetation data (contained in the routines VEGPAR_FIX and VEGPAR_VAR) will be used. On the contrary, if this variable is false, UTOPIA read directly by the parameter file the following parameters:

- SIGMAF (vegetation cover);
- D0LSPM (2nd dimension of the leaf);
- AFFH (vegetation albedo);
- RMINLSPM (minimum stomatal resistance);
- LAILSPM (leaf area index);
- HLSPM (height of the vegetation);
- EPSF (emissivity of the vegetation);
- DRLSPM (vegetation root depth).

Finally, if ILOGCOE is true, the vegetation class LVEG according with the Wilson and Henderson-Sellers (1985) archive is read. This variable allows the selection of the parameters in the routines VEGPAR_FIX and VEGPAR_VAR.

The next code allows the choice of soil freezing parameterization. The code ***INP_SOIL*** allows to select among the three soil freezing parameterizations currently implemented in UTOPIA and described in section 9.: 'SC01' (section 9.1.), 'VI99' (section 9.2.) and 'BO10' (section 9.3.). The allowed values of INP_SOIL code are:

- 0 = the soil freezing is not considered;
- 1 = the SC01 parameterization is used only for soil temperature;
- 2 = the full SC01 parameterization is used;

- 3 = the VI99 parameterization is used only for soil temperature;
- 4 = the full VI99 parameterization is used.
- 5 = the full BO10 parameterization is used.

Soil freezing parameterization takes into account the energy needed to freeze the water into the soil (SC01) and also the fact that the water freezing occurs at temperatures lower than 0 °C in the soil (VI99 and BO10). The expression 'full parameterization' means that the coupling with soil moisture allows the explicit calculation of soil ice content and its update during the simulation.

The following section of parameters is dedicated to the initialization of the soil layers: the number of soil layers is firstly required, and then for each layer the values of soil temperature, moisture and depth are required. ***NSOIL*** is the number of soil layers. The number of levels can be chosen by the user; according with some studies carried out at UK Met Office, it is recommended a number greater or equal to 4 soil layers for a multilayer scheme, and their depths should increase exponentially (or at least repeat, never decrease with depth); the first soil layer should be not larger than 5-10 cm (better 5 cm), in order to keep the numerical stability of the soil moisture and temperature schemes. Of course, higher is the number of soil layers, higher is the simulation time. Simulation time is approximately one minute for one year of simulation on a standard Linux PC for a single station, with KDATA=2. If there are some observations to be used for the intercomparison, it could be better to try to choose soil depths in order to match the observation levels: due to the exponential dependence of soil temperature and to the high exponent in the soil moisture dependence from soil properties, there is not linearity for soil variables, thus interpolations could give non-realistic values. Note also that the

number of soil layers should be lower than *NSOILMAX*; the latter value is currently set equal to 11, but it can be modified in the source code: there are no limitations about the number of soil layers; of course, if *NSOILMAX* will be modified, then the source code must be recompiled;

NSO, ***TILSPM***, ***QILSPM***, ***DEP*** are, respectively, the soil code type, initial soil temperature [K], initial soil saturation ratio [$m_{void}^3 m_{soil}^{-3}$] and soil depth [m]. In table 10 there is an example of initialization with 8 levels of soil extending to a total soil depth of 12.75 m.

Note that soil moisture is expressed in units of saturation ratio, i.e. volumetric soil moisture (volume of water per volume of soil) per units of porosity (maximum volume of water per units of volume of soil). This number ranges from zero (no moisture, almost impossible to be observed) to one (complete saturation: this value is also rare).

In the same section, it is also possible to set soil texture composition by giving in input the percentages of clay (***CLAY***), sand (***SAND***) and organic matter (***OM***). From those variables it is possible to estimate soil water characteristics through some empirical equations taken from (Saxton and Rawls (2006)). UTOPIA initializes these variables to error, then it read from the FILEPA; if these variable are present, UTOPIA ignore the soil water characteristics taken from the soil category (i.e. Those inserted in the database of the SELECT_SOIL subroutine: see section 10.2.) and calculate them by using the Saxton and Rawls (2006) equations (implemented in the SAXTON subroutine).

Since these equations do not allow to obtain empirically the dry soil thermal capacity $(\rho c)_d$ on the basis of CLAY, SAND and OM percentages, the $(\rho c)_d$ values are taken

from the soil category of texture triangle. It is also important to stress the fact that these empirical equations are not valid for OM>8% or CLAY>60%. In fact, a high content of organic matter is typical of a soil that is not representative of typical mineral soils. On the other hand, soils with high clay content often have pore structure and mineralogical effects different than those containing higher portions of sand or silt fractions.

In the same section of parameters, it is also possible to set the following soil parameters values:

- η_s (***ETAS***): porosity $[m^3_{voids} m^{-3}_{soil}]$;
- ψ_s (***PSIS***): saturated moisture potential [cm];
- $K_{\eta s}$ (***CAPPAETAS***): soil saturated water conductivity $[dm^2 s^{-1}]$;
- b (***BSOIL***): dimensionless exponent in delendencies from soil moisture;
- η_{wi} (***ETAWI***): soil volumetric wilting point $[m^3_{voids} m^{-3}_{soil}]$;
- $(\rho c)_d$ (***ROCI***): dry soil volumetric heat capacity $[\mu J\, m^{-3} K^{-1}]$.

If all of these last parameters are given for a particular soil layer, UTOPIA will ignore the soil characteristics taken from the soil category (or from empirical equations of Saxton and Rawls (2006) if CLAY, SAND and OM have been specified).

In the empirical equations of Saxton and Rawls (2006), the values of b and η_s are calculated from the field capacity η_{fc} and wilting point η_{wi} values, whereas $K_{\eta s}$ is calculated from η_s and η_{fc} values. In turn, η_{wi} and η_{fc} are evaluated from the percentages of clay, sand and organic matter. If, in the FILEPA, the empirical equations

of Saxton and Rawls (2006) are used for the calculation of soil characteristics (giving the percentages of CLAY, SAND and OM), but at he same time η_s and/or η_{wi} and/or η_{fc} are known, the values of b , η_s and $K_{\eta s}$ are recalculated still by means of empirical equation of Saxton and Rawls (2006), but on the basis of the experimental values of η_s , η_{wi} and η_{fc} .

In the next session, other data relative to the soil are given. α_{sd} (***ALBSD***) is the bare soil albedo (whose typical value for most soil types is 0.31), τ (***TORTUOS***) is the tortuosity coefficient (used in the parametrization of soil water vapor flux: its typical value for most soil types is 40.0). It is not easy to specify the value of τ , but the exact value of this parameter is useful only in arid conditions, where water vapor could play an important role for the calculation of evapotranspiration in absence of liquid water; in non-arid conditions, this parameter is not essential. c_{drain} (***C_DRAIN***) is the drainage coefficient, which can range between 0 and 1: 0 means that it is not allowed the drainage out of the bottom layer of soil, while 1 means that the drainage out of the bottom layer of soil is equal to the hydraulic conductivity in that layer.

The subsequent group of data is dedicated to the date and time of the initial instant of the simulation. ***YYYY***, ***MM***, ***DD***, ***hh*** and ***mm*** are the year, month, day, hour and minutes of the first instant of the simulation, respectively. ***CLEG*** is the summertime code, usually equal to zero unless local hour is used for some locations in which summertime is active: in this case, the value must be set to "+1". ***LUTCFLAG*** is a logical variable that is true when the hours in the input file are expressed in UTC reference time: if this variable is not present in the FILEPA, LUTCFLAG is set by default as false.

The next group of parameters describe the site in which the simulation is performed. ***ALON_INI*** and ***ALAT_INI*** are the longitude and the latitude of the station (degrees and decimals), respectively; ***QUOTA*** is the station height (in m a.s.l.). ***ZLSPM*** and ***ZVLSPM*** represent the height of all observations (but wind) and wind above QUOTA, respectively. ***RRR*** is the second Linke turbidity factor (see section 3.2. and [Page, 1986]), the two angles of the terrain slope (the slope azimuth ***ESSE*** and the slope orientation ***GAMMA***: see section 3.2.1.). Note that ZLSPM and ZVLSPM are defined because UTOPIA requires that the observation data are at the same height, but normally meteorological stations put the thermo-hygrometer at the height of about 2 m, while the reference height of the anemometer is 10 m. Take into account the different heights is important to correctly evaluate the Richardson number and some other quantities related to the stability.

Then, the logical variable ***ECO_CHOICE*** (see also section 10.1.), which – if true - allows to use Ecoclimap database, is present. Last number in the FILEPA is ***HSN***, the initial snow height present at the beginning of the simulation [m].

The final part of FILEPA set a list of logical variables. They are:

- ***L360DAYS_CALENDAR***: if true, 360 days climatic calendar is used;
- ***ILOGALB***: if false, soil albedo changes, otherwise soil albedo is fixed;
- ***ILOGFUN***: if true, the haze function is activated;
- ***LDATA***: if true, date is fixed;
- ***LVAP***: if true, water vapor effects in the soil will be evaluated;

- L***TCAN_NEW***: if true, the new untested canopy temperature scheme is used.

If these variables are not set, the following default values within the model setup are assumed: L360DAYS_CALENDAR, ILOGALB, LDATA and LTCAN_NEW are set to false, and ILOGFUN and LVAP are set to true.

In summary, an important thing to emphasize is that the elder versions of FILEPA used in the elder versions of UTOPIA (prior 2010) and in LSPM are compatible and readible by UTOPIA (however, the configuration file 'memoryout.config' must necessarily be present.

13.3. INPUT: BOUNDARY CONDITIONS

The environment of the UTOPIA is bordered by two levels: an upper level located in the atmosphere, above the vegetation, and a lower level, located in the deepest soil layer. Concerning the lower level, the current structure of the model assumes that the user will select a sufficiently deep total soil layer in order that the energy flux at the bottom could be considered negligible, while the water flux will be selected according to the drainage code C_DRAIN (see section 7.5.). Thus, only the data at the upper level are needed for the simulation.

The management of input file is performed by the routine READ_INP. The procedure has been created in order that the model is able to read from many kinds of input files. UTOPIA is expecting to have NDATI columns for any record of the input file, which is generally an ASCII file of extension INT, with the data stored in columns. The maximum number of input (columns) presently considered by UTOPIA is 15. The first five columns

are reserved for the date-time group and are considered as a single column (number 1), while the other columns contains all available input data (see figure 1.2).

date			pressure		v wind		Precipitation		cloudiness
	time	temperature		u wind		relative humidity		solar radiation	
2005 06 01	00 00	299.85	998.00	0.56	-1.50	21.20	0.00	0.00	0.69
2005 06 01	00 30	300.30	998.00	0.83	-1.58	20.95	0.00	0.00	0.69
|---column 1-----|		|--2---|	|---3---|	|--4-|	|--5--|	|--6--|	|--7-|	|--8-|	|--9-|

Figure 13.1: Example of input data file.

The vector IC must contain the number of the column number corresponding to each variable required by UTOPIA. The total number of data required (inclusive of first column) is contained in the variable M (its maximum value is 15). The order of the data is prescribed: UTOPIA is searching input data in the order shown in table 11. The vector IC contains the number of the column in which the data are stored in the input file. If any of the above data is missing, a negative number should be given to IC. As an example, if the input data file contains the following columns: time, U wind, total cloudiness, low cloudiness, V wind, pressure, relative humidity, precipitation, and temperature, the following values should be given:

M=8

IC=/9,6,-1,3,2,5,8,4,-1,7/.

Table 11 summarizes the variables, their expected range of variations, and clarify whether a variable is needed or not: the mandatory data (i.e. the data needed by UTOPIA: without these data, it is impossible to run the model) are identified by a "y" in the first column; regarding humidity data, specific and relative humidity (indicated with "*") are complementary; also data of cloudiness and global radiation (indicated with "**") are

complementary. Last two columns indicate the minimum and maximum allowed values for the input variables, if any.

y		1	Air temperature	K	200	330
		2	Atmospheric pressure	hPa	600	1050
y	*	3	Specific humidity	g/kg	$1.3\ 10^{-8}$	0.63
y	**	4	Total cloudiness	Unity	0	1
y		5	X component wind velocity U	m/s	-50	50
y		6	Y component wind velocity V	m/s	-50	50
y		7	Precipitation rate (rain+snow)	mm/s	0	$2\ 10^{-5}$
y	**	8	Low cloudiness	Unity	0	1
y	**	9	Solar global incoming radiation	W/m2	0	1200
y	*	10	Relative humidity	%	1	100
	**	11	Long wave downward radiation	W/m2	-650	650
	***	12	vegetation height	m	0.7	30
	***	13	LAI	m2/m2	1	20
	***	14	vegetation cover fraction	Unity	0.2	1
	***	15	CO2	ppm	100	1000

Tab 11: List of possible input variables for UTOPIA.

Regarding the data remarked as non mandatory, when they are not provided in input, they will be calculated in specific routines of UTOPIA. In particular:

- Humidity can be given as specific or relative humidity;
- if atmospheric pressure is missing, is reconstructed by UTOPIA in the READ_INP routine using the hypsometric formulation:

$$p_a = 1013.25 - \rho_a g \frac{quote}{100} \quad ;$$

- longwave downward radiation will be evaluated as shown in section 3.3.;
- Regarding solar radiation, if this variable is not available, it is mandatory to have information about (at least) the total cloudiness. In fact, UTOPIA has an internal package to evaluate an estimate of solar radiation using the cloudiness data. On the contrary, if cloudiness data are not available, it is mandatory to have the solar radiation: in this case, UTOPIA will evaluate the cloudiness by comparing the

observed solar radiation with the empirically estimated one, while it will use the daily mean during nighttime. Thus, in a certain sense, cloudiness and solar radiation are alternative data. Nevertheless, if solar radiation is available and cloudiness is not available, the information about shortwave radiation will be very accurate but the information about longwave radiation will be not accurate, due to the greatest uncertainity on the cloudiness, and vice versa.

- vegetation height, LAI and vegetation cover fraction are not mandatory data; if they are not observed, they will be evaluated from the internal routines or from the vegetation databases (see section 10.1.). However, if the latter is missing, the fixed value of 393.84 ppm will be used in the photosynthesis calculation, while in the resistance formulation, the subfunction linked to CO_2 will be set to 1 (i.e. the depencence of canopy resistance from CO_2 will not be considered).

Regarding the input data, the following checks and calculations are performed in the routine READ_INP:

- there is a check on temperature data: if in °C, they will be converted into K;
- the UTOPIA read specific and/or relative humidity, and calculates the other variable;
- the precipitation rate is converted in $mm\,h^{-1}$;
- the cloudiness is set equal to one (overcast sky) in case of non-null precipitation;
- in the case in which low cloudiness is not observed, it will be evaluated as the half of high cloudiness;

- in the case in which solar radiation is not observed, it is calculated using the observations of low and middle-high cloudiness according with the formulations of section 3.2.;
- if solar radiation is observed, but cloudiness data are not observed, the theoretical clear-sky solar radiation is calculated according with the formulations of section 3.2., and then total cloudiness is calculated on the basis of the following equation:

$$c_n = 1 - \frac{Gr}{Gr_{theo}}$$

where Gr is the observed datum and Gr_{theo} the theoretical clear-sky solar radiation.

13.4. OUTPUT

The management of the output variables is performed basically in two subroutines, MEMORYOUT_CONFIG and DYNAMIC_MEMORYOUT. The basic idea of this feature is that no modifications of the source code are needed to configure the UTOPIA output management.

The set of available variables for output contains many variables, also for developing and diagnostic purposes (some diagnostic output can be required to the model without modifying its code, and making much easier and faster for developers to understand the reason of some behaviors of the model, keeping the source code as clean as possible).

13.4.1. Configuration of the required UTOPIA output

The configuration file for the output routines has been conventionally named ***memoryout.config*** and UTOPIA looks for that in the default ***par/*** directory.

A sample of lines of this file is shown in Table 12.

```
!Configuration file for subroutine DYNAMIC_MEMORYOUT.[...]
AGRLSPM n    F8.3     !  global radiation (INPUT) [Wm-2]
RNLSPM y    F8.3     !  net radiation [Wm-2]
HALSPM y    F8.3     !  sensible heat flux [Wm-2]
FALSPM y    F8.3     !  latent heat flux [Wm-2]
QGTOT y    F8.3     !  atmosphere-surface total conductive flux [Wm-2]
PQLSPM     1-3&5-7    F8.3     !  soil humidity [% of por]
TLSPM n    F8.3     !  soil temp. [C]
CAPPAETA y    EN16.6  !  soil hydraulic conductivity [m/s]
```

Tab 12: Sample of file memoryout.config

This file contains a first line of caption. Then, a table of 5 columns follows. The columns of this table contain, respectively, the name of an UTOPIA variable, a “yes or no” column, a format descriptor, a short variable descriptor and its units (last two are text fields useful only for a memo). The file contains all variales available for the output. The only column the user should modify are the second (“yes or no”) and the third (format descriptor). The latter is just a valid Fortran format descriptor that will be used for that particular variable. A “yes” in the “yes or no” column means that the variable indicated in that line will be included in the output. Scalar variables can just have a “yes” (y, t) or a “no” (n, f), upper or lower case, to include or not that particular scalar. In the example of Table 12, the global radiation (AGRLSPM) is not printed, but all other components of the energy balance are.

Array variables present a little bit more complicated syntax for the specification of the required output. Sometimes it could be useful to check the desired variables just on some soil layers and not in all of them. We provided a syntax to match this output possibility. As a first point, if a syntax like the scalar ones is found, it applies to all the elements of

the array variable: in the example of Table 12, soil temperature (TSOIL) is not printed, while soil hydraulic conductivity (CAPPAETA) is printed for every layer.

In the line relative to soil humidity, a different syntax appears. The user can select the output layers one by one by the use of an ampersand (&) separated list, or an interval of layers, extremes included, using an hyphen(-). For instance, to select just the first four layers of a particular array, it is possible to write ***1&2&3&4*** or just ***1-4***. Any valid combination of these choices is valid: for instance, in Table 12, for the soil moisture PQLSPM, the syntax means the user has selected to include in the output of the model the data of soil layers number 1, 2, 3, 5, 6, and 7, but not the 4th.

Very important note: it is required to not leave any blank within the layer selector of array variables, in order to not make the model crash. For instance, a command line like ***1 & 2&3&4*** is not allowed.

13.4.2. Developers' notes: how to make a new variable available for output

In order to make a new variable available for output, that variable must be passed from the main program to the two called subroutines MEMORYOUT_CONFIG and DYNAMIC_MEMORYOUT.

Then, the file *${LSPM_ROOT}/par/memoryout.config* must be updated. A new line must be introduced, at its bottom, containing the name of the variable, a flag of yes or no, a reasonable output format, then a short descriptor with the units.

Since UTOPIA is configured to read a fixed number of lines from this file (which is stored in the integer parameter NSUDYN in the CONSTANTS module), it is necessary to

update NSUDYN increasing its value by the number of new variables (scalars or arrays) added.

The following operations are different according to the type of variable added (scalar or array).

Scalar variables: specific steps

The only operation regards the subroutine DYNAMIC_MEMORYOUT, in which it is necessary to add the new output variable in the calling arguments (both in the actual arguments in the main program, and in the dummy arguments in the subroutine declaration), then declare the new variable in the subroutine. In the subroutine code, one must assign a new element to the SU_POSSIBILITIES array; in particular the last one.

So, for example, if 42 elements are assigned in the SU_POSSIBILITIES array before adding one new output variable, and NSUDYN has been already updated from 42 to 43 as stated in the previous step, the 43rd element of SU_POSSIBILITIES array must be assigned with the value of the new output variable.

Array variables: specific steps

In this case, the procedure is rather complicated, as several steps are required. Let suppose to add the new array NEWARRAY.

As a preliminary step, in the main program, a new logical array variable must be created. Its declaration should be done as follows:

```
LOGICAL,DIMENSION(:),ALLOCATABLE :: LAYERS_OUT_NEWARRAY
```

Then, in the part of the main program in which all the dynamic memory allocations are made, this array must be allocated by adding the line (note that, in this section of the code, like in many others, the variables appear in alphabetical order):

```
ALLOCATABLE LAYERS_OUT_NEWARRAY
```

Then, the subroutine MEMORYOUT_CONFIG must be changed. At first, the newly created variable LAYERS_OUT_NEWARRAY must be made an output argument of the subroutine, so it must be put in its calling sequence and in the dummy argument list, and declared similarly to the other arrays of the same kind. Then, the MEMORYOUT_CONFIG subroutine must be configured to take into account the fact that the variable is an array. This can be done by modifing the first IF block after the VARIABLE_NAME, SELECT_OUTPUT and FORMAT_OUTPUT_SINGLEVAR are read from memoryout.config. That IF selection verifies if the variable name corresponds to an array. Here, a new verification line similar to the ones above must be inserted:

```
IF(VARIABLE_NAME(I)=='PQLSPM'.OR.VARIABLE_NAME(I)=='TLSPM'.OR.&
VARIABLE_NAME(I)=='CAPPAETA'.OR.VARIABLE_NAME(I)=='CAPPAETAM'.OR.&
VARIABLE_NAME(I)=='CAPPAM'.OR.VARIABLE_NAME(I)=='DIFFSUMM'.OR.&
VARIABLE_NAME(I)=='DIFFSUM'.OR.VARIABLE_NAME(I)=='DIFFVTM'.OR.&
VARIABLE_NAME(I)=='NEWARRAY')THEN
[...]
END IF
```

Since the subroutine uses a generic logical array to understand the user's output require, the information stored in this generic array must be associated to the new output variable:

```
!Assignement of the LAYERS_OUT_GENERIC to the correct LSPM field
IF(VARIABLE_NAME(I)=='PQLSPM')THEN
LAYERS_OUT_PQLSPM=LAYERS_OUT_GENERIC
ELSE IF(VARIABLE_NAME(I)=='TLSPM')THEN
LAYERS_OUT_TLSPM=LAYERS_OUT_GENERIC
ELSE IF(VARIABLE_NAME(I)=='CAPPAETA')THEN
LAYERS_OUT_CAPPAETA=LAYERS_OUT_GENERIC
ELSE IF(VARIABLE_NAME(I)=='CAPPAETAM')THEN
LAYERS_OUT_CAPPAETAM=LAYERS_OUT_GENERIC
```

```
ELSE IF(VARIABLE_NAME(I)=='CAPPAM')THEN
LAYERS_OUT_CAPPAM=LAYERS_OUT_GENERIC
ELSE IF(VARIABLE_NAME(I)=='DIFFSUMM')THEN
LAYERS_OUT_DIFFSUMM=LAYERS_OUT_GENERIC
ELSE IF(VARIABLE_NAME(I)=='DIFFSUM')THEN
LAYERS_OUT_DIFFSUM=LAYERS_OUT_GENERIC
ELSE IF(VARIABLE_NAME(I)=='DIFFVTM')THEN
LAYERS_OUT_DIFFVTM=LAYERS_OUT_GENERIC
ELSE IF(VARIABLE_NAME(I)=='NEWARRAY')THEN
LAYERS_OUT_NEWARRAY=LAYERS_OUT_GENERIC
END IF
```

Where the new part has been indicated in red color.

Regarding the subroutine DYNAMIC MEMORYOUT, the new array in output must be inserted in the calling sequence and in the dummy arguments of the subroutine DYNAMIC_MEMORYOUT, both the variable itself and the related logical array LAYERS_OUT_*. The order of the dummy variables of subroutine DYNAMIC_MEMORYOUT is such that the first group of variables are the output format, then the LAYERS_OUT_* arrays (for every array for which is possible to have as an output), then the actual values of the array variables, then the scalar variables, then date and time and some variables useful for determining the writing mode.

Then the SU_POSSIBILITIES array must be updated. The actual dimension of the array should be already updated, ok after having completed the procedures described at the very beginning of this section. Even if an array will be added to the output, just one element of the SU_POSSIBILITIES array must be added. Even if the specific value assigned to the new SU_POSSIBILITIES element will not be important, for convenience it has been decided to set it equal to -999.9, with a comment stating why that value was set to -999.9. As an example, the following two lines refer to the addition of two variables in output: the scalar SOL_ALFA and the array CAPPAETA:

```
SU_POSSIBILITIES(36)=SOL_ALFA
SU_POSSIBILITIES(37)=-999.9!Will fill with CAPPAETA array
```

After having defined the newer element in the SU_POSSIBILITIES array, it is necessary to update its dynamic filling.

The code section dedicated to the dynamic filling consists basically in a long sequence of: IF() THEN . . . ELSE IF()THEN . . . ELSE . . . END IF. The last element of this sequence is slightly different, but it is not important for the introduction of a new array variable in the output possibilities (it deals with the output of scalar variables, but it is not affected by the introduction of a new output possibility, so it should not be modified). Thus, each block of this sequence will look as:

```
[ELSE] IF(VARIABLE_NAME(I_POSSIB)=='NEWARRAY')THEN
DO K_NSOILLSPM=1,NSOILLSPM
IF(LAYERS_OUT_NEWARRAY(K_NSOILLSPM))THEN
SU6(J_SU)=NEWARRAY(K_NSOILLSPM)
J_SU=J_SU+1
END IF
END DO
```

Except the first one (no leading ELSE) and the last one (non array behaviour). The developer must just insert a new block similar to the one above shown, obviously changing the string containing the variable name to be verified in the IF statement, the verification on the LAYERS_OUT* to output and the assignment to the SU6(J_SU) array.

14. References

Allen R. G., Trezza R., Tasumi M., 2006: Analytical integrated functions for daily solar radiation on slopes. . *Agricultural and Forest Meteorology*, **139**, 55–73

Anderson, E. A., 1976: *A point energy and mass balance model of a snow cover. ,* . NOAA Tech. Rep., Off. Hydrol., Nat. Weather Ser., Silver Spring, Md.., NWS 19. .

Anten N. P. R., E. Schieving, and M. J. A. Werger, 1995: Patterns of lightand nitrogen distribution in relation to whole canopy carbon gain in C3 and C4 mono- and dicotyledonous species. *Oeeologia*, **101**, 504–513

Arora V., 2002: Modeling vegetation as a dynamic component in soil-vegetation-atmosphere transfer schemes and hydrological models. *Reviews of Geophysics*, **40**, 1006–1019

Arrhenius S.A., 1889: Über die Dissociationswärme und den Einflusß der Temperatur auf den Dissociationsgrad der Elektrolyte. *Z. Physik. Chem.*, **4**, 96–116

Arya, S. P., 1988: . Academic Press (San Diego), 307 pp

Avissar R., Pielke R. A., 1991: The impact of plant stomatal control on mesoscale atmospheric circulations.. *Agricultural and Forest Meteorology*, **54**, 353–372

Avissar R., Verstraete M. M., 1990: The representation of continental surface processes in atmospheric models. *Reviews of Geophysics*, **28**, 35-52

Ball J. T., I. E. Woodrow, and J. A. Berry, 1987: *A model predictingstomatal conductance and its contribution to the control of photosynthesis under different environmental conditions*. In Progress in Photosynthesis Research. , 221–224

Beljaars A. C. M., Viterbo P., Miller M. J., Betts A. K., 1996: The anomalous rainfall over the United States during July 1993: sensitivity to land surface parametrization and soil moisture anomalies.. *Monthly Weather Review*, **124**, 362–383

Bernacchi C. J., A. R. Portis jr, H.????????????????, S. V. Nakano, and S. P. Long, 2002: Temperature response of mesophyll conductance. Implications for the deter-mination of Rubisco enzyme kinetics and for limitations to photosynthesisin vivo. *Plant Physiol.*, **130**, 1992–1998

Bernacchi C. J., C. Pimentel, and S. P. Long, 2003: In vivo temperatureresponse functions of parameters required to model RuBP-limited photo-synthesis. *Plant Cell Environ*, **26**, 1419–1430

Bernacchi C. J., D. M. Rosenthal, C. Pimentel, S. P. Long, and G. D. Farquhar, 2009: *Modeling the Temperature Dependence of C3 Photosynthesis*. In Photosynthesis in silico: Understanding Complexity from Molecules to Ecosystems. Springer Science + Business Media B.V., 231–246

Bernacchi C. J., E. L. Singsaas, C. Pimenntel, A. R. Portis jr, and S. P. Long, 2001: Improved temperature response functions for models ofRubisco-limited photosynthesis. *Plant, Cell and Environment*, **24**, 253–259

Betts A. K., Ball J. H., Beljaars A. C. M., Miller M. J., Viterbo P. A., 1996: The land surface–atmosphere interaction: a review based on observational and global modeling perspectives.. *Journal of Geophysical Research*, **101**, 7209–7225

Blondin (1988): Blondin, C., Research on Land Surface Parameterization Schemes at ECMWF, 1988

Bonan G. B., 2002: *Leaves and plants*. In Ecological climatology: concepts and applications. Cambridge University Press, 690 pp

Bonan G.B., 1996: *A Land Surface Model (LSM version 1.0) for ecological, hydrological and atmospheric studies: technical description and user's guide*. NCAR technical note, NCAR, Climate and global division, Boulder, Colorado, NCAR/TN-417+STR. missing.

Bonanno, R., N. Loglisci, S. Cavalletto, and C. Cassardo, 2010: Analysis of Different Freezing/Thawing Parameterizations using the UTOPIA Model. *Water*, **2**, 468-483

Boone, A., and P. J. Wetzel, 1996: Issues related to low resolution modeling of soil moisture: Experience with the PLACE model. *Global and Plan. Change*, **13**, 161-181

Brutsaert, W., 1982: . D. Reidel, Hingham, Mass., 299 pp

Cassardo C., 2006: *The Land Surface Process Model (LSPM) version 2006. The complete manual.*. , Department of General Physics "Amedeo Avogadro", University of Torino, Italy., DFG Report – 01/2006. . Available from claudio.cassardo@unito.it

Cassardo C., Carena E., A. Longhetto A., 1998: Validation and sensitivity tests on improved parametrizations of a land surface process model (LSPM) in the Po Valley.. *Il Nuovo Cimento C*, **21(2)**, 189-213

Cassardo C., Ji J. J., Longhetto A., 1995: A study of the performance of a land surface process model (LSPM). *Boundary Layer Meteorology*, **3**, 87-121

Cassardo C., Loglisci N., Gandini D., Qian M. W., Niu G. P., Ramieri P., Pelosini R. Longhetto A., 2002: The flood of november 1994 in Piedmont, Italy: a quantitative simulation.. *Hydrological Processes*, **16**, 1275–1299

Cassardo C., Loglisci N., Paesano G., Rabuffetti D., Qian M. W., 2006: The hydrological balance of the October 2000 flood in Piedmont, Italy: quantitative analysis and simulation.. *Phys. Geogr.*, **27(5)**, 411-434

Cassardo C., Loglisci N., Romani M., 2005: Preliminary results of an attempt to provide soil moisture datasets in order to verify numerical weather prediction models.. *Il Nuovo Cimento C*, **28(2)**, 159–171

Cassardo C., Mercalli L., Cat Berro D., 2007: Charateristics of the summer 2003 heat wave in Piedmont, Italy, and its effects on water resources.. *Journal of the Korean Meteorological Society*, **43(3)**, 195-221

Cassardo C., Park S. K., Malla Thakuri B., Priolo D., Zhang Y., 2009: Soil surface energy and water budgets during a monsoon season in Korea.. *J. Hydrometeorol.*, **10(6)**, 1379–1396

Cassardo et al. (2003): Cassardo, C., Loglisci N., Manfrin M., and Spanna F., The estimate of surface wetness of the vegetation: experiments and numerical methods, 2003

Cerenzia, I., 2012: *Ecophysiological processes in a Big-Leaf model*. , , 189 pp.. Available from the author.

Chen F., Mitchell K., Schaake J., Xue Y., Pan H.-L., Koren V., Duan Q. Y., Ek M., Betts A., 1996: Modeling of land surface evaporation by four schemes and comparison with FIFE observations.. *J. Geophys. Res.*, **101(D3)**, 7251-7268

Chen T. H., Henderson-Sellers A., Milly P. C. D., Pitman A. J. , Beljaars A. C. M., Polcher J., Abramopoulos F., Boone A., Chang S., Chen F., Dai Y., Desborough C. E., Dickinson R.E., Dümenil L., Ek M., Garratt J. R., Gedney N., Gusev Y. M., Kim J., Koster R., Kowalczyk E. A., Laval K. , Lean J., Lettenmaier D., Liang X., Mahfouf J.-

F., Mengelkamp H.-T., Mitchell K., Nasonova O. N., Noilhan J., Robock A., Rosenzweig C., Schaake J., Schlosser C. A., Schulz J.-P., Shao Y., Shmakin A. B., Verseghy D. L., Wetzel P., Wood E. F., Xue Y., Yang Z.-L., Zeng Q., 1997: Cabauw experimental results from the Project for Intercomparison of Land-surface Parameterization Schemes.. *Journal of Climate*, **10**, 1194–1215

Clapp, R. B., and G. M. Hornberger, 1978: missing. *Water Resour. Res.*, **14**, 601-missing

Collatz G. J., M. Ribas-Carbo, and J. A. Berry, 1992: Coupled photosynthesis-stomatal conductance model for leaves of C4 plants. *Aust. J. Plant Physiol.*, **19**, 519–538

Collatz G. J., T. J. Ball, C. Grivet, and J. A. Berry, 1991: Physiological and environmental regulation of stomatal conductance, photosynthesis and transpiration: a model that includes a laminar boundary layer. *Agricultural and Forest Meteorology*, **54**, 107–113

Cosby B. J., G. M. Hornberger, R. B. Clapp, and T. R. Ginn, 1984: A statistical exploration of the relationships of soil moisture characteristics to the physical properties of soils. *Water Resour. Res.*, **20**, 682-690

Cox, P. M., R. A. Betts, C. B. Bunton, R. L. H. Essery, P. R. Rowntree, and J. Smith, 1999: The impact of new land surface physics on the GCM simulation of climate and climate sensitivity. *Climate Dynamics*, **15**, 183–203

Crank, J., and P. Nicolson, 1947: A practical method for numerical evaluation of solutions of partial differential equations of the heat conduction type. *Proc. Camb. Phil. Soc.*, **43 (1)**, 50-67

Dai, Y. J., and Q. C. Zeng, 1988: A land surface model (IAP94) for climate studies. Part I: formulation and validation in off-line experiments. *Climate Dynamics*, **MISSING**, MISSING

Damour G., T. Simonneau, H. Cochard, and L. Urban, 2010: An overviewof models of stomatal conductance at the leaf level. *Plant, Cell and Environment*, **33**, 1419–1438

De Pury D. G. G., and G. D. Farquhar, 1997: Simple scaling of photosyn-thesis from leaves to canopies without the errors of big-leaf models. *Plant,Cell and Environment*, **20**, 537–557

Deardorff J. W., 1978: Efficient prediction of ground surface temperature and moisture with inclusion of a layer of vegetation.. *Journal of Geophysical Research*, **83**, 1889–1903

Dickinson R. E., Henderson-Sellers A., Kennedy P. J., Wilson M. F., 1986: *Biosphere–Atmosphere Transfer Scheme (BATS) for the NCAR Community Climate Model.*. NCAR Technical Note TN-275 + STR., , . missing.

Dickinson, R.E., 1984: *Modeling evapotranspiration for 3dimensional global climate models*. In Climate Processes and climate sensitivity. Am. Geophys. Union, Washington, DC, 58-72

Dingman, S. L., 1994: *Physical hydrology*. Macmillan College Pub. Com., N. York., US, MISSING

Douville, H., J. F. Royer, and J.-F. Mahfouf, 1995: *Douville, H., Royer, J.F. and Mahfouf, J. F. ; 1995 : A new snow parameterization for The meteo – france climate model. Note de travail n. 44, Centre national de Recherches meteorologiques, Meteofrance, France*. Note de travail, Centre national de Recherches meteorologiques, Meteofrance, France, 44. MISSING.

Ehleringer J. R., and O. Björkman, 1977: Quantum yields for CO2 uptake in C3 and C4 plants: Dependence on temperature, CO2 and O2 concentration. *Plant Physiol.*, **59**, 86-90

Ehleringer J. R., and Pearcy R. W., 1983: Variation in quantum yield for CO2 uptake among C3 and C4 plants. *Plant. Physiol.*, **73**, 555-559

Farquhar G. D., 1989: Models of integrated photosynthesis of cells and leaves. *Philosophical Transactions of Royal Society of London*, **323**, 357–367

Farquhar, G. D., and T. D. Sharkey, 1982: A point energy and mass balance model of a snow cover. *Annual Review of Plant Physiology*, **33**, 317–345

Farquhar, G. D., S. von Caemmerer, J. A. Berry, : A biochemicalmodel of photosynthetic CO2 assimilation in leaves of C3 species. *Planta*, **149**, 78–90

Feng J., Liu X., Cassardo C., Longhetto A., 1997: A model of plant transpiration and stomatal regulation under the condition of waterstress.. *Journal of Desert Research*, **17**, 59–66

Field C., 1983: Allocating leaf nitrogen for the maximization of carbon gain: leaf age as a control on the allocation program. *Oeeologia*, **56**, 341–341

Francone C., Katul G., Richiardone R., Cassardo C., 2011: Turbulent transport efficiency and the ejection-sweep motion for momentum and heat on sloping terrain covered with vineyards.. *Agr. Forest Meteorol.*, **missing**, missing

Garratt J. R., 1993: Sensitivity of climate simulations to land-surface and atmospheric boundary-layer treatments — a review.. *Journal of Climate*, **6**, 419–449

Garratt, J. R., 1984: *The atmospheric boundary layer*. Cambridge University Press, missing

Gel'fan, A. N., 1989: Comparison of two methos of calculating soil freezing depth. *Sov. Meteorol. Hydrol.*, **2**, 78–83

Gottib, L., : A general runoff model for snow – covered and glacierized basins. *Nord. Hydrol. Conf.*, **6**, 172-177

Goudriaan J., 1977: *Crop Micrometeorology: a Simulation Study*. PUDOC, Wageningen, missing

Grimmond, C. S. B., H. A. Cleugh, and T. R. Oke, : An Objective Urban Heat-StorageModel and its Comparison with Other Schemes. *Atmos. Environ.*, **25B**, 311–326

Hansen, M. C., R. S. Defries, J. R. G. Townshend, and R. Sohlberg, 2000: missing. *Int. J. Remote Sensing*, **21**, 1331-missing

Henderson-Sellers A., Dickinson R. E, Durbidge T. B., Kennedy P. J., McGuffie K., Pitman A. J., 1993: Tropical deforestation: modelling local to reg.ional-scale climate change.. *Journal of Geophysical Research*, **98**, 7289–7315

Hirose T. and M. J. A. Werger, 1987: Maximizing daily canopy photosyn-thesis with respect to the leaf nitrogen allocation pattern in the canopy. *Oecologia*, **72**, 520–526

IUPAC, 1997: *Compendium of Chemical Terminology*. Blackwell Scientific Publications, Oxford,

Jacquemin B., and J. Noilhan, 1990: Sensitivity study and validation of a land surface parameterization using the HAPEX-MOBILHY data set. *Bound.-Layer Meteor.*, **52**, 93-134

Jarvis P. G., 1976: The interpretation of the variations in leaf water potential and stomatal conductance found in canopies in the field.. *Philosophical Transactions of the Royal Society of London*, , 593–610

Kojima (1967): Kojima, K., Densification of seasonal snow cover,physics of snow and ice, 1967

Koren, V., J. Schaake, K. Mitchell, Q.– Y. Duan, F. Chen, and J. M. Baker, 1999: A Parametrization of snow pack and frozen ground intended for NCEP weather And climate models. *J.Geophys. Res.*, **104 (D16)**, 19569 – 19585

Loglisci N., Qian M. W. , Cassardo C., Longhetto A., Giraud C., 2001: Energy and water balance at soil-air interface in a Sahelian region.. *Advances in Atmospheric Sciences*, **18**, 897–909

Louis J.F., 1979: A parametric model of vertical eddy fluxes in the atmosphere. *Boundary-Layer Meteor.*, **17**, 187-202

Loveland T. R., B. C. Reed, J. F. Brown, D. O. Ohlen, Z. Zhu, L. Yang, and J. W. Merchant, 2000: missing. *Int. J. Remote Sensing*, **21**, 1303-missing

Makino A., H. Nakano, T. Mae, T. Shimada, and N. Yamamoto, 1999: Photosynthesis, plant growth and N allocation in transgenic rice plants withdecreased Rubisco under CO2 enrichment. *Journal of Experim. Botany*, **51**, 383–389

Manabe S., 1969: Climate and the ocean circulation: 1, the atmospheric circulation and the hydrology of the Earth's surface.. *Monthly Weather Review*, **97**, 739–805

Masson, V., J.-L. Champeaux, F. Chauvin, C. Meriguet, and R. Lacaze, 2003: V. Masson, J.-L. Champeaux, F. Chauvin, C. Meriguet and R. Lacaze, 2003 : A global database of land surface parameters at 1km resolution in meteorological and climate models, J. Climate, 16, 1261-1282. *J. Climate*, **16**, 1261-1282

Mc Cumber, M. C., 1980: *A numerical simulation of the influence of heat and moisture fluxes upon mesoscale circulations.*. Ph.D. Dissertation, University of Virginia, Charlottesville, MISSING.

Medlyn B. E., E. Dreyer, D. Ellsworth, M. Forstreuter, P. C. Harley, M. U. F. Kirschbaum, X. Le Roux, P. Montpied, J. Strassemeyer, A. Wal-Croftand, K. Wang, and D. Loustau, 2002: Temperature response ofparameters of a biochemically based model of photosynthesis. II. A review of experimental data. *Plant, Cell and Environment*, **25**, 1167–1179

Mintz, Y., 1984: *The Global Climate*. Cambridge University Press, 79-105

Monsi M. and T. Saeki, 1953: Uber den lichtfaktor in den pflanzenge-sellschaften und seine bedeutung fur die stoff produktion. *Japanese Journal of Botany*, **14**, 22–52

Monteith J. L., 1973: *Principles of Environmental Physics*. Edward Arnold, London, 241 pp

Murthy K. V. R., 2002: *Basic principles of agricultural meteorology*. BS Publications, 261 pp

Mutinelli F. (1988), 1988: *Study of physical processes involving the snow pack and their parameterization at the internal of a numerical model of energy balance.*. Master thesis in physics, University of Torino "Alma Universitas Taurinorum", Italy, 269 pp. In Italian. Available from the author.

Niu G. Y., S. F. Sun, and Z. X. Hong, 1997: Water and heat transport in the desert soil and atmospheric boundary layer in western China. *Bound.-Lay. Meteorol.*, **85**, 179–195

Noilhan J., Planton S., 1989: A simple parameterization of land surface processes for meteorological models.. *Monthly Weather Review*, **117**, 536–549
Oglesby R. J., 1991: Springtime soil moisture variability, and North American drought as simulated by the NCAR Community Climate Model.. *I. J. Climate*, **4**, 890–897
Oleson K. W., D. M. Lawrence, G. B. Bonan, M. G. Flanner, E. Kluzek, P. J. Lawrence, S. Levis, S. C. Swenson, and P. E. Thornton, 2010: *Technical Description of version 4.0 of the Community Land Model (CLM)*. Technical report, , missing. missing.
Page J. K., 1986: . D. Reidel Publishing Company,
Philip, J. R., and D. A. de Vries, 1957: Moisture movement in porousmaterials under temperature gradients. *Trans. Am. Geophys. Union*, **38**, 222-232
Pielke R. A. Sr., 2001: Influence of the spatial distribution of vegetation and soils on the prediction of cumulus convective rainfall.. *Reviews of Geophysics*, **39**, 151–177
Pielke R. A., Avissar R., Raupach M., Dolman A. J., Zeng X., Denning A. S., 1998: Interactions between the atmosphere and terrestrial ecosystems: influence on weather and climate.. *Global Change Biology*, **4**, 461–475
Pielke, R. A., 1984: *Mesoscale meteorological modelling*. San Diego Academic Press, missing
Pitman A. J., 2003: Review: the Evolution of, and Revolution in, Land Surface Schemes designed for Climate Models. *Int. J. Climatol.*, **23**, 479–510
Polcher J., B. McAvaney, P. Viterbo, M.-A. Baertner, A. Hahmann, J.-F. Mahfouf, J. Noilhan, T. Phillips, A. Pitman, C. A. Schlosser, J.-P. Schulz, B. Timbal, D. Verseghy, Y. Xue (1998), : A proposal for a general interface between land surface schemes and general circulation models.. *Global and Planetary Change*, **19**, 261–276
Prino, S., F. Spanna, and C. Cassardo, 2009: Verification of the stomatal conductance of Nebbiolo grapevine. *Journal of Chongqing University (English Edition)*, **8 (1)**, 17-24
Qian, M. W., N. Loglisci N., C. Cassardo, A. Longhetto, and C. Giraud, 2001: Energy and water balance at soil-interface in a Sahelian region. *Advances in Atmospheric Sciences*, **18 (5)**, 897-909
Robinson, D. and G. Kukla, 1984: Albedo of a dissipating snow cover.. *J. Climat. and Appl. Meteor.*, **23**, 1626–1634
Robock, A., K. Y. Vinnikov, C. A. Schlosser, N. A. Speranskaya, and Y. Xue, 1995: Use of midlatitude soil moisture and meteorological observations to validate soil moisture simulations with biosphere and bucket models. *J. Climate*, **8**, 15-35
Ruti P. M., Cassardo C., Cacciamani C., Paccagnella T., Longhetto A., Bargagli A., 1997: Intercomparison between BATS and LSPM surface schemes, using point mocrometeorological data set.. *Contrib. Atmos. Phys.*, **70**, 201–220
Sadras V. O., A. J. Hall, and D. J. Connor, 1993: Light-associated nitrogendistribution profile in flowering canopies of sunflower (Helianthus annuus L.) altered during grain growth. *Oecologia*, **95**, 488–494
Salvucci M. E., and S. J. Crafts-Brandner, 2004: Inhibition of photosyn-thesis by heat stress: the activation state of Rubisco as a limiting factor inphotosynthesis. *Phisiologia Plantarum*, **120**, 179–186
Saxton K. E. and Rawls W. J., 2006: Soil water characteristic estimates by texture andorganic matter for hydrologic solutions.. *Soil Sci. Soc. Am. J.*, **70**, 1569–1578
Schrödin, R., and E. Heise, 2001: *The Multi Layer Version of the DWD Soil Model TERRA_LM*. Technical Report, COSMO: Offenbach, Germany, 2. .

Sellers P. J., 1992: *Climate System Modelling*. Cambridge University Press,
Sellers P. J., Dickinson R. E., Randall D. A., Betts A. K., Hall F.G., Berry J. A., Collatz G. J., Denning A. S., Mooney H. A., Nobre C. A., Sato N., Field C. B., Henderson-Sellers A., 1997: Modelling the exchanges of energy, water and carbon between continents and the atmosphere.. *Science*, **275**, 502–509
Sellers P. J., Mintz Y., Sud Y. C., Dalcher A., 1986: A Simple Biosphere model (SiB) for use within general circulation models.. *Journal of the Atmospheric Sciences*, **43**, 505–531
Sellers P. J., Randall D. A., Collatz C. J., Berry J. A., Field C. B., Dazlich D. A., Zhang C., Collelo G., Bounoua L., 1996: A revised land-surface parameterization (SiB2) for atmospheric GCMs. Part 1: model formulation. *Journal of Climate*, **9**, 676–705
Sellers, P. J.,J. A. Berry, G. J. Collatz, C. B. Field and F. G. Hall, 1992: Canopy Reflectance, Photosynthesis, and Transpiration. III. A Reanalysis Using Improved Leaf Models and a New Canopy Integration Scheme. *Remote Sensing Environ*, **42**, 187-216
Shao Y, Henderson-Sellers A., 1996: Modeling soil moisture: a project for intercomparison of landsurface parameterization schemes phase 2(b).. *Journal of Geophysical Research*, **101**, 7227–7250
Singsaas E. L., D. R. Ort, and E. H. Delucia, 2001: Variation in mea-sured values of photosynthetic quantum yield in ecophysiological studies. *Oecologia*, **128**, 15–23
Skillman J. B., 2009: Quantum yield variation across the three pathways ofphotosynthesis: not yet out of the dark. *Journal of Experimental Botany*, **59**, 1647–1661
Sun, S. F., 1982: *Moisture and heat transport in a soil layer forcedby atmospheric conditions*. M. Sc. thesis, , missing.
Sun, S. F., I. Jin I., and Y. K. Xue, 1999: A simple snow-atmosphere-soil transfer model.. *J. Geophys . Res.*, **104 (D16)**, 19587-19597
Thornton, P. E. and Zimmermann, N. E. (2007), 2007: An improved canopy inte-gration scheme for a land surface model with prognostic canopy structure. *J. Climate*, **20**, 3902–3923
van 't Hoff J. H., 1884: *Etudes de Dynamique Chimique*. Kessinger Publishing, LLC, Amsterdam, 226 pp
Verseghy D. L., 1991: CLASS—A Canadian land surface scheme for GCMS. I. Soil model.. *Int. J. Climatol.*, **11**, 111–133
Verseghy D. L., Mc Farlane N. A., Lazare M., 1993: CLASS — a Canadian Land Surface Scheme for GCMs. II: vegetation model and coupled runs.. *International Journal of Climatology*, **13**, 347–370
Viterbo, P., A. M. Beljiard, J.-F. Mahnfouf, and J. Teixeira, 1999: The representation of soil moisture freezing and its impact on stable boundary layer. *Quart. J. Roy. Meteorol. Soc.*, **125**, 2401-2426
von Caemmerer, S., 2000: *Biochemical models of leaf photosynthesis*. CSIRO Publishing, missing
Wen L., Yu W., Lin C. A., Beland M., Benoit R., Delage Y., 2000: The Role of Land Surface Schemes in Short-Range, High Spatial Resolution Forecasts.. *Monthly Weather Review*, **128**, 3605-3617

Wetzel P., S. Argentini, and A. Boone, 1996: Role ofland surface in controlling daytime cloud amount: Two case studies in the GCIP-SW area. *J. Geophys. Res.*, **101**, 7359-7370

Wilson, M. F., and A. Henderson-Sellers, 1985: A global archive of land cover and Soils data for use in general circulation climate models. *Journal of Climatology*, **5**, 119-143

Wullschleger S., 1993: Biochemical limitations to carbon assimilation inC3 plants - A retrospective analysis of the A/Ci, curves from 109 species. *Journal of Experimental Botany*, **44**, 907–920

Yang Z. L., Dickinson R. E., Robock A., Vinnikov K.Y., 1997: 1997. On validation of the snow sub-model of the biosphere–atmosphere transfer scheme with Russian snow cover and meteorological observational data.. *Journal of Climate*, **10**, 353–373

Yang, Z.-L., and R. E. Dickinson, 1996: Yang, Z.-L., and R. E. Dickinson, 1996: Description of the Biosphere–Atmosphere Transfer Scheme (BATS) for the soil moisture work-shop and evaluation of its performance.. *Global Planet. Change*, **13**, 117-134

Zhang Y., Cassardo C., Ye C., Galli M., Vela N., 2011: A Landfall Typhoon Simulation in a Coupled Land Surface Process Model with WRF.. *Asia-Pacific J. Atmos. Sci.*, **47**, 63-77

15. Acknowledgments

The original version of UTOPIA model was called LSPM (Land Surface Process Model) and has been developed by Jin Jun Ji, Arnaldo Longhetto and myself in 1989. In the long period elapsed since that date, several persons have worked in adjusting mistakes, upgrading old parameterizations or developing new parameterizations, and generally improving the model: despite the list of persons is not exhaustive, I want to thank Elena Carena, Paolo Michele Ruti, Ying Feng, Guang Ye Niu, Min Wei Qian, Paolo Ramieri, Federica Mutinelli, Gianpaolo Balsamo, Mattia Romani, Massimiliano Trevisan, Nicola Loglisci, Massimiliano Manfrin, and Silvia Cavalletto.

Since the model name was changed in UTOPIA, I would like to remember and thank other people that has collaborated with me in managing and improving the model: Ying Zhang, Seon Ki Park, Caterina Francone, and in particular Riccardo Bonanno, who improved the routines on soil freezing and corrected several mistakes, and Ines Cerenzia, who implemented the routines relative to photosynthesis and carbon budget. Finally; I want to thank Silvia Terzago and Jost von Handemberg who helped me in optimizing the routines for the compilation in Fortran.

UTOPIA : The Manual of Version 2015

Claudio Cassardo

CCCPR
Center for Climate/Environment Change Prediction Research

Severe Storm Research Center
SSRC

DEPARTMENT OF ATMOSPHERIC SCIENCE AND ENGINEERING

INNOVATION EWHA

UNIVERSITÀ DEGLI STUDI DI TORINO